



TECHNISCHE
UNIVERSITÄT
WIEN

Vienna University of Technology

MASTER THESIS

Mechanical Properties of Friction Stir Welded and Laser Hybrid Welded Joints

performed in order to obtain the academic degree of graduate-
engineer under the direction of

Ao.Univ.Prof. Dipl.-Ing. Dr.techn. Sonja Felber

E206

Institute for Building Construction and Technology

submitted at Vienna University of Technology,
Faculty of Mechanical and Industrial Engineering

Ugis Groza

0626105

Kölblgasse 2-44 A-1030 Vienna

Vienna, February, 2014

At this point I want to give my sincere thanks to my advisor Ao.Univ.Prof. Dipl.-Ing. Dr.techn. Sonja Felber for supervising my master thesis, as well as for offering this topic.

Furthermore I want to express thanks to Dipl.-Ing. Peter Herzog and the team of his students, with whom it was a great pleasure to undertake the first trials and discover the world of friction stir welding. I would also like to thank the staff of the TGM (Technologisches Gewerbemuseum), who were involved in the process of this thesis.

I am especially grateful to Dipl.-Ing. Matthias Michl and Dipl.-Ing. Dr. tech. Herbert Stauffer at Fronius welding, for carrying out the laser hybrid welds.

On a private behalf I would like to thank my family, who supported me during my studies at the Vienna University of Technology, Lucia, for being there for me in the last year, and all of my friends.

Abstract

Friction stir welding (FSW) and laser hybrid welding (LHW) are two relatively new welding technologies, which are gaining importance in industrial applications. The focus of this master thesis lies in studying the basics of the FSW technology. A literature study provides an overview about welding, aluminum and its alloys, as well as the FSW and LHW processes. The practical part describes experiments, which were carried out, including the manufacturing of FSW tools, parameter variation during FSW welding, and the testing of FSW and LHW welds according to relevant standards. The base material used in the experimental part is the aluminum alloy AW-5747.

Zusammenfassung

Rührreibschweißen (FSW) und Laser-Hybrid Schweißen (LHW) sind zwei relativ neue Schweißverfahren, die zunehmende Bedeutung in industriellen Anwendungen finden. Der Schwerpunkt dieser Diplomarbeit, liegt in der Erforschung der Grundlagen des Rührreibschweißens. Eine Literaturstudie bietet eine Übersicht über Schweißen, beschreibt Aluminium und seine Legierungen und erläutert die FSW und LHW Prozesse. Im praktischen Teil werden die durchgeführten Versuche beschrieben. Diese beinhalten die Herstellung von FSW Werkzeugen, eine Parameterstudie des FSW-Schweißprozesses, sowie das Prüfen von FSW und LHW Schweißnähten nach gültigen Standards. Der Grundwerkstoff für die Schweißnähte, die im experimentellen Teil verwendet wurden, ist die Aluminiumlegierung AW-5747 (AlMg3).

Table of Contents

1 INTRODUCTION	1.1
1.1 History of welding	1.4
1.2 History of aluminum and aluminum production	1.6
1.3 Friction stir welding (FSW)	1.8
1.4 Laser hybrid welding	1.9
2 WELDING	2.1
2.1 Fusion welding processes	2.5
2.1.1 Gas welding	2.5
2.1.2 Arc welding processes	2.7
Manual metal arc welding	2.8
Submerged arc welding	2.9
Gas shielded arc welding	2.10
Gas metal arc welding MIG/MAG	2.11
Gas tungsten arc welding TIG	2.13
Plasma welding	2.14
2.1.3 Power beam welding	2.15
Laser-beam welding	2.15
Hybrid welding	2.16
Electron beam welding	2.17
2.2 Pressure welding processes	2.18
2.2.1 Friction welding	2.18
Orbital friction welding	2.19
Radial friction welding	2.19
Linear friction welding	2.20
2.2.2 Ultrasonic welding	2.20
2.2.3 Cold pressure welding	2.21
3 ALUMINUM AND ALUMINUM ALLOYS	3.1
3.1 Production of aluminum	3.4
3.2 Aluminum alloys	3.7

3.2.1 Wrought aluminum alloys	3.7
3.2.2 Cast aluminum alloys	3.11
3.3 Temper designations of aluminum alloys	3.12
3.4 Strengthening mechanisms for aluminum alloys	3.14
3.4.1 Grain size control	3.14
3.4.2 Solid solution strengthening	3.15
3.4.3 Strain hardening	3.16
3.4.4 Precipitation (age) hardening	3.17
3.5 Problems associated with welding of aluminum	3.18
3.5.1 Porosity	3.18
3.5.2 Crack sensitivity during welding	3.19
3.5.3 Oxide film entrapment	3.21
3.5.4 Degradation of the heat affected zone (HAZ)	3.21
4 FRICTION STIR WELDING (FSW)	4.1
4.1 Description of the friction stir welding process	4.3
4.2 FSW variables	4.5
4.3 Friction stir tools	4.6
4.3.1 Tool materials	4.7
4.3.2 Tool geometry	4.10
Design of the tool shoulder	4.10
Design of the tool pin	4.12
4.3.3 Special tool designs	4.16
Complex motion tools	4.16
Bobbin tools	4.18
Retractable pin tools	4.19
4.4 Influence of FSW welding parameters	4.19
4.5 Microstructure of FSW welds	4.21
Dynamically recrystallized zone (DXZ)	4.21
Thermo-mechanically affected zone (TMAZ)	4.22
Heat affected zone(HAZ)	4.22

4.6 Possible welding flaws during the FSW process	4.22
Voids	4.22
Joint line remnants	4.23
Root flaws	4.24
4.7 Applications of FSW	4.24
FSW in maritime applications	4.24
FSW in the aeronautic industry	4.24
FSW in the automotive industry	4.26
Other FSW applications and future outlook	4.26
5 LASER HYBRID WELDING (LHW)	5.1
5.1 LHW process	5.3
The CO ₂ laser	5.4
The Nd:YAG laser	5.4
5.1.1 LHW process parameters	5.5
Laser power	5.5
Welding speed	5.6
Relative arrangement of the laser and the MIG torch	5.6
Focal point position	5.6
Angle of the electrode	5.6
Shield gas composition	5.7
Power source of the MIG/MAG welding unit	5.7
Weld geometry and preparation	5.7
5.1.2 LHW advantages and applications	5.8
LHW in the automotive industry	5.9
LHW in the maritime industry	5.9
LHW in pipeline construction	5.9
6 WELDING OF THE SPECIMENS	6.1
6.1 Welding of the FSW specimens	6.3
6.1.1 Selection of the workpiece material	6.3
6.1.2 Selection of the FSW welding equipment	6.4

6.1.3 Designing and manufacturing of FSW tools	6.4
6.1.4 Experimental setup	6.5
6.1.5 Variation of FSW parameters	6.6
6.2 Welding of the LHW specimen.....	6.7
7 TESTING OF THE SPECIMENS	7.1
7.1 Testing methods for FSW and LHW welds	7.3
7.1.1 Non destructive testing (NDT) methods	7.3
Visual testing (VT)	7.3
7.1.1 Destructive testing (DT)	7.5
Tensile testing	7.5
Metallography and macroscopic examination	7.8
7.2 Testing of the FSW specimens	7.9
VT of FSW specimens	7.9
Inspection before welding	7.9
Inspection during welding	7.9
Inspection after welding	7.10
Tensile tests of the FSW specimens	7.12
Macroscopic examination of FSW specimens	7.13
Specimen 2	7.14
Specimen 3	7.14
Specimen 4	7.14
7.3 Testing of the LHW specimen	7.15
VT of the LHW specimen	7.15
8 SUMMARY AND DISCUSSION OF THE RESULTS	8.1
8.1 FSW results	8.3
8.1.1 Influence of the welding tool shoulder diameter	8.3
8.1.2 Influence of the edge preparation	8.4
8.1.3 Influence of the dwell time prior to welding advance	8.5
8.1.4 Influence of the welding speed	8.5
8.1.5 Conclusions of the FSW parameter study	8.6

8.2 LHW results	8.7
8.3 Comparison of FSW and LHW test results	8.7
8.4 Comparison of FSW and LHW technologies	8.8
R REFERENCES.....	R.1
A APPENDIX.....	A.1
S SUPPLEMENTS.....	S.1

LIST OF ABBREVIATIONS, UNITS AND SYMBOLS IN FORMULAS

A	...	Cross section of a tensile specimen
A	...	Tensile elongation
AC	...	Alternating current
AlMg3	...	Aluminum alloy AW-5754
Al ₂ O ₃	...	Aluminum oxide
ASME	...	American Society of Mechanical Engineers
B	...	Breaking strength
CaF ₂	...	Calcium fluoride
CNC	...	Computer numerical control
CO ₂	...	Carbon-dioxide
d	...	Grain size
DC	...	Direct current
DT	...	Destructive testing
d _s	...	Shoulder diameter of friction stir welding tools
DXZ	...	Dynamically recrystallized zone
EBW	...	Electron beam welding
EN	...	European standard
E ^w	...	Welding energy
F	...	Force
FRW	...	Friction welding
F _z	...	Downward force
FSW	...	Friction stir welding
GMAW	...	Gas metal arc welding
GSAW	...	Gas shielded arc welding
H ₂ PO ₄	...	Phosphoric acid
HAZ	...	Heat affected zone
HF	...	Hydrofluoric acid
I	...	Electric current

k_y	...	Metal constants
l_0	...	Original length of a tensile specimen
LBW	...	Laser beam welding
L_f	...	Laser focus
LFW	...	Linear friction welding
L_P	...	Laser power
l_p	...	Length of pin of friction stir welding tool
LHW	...	Laser hybrid welding
LOM	...	Light optical microscope
MAG	...	Metal active gas welding
MIG	...	Metal inert gas welding
Mg_2Si	...	Magnesium silicide
MMA	...	Manual metal arc welding
n	...	Rotation rate per minute
Na_3AlF_6	...	Cyrolite
NDT	...	Non destructive testing
PA	...	Flat or downhand welding position
PAW	...	Plasma arc welding
PC	...	Horizontal/vertical welding position
PCBN	...	Polycrystalline cubic boron nitride
PE	...	Overhead welding position
PF	...	Vertical up welding position
PG	...	Vertical down welding position
R	...	Resistance across weld
R_e	...	Yield strength
R_m	...	Tensile strength
R_p	...	Proof strength
$R_{p0.2}$...	0.2% proof strength
r_p	...	Radius of pin of friction stir welding tool
r_s	...	Radius of tool shoulder

Q	...	Thermal energy
SAW	...	Submerged arc welding
SEM	...	Scanning electron microscope
t	...	Thickness of the base material
t	...	Welding time duration
t _D	...	Dwell time before start of welding
T _f	...	Liquidus temperature interval
TiC	...	Titanium carbide
TIG	...	Gas tungsten arc welding
TEM	...	Transmission electron microscope
TGM	...	Das Technologische Gewerbemuseum
TMAZ	...	Thermo-mechanically affected zone
TWI	...	The Welding Institute
USW	...	Ultrasonic welding
v	...	Advance speed
VT	...	Visual testing
WAZ	...	Weld affected zone
WPS	...	Welding procedure specification
WC	...	Tungsten carbide
1...7	...	Specimen number of a friction stir welded specimen
Δl	...	Elongation of a tensile specimen
ε	...	Strain
ε	...	Maximum strain
σ	...	Stress
σ ₀	...	Metal constant
σ _y	...	Actual yield strength
μ	...	Coefficient of friction between tool and workpieces
✓	...	Test passed
✗	...	Test not passed
---	...	Test not relevant for specific welds

1 INTRODUCTION

1 INTRODUCTION

Research today is state of the art of technology tomorrow. These words can be applied to almost any invention made by humans throughout history. This master thesis will take a closer look at a relatively new welding technique called friction stir welding (FSW). Ever since its discovery in the early 90ies, in a laboratory at the University of Cambridge UK, FSW welds have found their way to outer space in a mere time lapse of little more than 15 years.

In 1993, NASA challenged Lockheed Martin Laboratories in Baltimore, to develop a high-strength, low-density, lighter-weight replacement for the aluminum alloy Al 2219, used on the original Space Shuttle External Tank. A new aluminum-lithium alloy, known as Al-Li 2195, was developed by Lockheed Martin, and the laboratories at Marshall Space Flight Center. The weight of the external tank, (shown in *Figure 1-1*) was reduced by 3.500 kilograms. The lithium component proved to be problematic, when welding the new alloy. Repair welds were difficult to make, and the joint strength of the external tank had much lower mechanical properties. Alternative welding techniques were thoroughly researched. The solution was found in friction stir welding. FSW is a process, which transforms metals from a solid state into a "plastic-like" state, using a rotating pin tool to soften, stir, and forge a bond between two metal plates to form a uniform welded joint [1].



Figure 1-1: The dome of a space shuttle fuel tank produced using FSW technology [1]

1.1 History of welding

Nowadays, it would be hard to imagine our daily lives without products that use welding in part of their manufacturing process. Almost every mean of transportation, from a bicycle to a space rocket, household goods, as well as industrial machines, and many more are produced involving at least some welding in their production cycle.

Next to the use of adhesives, mechanical attachment, and fastening, welding is one of the oldest methods for joining materials. Welding is an ancient art, which in the old days was a challenging problem for our ancestors, as heat sources were limited. The first welding, in the sense of its definition, was achieved by forming small pieces of metal into larger assemblies, through the process of what has been called adaptive metallurgy. Joining of larger assemblies required evolving of joining processes, such as coforging or riveting. The first crude welds were also produced. Forge welding took off, as first bracelets were crafted by hammering nuggets of gold or silver into rods, which then were formed into rings by connecting together the ends of the circle segments. As the complexity of shapes grew, casting was preferred to forging, as large and intense heat sources were needed for bigger and better welds. Nevertheless, the superiority of mechanical properties, such as strength and toughness of wrought metals to cast metals, was recognized even back in the Bronze Age [2].

The key discoveries that enabled welding to take off were made in the later half of the 19th century. The physical properties of acetylene were examined, and the knowledge applied in first gas arc welds. The advances in the exploration of electricity led to the introduction of welding using an electric arc. In 1885, Nicolai N. Benardos and Stanislaw Olzewaski declared a British patent, which used carbon dioxide (resulting from the oxidizing of a carbon electrode) as a shielding gas in the arc welding process. This helped to avoid the unwanted brittle nature of oxidized metal. The first patent for welding with a metal filler material was granted to C. L. Coffin in 1890. In 1900, the first oxyacetylene torch was developed by E. Fouch and F. Picard in France. Just three years later, the torch was already

applied commercially. In the following years, further inventions led to coated electrodes, thermite welding of aluminum, electroslag welding, as well as plasma arc welding. During the Industrial Revolution and World War I, the new technologies were extensively used. Inventions were made, and patents registered at a never before seen rate. In 1911, a first attempt to lay 11 miles of pipeline, using oxyacetylene welding, was undergone in the USA. Milestone achievements, such as the first all-welded bridges, building frames, and ships, emphasized the importance of this relatively new crafting technique. Institutions such as the American Welding Society were set up.

In the early 1930s, submerged arc welding was introduced and applied in shipbuilding and fabrication of pipes. The German shipbuilding industry used welding extensively to reduce the weight of warships and to increase their overall size, as strict weight limitations were set up after World War I. A major development was the patent of gas tungsten arc welding in 1942, which was specifically designed for the aircraft industry. In the second half of the 20th century new technologies, such as electron beam welding, friction welding, laser beam welding, explosive welding, and friction stir welding (FSW) were invented. The space exploration programs, by the USA and the Soviet Union, pushed the limits for both materials and fabrication techniques [3].

The most actual developments, to present, have brought about processes, such as magnetic pulse welding, diode laser welding, and conductive heat resistance seam welding. These still might seem exotic at present, but as the preceding overview of history of welding shows, they might become state of art technology for future generations.

1.2 History of aluminum and aluminum production

In 1787, the French chemist Antoine Lavoisier identified aluminum as an oxide, of a still undiscovered metal, in alum. The name aluminum was assigned by Sir Humphrey Davy in 1807, originating from the Latin word 'alumen', which literally means 'bitter salt' [4]. The first isolation of aluminum was achieved by Hans Christian Oersted in 1825. In a painstaking process, anhydrous aluminum chloride with potassium amalgam was heated and then the mercury distilled away. For the following 30 years aluminum remained a laboratory curiosity. During these years Friedrich Wöhler and Henri Saint-Claire Deville managed to improve the technique by replacing potassium with the more abundant and less expensive sodium. First commercial quantities of aluminum were produced in this manner. As often seen in history, the potential of aluminum was initially recognized by the military. Napoleon the Third foresaw its use in lightweight body armor and supported the investigation in the production of aluminum. However the aluminum produced by the Saint-Claire Deville's process was less than 95% pure, and the price proved to be more expensive than gold at that time. It is reported that the only result of the Emperors investment were just some decorative military helmets, an aluminum dinner set, and some aluminum toys for children of the Imperial Court.

In 1886, a breakthrough in the production of aluminum occurred. Two young scientists, Charles Martin Hall in the US and Paul L. T. Heroult in France, both 22 years old at that time, discovered and patented almost simultaneously a process, in which aluminum is produced by dissolving alumina into molten cryolite, and then decomposing it electrolytically. Known as the Hall-Heroult process, it has proven to be the most efficient way of aluminum extraction and is still by far the major source of aluminum at present [5].

With the production process in place, aluminum got affordable and more abundant. At the same time the applications of aluminum took off. An example, where this can be taken literally, occurred in 1903, when the Wright brothers introduced aluminum in the engine of their first powered aircraft, the Flyer I. They successfully proved to the world, that flying a device, which is heavier-than-air, is

possible [6]. At the beginning of the 20th century, aluminum was not yet widely used, as the quantities smelted, compared to iron, were very small. Many scientists set themselves the goal to solve the task of aluminum reinforcement. Among them was Alfred Wilm, a German physicist, who achieved a remarkable increase of strength by coincidence. During experiments with the chemical composition of aluminum, he discovered the favorable effect of aging. This eventually resulted in one of the first aircraft alloys, called Duralumin (first produced in Dürener Metallwerke AG). It was successfully used in the military aircraft planes Junk J1 by the German army during World War I. At this time, the scientists in Soviet Russia were still ignorant of the secret of this high-strength alloy. Their chance came about, when in 1922 a German plane was shut down. A thorough chemical analysis revealed the trick, and by the end of the year Soviet Russia started the production of Kolchougaluminum. This high-strength alloy was also applied in military aircrafts. During World War II, aluminum played an important role, as it was applied in airplane parts such as body, engines, chassis, and fuel tanks. Aluminum powder was used for bombs, shells, and flares [7]. After World War II, both superpowers set up space exploration programs, which largely depended on aluminum alloys. At present, 70% of the weight of modern civil aircrafts, like the Airbus A330 or Boeing 777, is attributed to high strength aluminum alloys. Research in producing new, even lighter, and stronger aluminum alloys is never ending, as carbon reinforced polymer composites start to become a serious competitor in the field of high-strength, low-weight materials [8].

At present, the favorable properties of aluminum, such as the low density, high strength, excellent corrosion resistance, and other, have made this metal to be first choice of engineers and designers. Aluminum is used in a wide variety of applications, such as transportation, packaging, construction, household items (cooking equipment, laptop shells,...), and many more [9].

1.3 Friction stir welding (FSW)

Invented in 1991 by Wayne Thomas, at The Welding Institute (TWI) in Cambridge UK, this relatively new welding technology has evolved impressively during the last 20 years. The first patent in the US, with the No. 5.460.317, was filed in November 1992, and assigned to TWI, with W. H. Thomas et al. as inventors. The TWI is one of the world's foremost independent research and technology organizations, with a specialty in welding, and has a long history of innovation and knowledge transfer. After its invention, the FSW process found its way quickly out of the laboratories of TWI into industry. The first production application was initiated already in 1995, by Marine Aluminum in Norway. FSW welds were applied on 6xxx aluminum extrusions to make large panels for decking of fast ferries [10]. Since this time, the FSW process has made its way into many other applications, one of the most spectacular being a five-meter diameter fuel tank, used by NASA. The dome of the tank is shown in *Figure 1-1*. The first spacecraft, with a fuel tank manufactured using the FSW technology, flew into space in 2009, and further research aims to implement the process into the new generation of NASA's Space Launch System [11]. More recently the process has expanded into fabrication of more complex assemblies for the automotive, medical, semiconductor, and oil and gas industries. To date, most of the applications have involved welding of aluminum. In the last couple of years however, FSW welding of copper and steel have been initiated and implemented. Currently, the FSW technology is researched at facilities throughout the world, as publications of different character are reaching the public at a never before seen rate.

1.4 Laser hybrid welding (LHW)

The combination of laser light and an electrical arc into an amalgamated welding process has existed since the 1970s, but has only been used recently in industrial applications. First attempts of combining a laser and an arc for welding, were performed by a group, led by William Steen, at Imperial College, London. The advantages of the process, such as increased welding speeds and process stability were immediately shown. Practical applications had to wait for the laser technology to mature, as the early process was not viable on an industrial scale.

As advances in the laser technology made the equipment more reliable and cost effective, possibilities and limitations of the hybrid laser-arc welding technique were investigated all over the world by both, public and private sector. The driving forces behind the innovations were, among others, the need for higher production rates for military equipment. The manufacture of modern submarine vehicles involves the production of tailored blanks, which require wide, high quality welds made at high speed. The automotive, ship building, and the pipeline industry became interested in this relatively new welding technology, and it was just a matter of time, before the first industrial applications emerged.

One of the first companies to adapt the hybrid laser-arc welding technique was Meyer Werft shipbuilding company, in Germany, in 2000. The new panel production line proved to be so successful, as to replace the conventional panel line by 2002. The amount of laser hybrid welds account for approximately 50% of total weld length, which for a large cruise ship total to a length of up to 500 km. Innovations, such as integrated hybrid welding heads (by Fronius) have made this welding process attractive for the automotive industry, as hybrid welds are applied in the production of higher class models of companies, such as Volkswagen and Audi.

The outlook of the laser hybrid welding technology is to increasingly weld high strength alloys and the introduction of the process into pipeline construction **[12]**, **[13]**, and **[14]**.

2 WELDING

2 WELDING

Welding is commonly described as a fabrication or sculptural process, in which materials of the same type, usually metals or thermoplastics, are joined causing coalescence. Different definitions exist, but there seems to be a common core in all of them. The central aspect is that multiple entities are made one by establishing continuity. This does not imply homogeneity of chemical composition but a continuation of similar atomic structure. A second essential point is that welding applies not just to metals but also a wide variety of materials, such as polymers, ceramics, inter-metallic compounds, and glass. Furthermore, a third important aspect of welding is, that it is the result of combined action of heat and pressure. This is often neglected, as the classical idea of welding is the melting up and joining of materials. Last but not least, it is important to realize, that welding is used to join parts, which it does by joining materials. The joining of materials is mainly a challenge of creating chemical bonds, through the combined action of heat and pressure, using the knowledge, obtained through the study of metallurgy. The joining of parts adds additional constraints, such as shape restrictions, critical energy input levels to avoid intolerable levels of distortion, residual stresses or disruption of chemical composition, and microstructure. The key point is to understand, that welding is a secondary manufacturing process to produce an assembly or structure from parts or structural elements [2].

When looking at the definition of welding, it is clear that a wide variety of processes can lead to obtaining material continuity. Therefore, it is essential to classify the processes in order to clarify fundamental differences and identify technology gaps. For complex entities, such as welding, there can be many bases for classification for creating a taxonomy.

Commonly, when classifying a welding technology, the first distinction is made between fusion and non fusion welding processes. Most welding processes rely on heat more than on pressure to accomplish joining by creating atomic bonding across the joint interface. When significant melting is involved and necessary for welding, and pressure is mainly used for fixing the workpieces position, the

processes are called fusion welding processes. If, however, melting does not occur or is not principally responsible for the bond creation, the term non fusion or pressure welding processes applies. A schematic overview of the most common welding methods is shown in *Figure 2-1*.

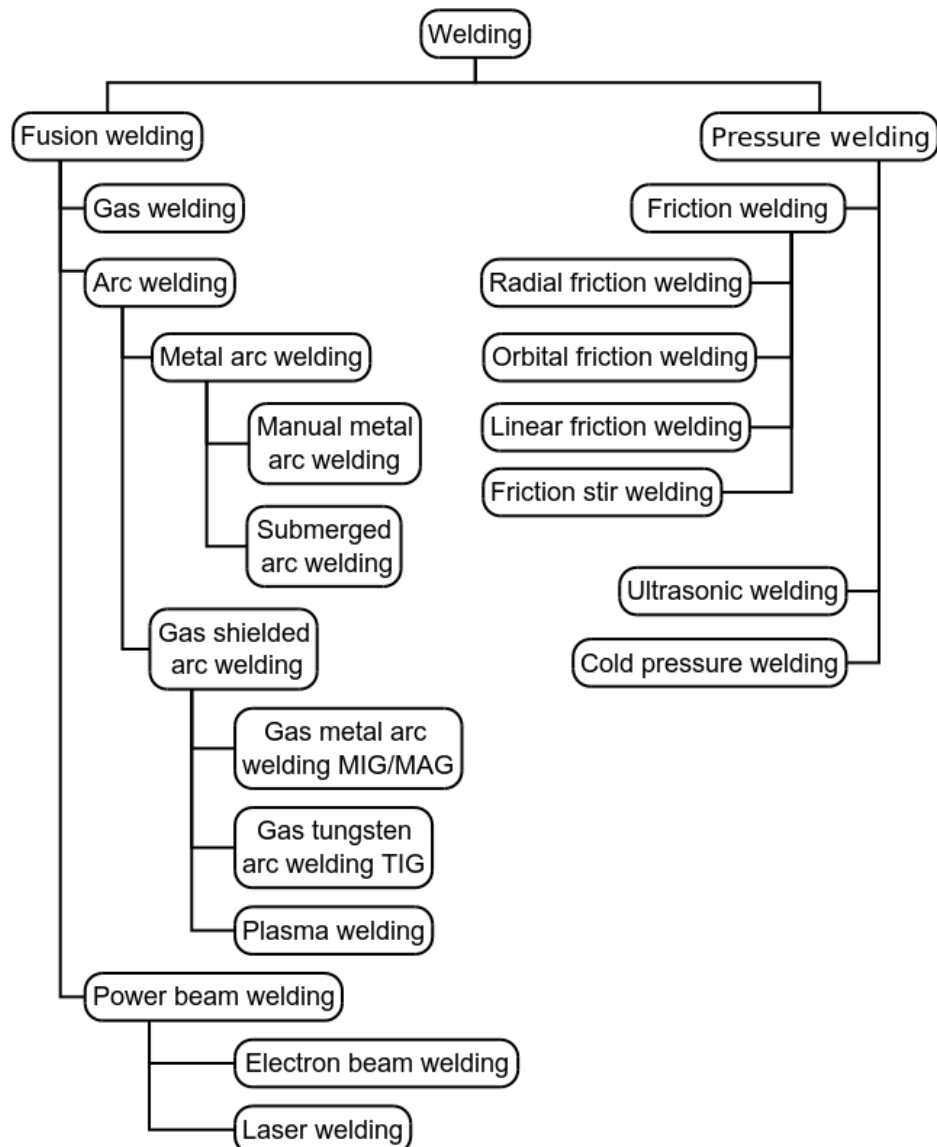


Figure 2-1: Schematic overview of the most common welding methods [2], and [15]

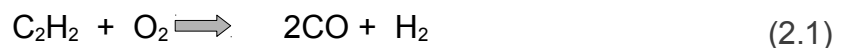
2.1 Fusion welding processes

In fusion welding processes the workpiece material is heated up to a temperature above its melting point or liquidus line for alloys. The atoms are brought together in the liquid state to establish material continuity and create a large number of primary bonds across the interface, after solidification has taken place. Depending on the welding method, filler material also has to be melted and added to completely fill the joint gap. The energy, mainly in form of heat is generated by one or a combination of the following energy sources:

- Electric arc employing an non-consumable or a consumable electrode,
- Heat generation through resistance or Joule heating of the workpiece, which is subjected to direct or alternating current,
- High intensity radiant energy source, such as a beam, where the heat is generated by conversion of the kinetic energy of fast-moving particles, or
- A chemical energy source, such as the heat generated by combustion of a fuel, or an highly exothermic reaction between the solid workpiece and a solid or gaseous reactant.

2.1.1 Gas welding

Gas welding used to be the most widely used welding method for many years, but it is less common today. Gas welding is versatile, uses simple and relatively cheap equipment and is used, where there is no access to power sources. By adjusting the levels of acetylene and oxygen, the welder can influence the type of flame. Depending on the level of oxygen a flame can be carbonizing (reducing), neutral or oxidizing. The heat is generated by two steps of combustion. In the first step acetylene is combusted in oxygen, as described in the following formula:



The first step of combustion occurs in the smaller inner flame cone. It has a typical

2 WELDING

light blue color and can reach a temperature of up to 3500°C. The second step of combustion, takes place immediately afterwards in the outer envelope of the flame. During this process, carbon monoxide, resulting from partial combustion of the carbon, which is dissociated from the acetylene (or other fuel gas), reacts further with oxygen, this time from the surrounding air to form carbon-dioxide. The hydrogen from the primary combustion (or the fuel gas) also reacts with oxygen to form water, as can be seen in the following formulas:



Figure 2-2 shows a schematic view of the gas welding flame with the corresponding temperatures and a schematic overview of welding in progress.

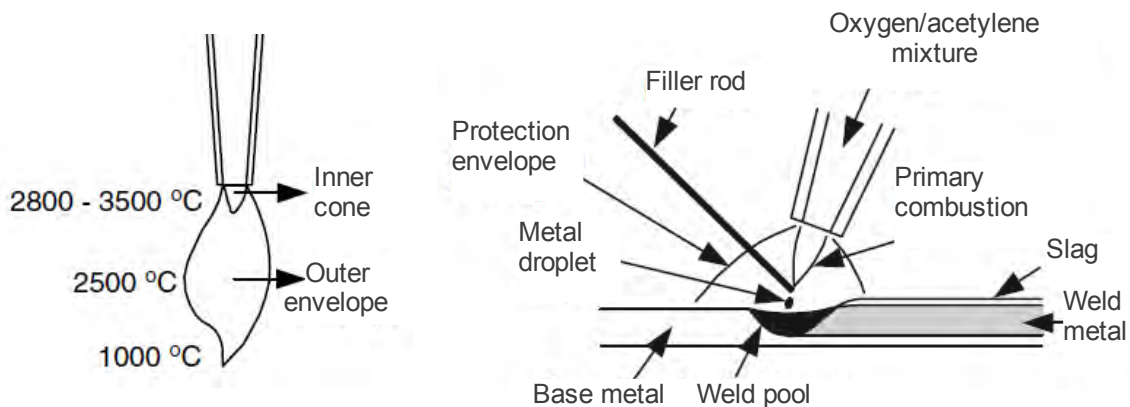


Figure 2-2: Schematic overview of gas welding [16]

The benefits of gas welding include:

- The ability to influence the temperature by slow heating and cooling to avoid hardening of the weld,
- The ability to weld metal with a thickness of up to 6 mm with a I-joint configuration,
- The independence of electrical supply and portability of the equipment,

- Gas welding processes can also be used for metal cutting, gouging or piercing. Here the molten base metal is blown away with a jet of oxygen or air from a compressed source.

The drawbacks of gas welding are mainly the limited source of energy, which can result into a rather slow welding velocity, and a high total energy input. The nature of the process limits the amount of protective shielding provided to the weld, so welding of the more reactive metals (e.g. titanium) is generally impossible. To offset this shortcoming, oxyacetylene welding may employ a flux or fluxing agent to provide additional protection to the weld, to prevent oxidation during welding, and/or to clean the workpiece of oxide, and to promote flow and wetting by any filler metal [15] and [16].

2.1.2 Arc welding processes

Fusion welding technologies that employ an electric arc as a heat source are called arc welding processes. Arc welding processes are the most commonly used welding processes, as the energy source can be effectively generated, concentrated, and controlled. The arc, in arc welding, is created by an electric current, which flows from an electrode to the workpiece, both subjected to different polarities. The arc itself is an electric breakdown of a gas, which produces an ongoing plasma discharge. The electrons and positive ions, from the electric breakdown, are accelerated by the potential field between the electrodes and produce heat, when converting their kinetic energy upon collision with the workpiece. The arc welding processes can be separated, depending on whether the electrode of the welding apparatus is permanent, serving solely as a source of electrons, or is being consumed providing filler material to the weld. Non-consumable electrodes are usually composed of tungsten or carbon (graphite), because of their very high melting temperatures. A shielding gas must be provided in order to protect the electrodes from oxidation. Consumables are composed of the metal or alloy, needed in the filler, and come as rods or continuous wires [15].

Manual metal arc welding

Until the beginning of 1980s, manual metal arc (MMA) welding was the predominant form of fusion welding, using consumable electrodes. The process is versatile and the equipment required fairly simple. A MMA welding kit is depicted in *Figure 2-3* and consists of an electrode holder, a power source, a welding cable, which is attached to the electrode holder, and a return cable, which has an electric contact to the workpiece. A wide range of electrodes is available, depending on the requirements for the particular welding tasks. Shielding is provided by the coating of the electrode, which forms a slag upon the weld, and needs to be removed after the weld is finished.

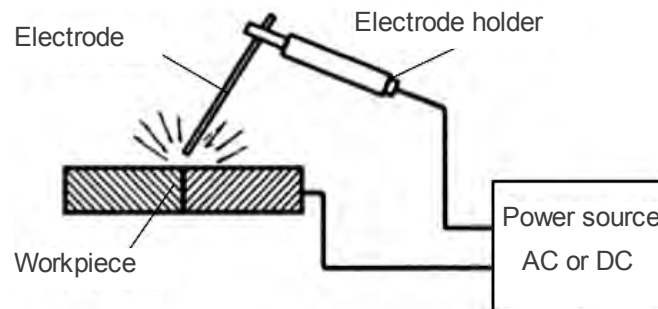


Figure 2-3: Schematic diagram of MMA welding [15]

Depending on the metal type, welding position, the current range used or particularities of the welding environment, the welder has a wide variety of electrodes to choose from. Electrodes are divided into four groups, depending on the chemical composition of the slag: acid, basic, rutile and cellulose. While the metal rod of the electrode is of a similar alloy, as the workpiece, the coating of the electrode consists of various mixtures of finely powdered chemicals and minerals, held together by a suitable binder. The functions of the electrode coating include, among others, the protecting of the weld pool from the surrounding atmosphere, improving the stability of the arc, increasing the yield by providing additional metal powder, cleaning of the weld pool of sulfur and phosphor, and shaping the upper surface of the weld [17].

Acid electrodes are coated by iron- and manganese oxides as well as silica and produce a viscous and easily removable slag. Smooth and shiny weld beads are characteristic to these electrodes, yet a lower yield- and ultimate tensile strength can be expected compared to other types of electrodes.

Rutile electrodes contain titanium-oxide (TiO_2) in their coating. Large amounts of H_2 is generated during welding, which acts as a shielding gas, but also increases the risk of hydrogen embrittlement and cracking [2]. Rutile electrodes are easy to strike and re-strike and produce neat welds with an easily removable slag.

The coating of basic electrodes is mainly composed of calcium fluoride (CaF_2). The slag reacts as a base, leaving low sulfur and oxygen contents in the weld metal, resulting in high-strength and high-toughness welds with a good resistance to hot cracking.

Using cellulose electrodes produces excellent penetration, by providing a high hydrogen content in the arc. Cellulose electrodes are mainly used for the construction of gas and oil pipelines, and are applied in all welding positions [15] and [17].

The advantages of the MMA include the versatility of the method and the simple, and relatively cheap equipment. The main drawbacks are increased operating costs due to time consumed by slag removal and changing of the electrodes. As MMA is limited in terms of mechanization, weld quality and reproducibility largely depends on the skill of the welder [15] and [17].

Submerged arc welding

Submerged arc welding (SAW) is a high-productivity welding method, which usually is mechanized and uses one to three continuous wire consumables. Similar to manual metal arc welding, the shielding of the weld is provided by a solid substance in form of flux powder, which is supplied to the welding head, while welding is in progress. As can be seen in *Figure 2-4*, the excessive flux is sucked up, returned, and reused. The flux has the same functions as the coating of the MMA electrodes. The excessive flux also serves as a cover for light, and

2 WELDING

there is no smoke or splatter from the weld. However due to the fact, that the flux powder is not bounded, only horizontal flat welding position can be carried out.

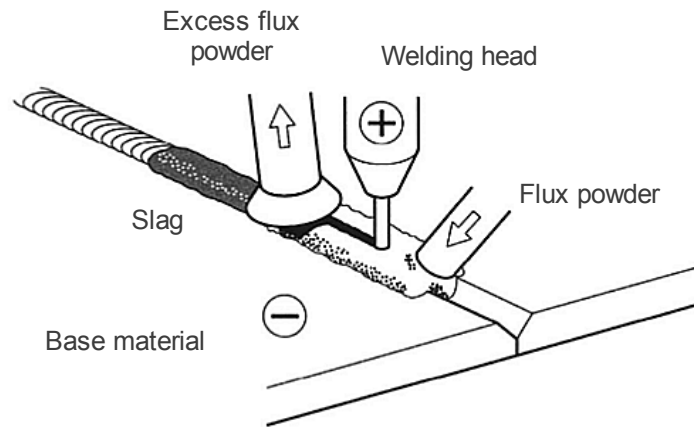


Figure 2-4: Principle of submerged arc welding [15]

If the welding parameters are properly set, the appearance of the weld is often very uniform and bright, merging smoothly into the workpiece material. Welding can be carried out with both DC or AC power supply. The advantages of the submerged arc welding include a high deposition rate, deep penetration, and high and reproducible weld quality. The SAW method is used for both butt and fillet welds and is most commonly applied for large items such as plates in shipyards, longitudinal welding of large tubes, or large cylindrical vessels [15].

Gas shielded arc welding

Whereas the previously described electric arc processes use solid material to protect the weld, gas shielded arc welding (GSAW) processes rely on a continuous flow or a sealed atmosphere of shielding gas in order to prevent oxygen and nitrogen from the air to come in contact with the melted metal. Oxygen is very reactive at elevated temperatures and oxidizes the alloying elements, creating slag inclusions in the weld pool. Nitrogen is solved in the melted material, yet as the temperature decreases, so does the solubility of nitrogen, which results in pores of the evaporating gas. Nitrogen can also be the cause of brittleness of the

workpiece. The shielding gas influences the welding properties, the penetration, and weld bead geometry [15].

The most commonly used shielding gases are argon (Ar), helium (He), carbon dioxide (CO₂), and, for some applications, small additions of hydrogen (H), oxygen (O₂), and nitrogen (N₂) have a favorable effect. Argon is the most widely used shielding gas. Being an inert gas, it does not chemically react with other materials and can be applied for sensitive materials such as aluminum, and stain-less steel. Helium is also an inert gas, but more expensive and less dense than argon. Compared to argon, the heat input into the weld is higher, which is advantageous when welding materials with a high heat conductivity such as aluminum or copper. CO₂ is much less expensive than argon and helium. A disadvantage is the spatter resulting from the welding process. Hydrogen, when used properly, increases the heat input into the weld and can be used in root gases. However, the risk of cracks only makes it suitable for austenitic stainless steel applications. Oxygen, in small doses, has a stabilizing effect on the arc when used in the MIG welding process. Small additions of nitrogen in the shielding gas composition compensate for the losses of alloying nitrogen when welding austenitic steels [15].

Gas metal arc welding MIG/MAG

Gas metal arc welding (GMAW) has emerged as the leading welding method in most industrial countries today. Depending on which shielding gas is used, the GMAW method is most commonly known as metal inert gas (MIG) welding or metal active gas (MAG) welding. The MIG welding process uses chemically inert gases such as helium or argon. The shielding atmosphere, used in MAG welding, has an active component, such as CO₂. The gas metal arc welding process is an all-position welding process. However, each of the variations has its own position capabilities, depending on the electrode size and the metal transfer. The most popular method of applying is the semi-automatic method, where the welder provides manual ravel and guidance of a welding torch. The principle of operation and the equipment are shown in *Figure 2-5*. The arc is struck between the work-

2 WELDING

piece and a continuous, consumable metal wire electrode that is fed forward into the arc. The wire is supplied on a reel and is fed to the welding gun by drive rollers. These push the wire through a flexible conduit, through the hose package to the gun. Electrical energy for the arc is passed to the electrode through the contact tube in the welding gun. The workpiece is connected to the power source, which most commonly operates on DC. The gas nozzle that surrounds the contact tube supplies the shielding gas for the stabilization of the arc, and protection of the weld pool. Welding parameters, such as wire feed speed and current, electrode diameter, voltage, welding speed, inductance, electrode stick-out, as well as the type and flow rate of the shielding gas influence the MIG/MAG welding process. They need to be matched with each other, for optimum welding performance. The main advantages of the MIG/MAG process include a high deposition rate and operator factor, elimination of slag and flux removal, reduction of fumes and smoke, but most of all, the extreme versatility and its broad application ability. The skill level in the semiautomatic method is also slightly lower, compared to manual metal arc welding [15].

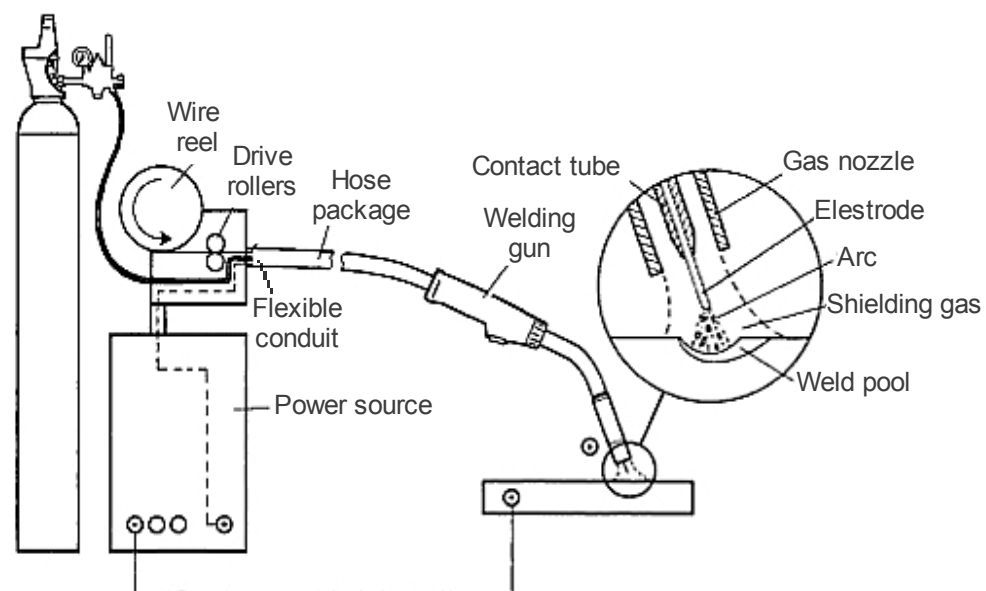


Figure 2-5: Schematic overview of an MIG/MAG welding unit: [15]

Gas tungsten arc welding TIG

TIG welding uses a non-consumable tungsten electrode, shielding gas, and if needed, a manually supplied filler rod. Stability of the arc and the excellent control of the welding process make TIG welding suitable for joining of stainless steels, and light metals, such as aluminum. The equipment is depicted in *Figure 2-6*.

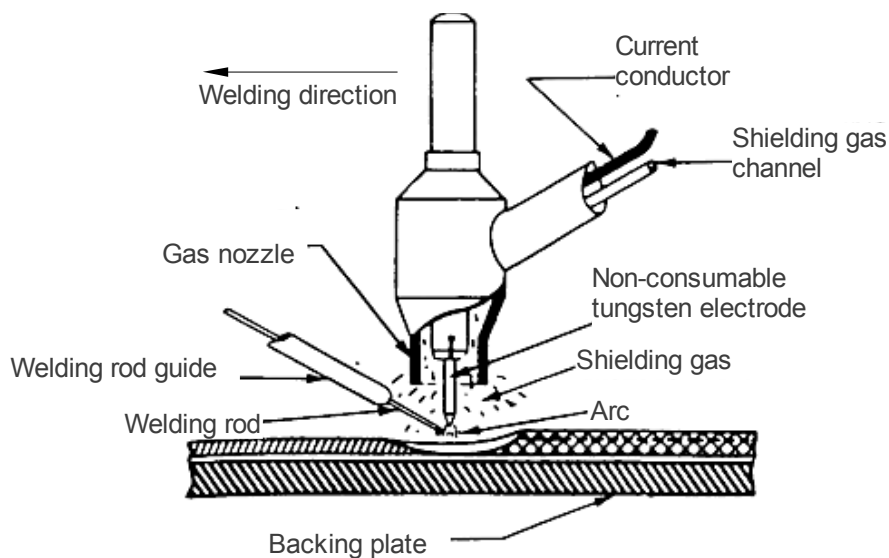


Figure 2-6: TIG welding process [18]

The electrode must fulfill requirements such as low electrical resistance, high melting point, good emission of electrons, and good thermal conductivity. These are best met, using tungsten as the base electrode material. In order to improve the stability of the arc, and ease the arc striking process, small proportions (up to 3%) of thorium oxide, zirconium, lanthanum or cerium may be included. The electrode is subjected to a high temperature, and might break due to the brittle nature of tungsten. In order to maintain a sharp tip of the electrode, which is needed to produce a stable arc, the welder needs to grind the electrode in-between the welding cycles [15]. Filler material for TIG welding comes in form of a wire, which is fed into the joint by hand or mechanically. The deposition rate is comparatively slow (0.5 – 1 kg per hour) [2], but can be enhanced using a 'hot wire' variation, where the wire is resistance-heated prior to its introduction into the weld pool. The

shielding gases used are similar to those of the MIG process, with argon being the most widely used. When welding materials, which are easily oxidized, a root gas can be applied in order to protect the root side of the weld.

TIG welding is usually carried out, using DC, with the negative pole connected to the electrode. This constellation generates more heat in the workpiece. However, when welding aluminum or magnesium the problematics of the oxide layer require an AC power source. The oxide layer is only broken down, when subjected to the negative pole, yet this would result in excessive temperature of the electrode, so AC is used. In order to prevent the arc from extinguishing, square wave AC power sources are applied. These enable the variation of the proportions of the positive and negative polarity currents and empower the welder to control the penetration, and oxide breakdown. The main advantages of the TIG welding process are the excellent control of the welding, resulting in precise, high quality welds, absence of slag, and versatility of the process. Little amounts of spatter, and the good visual appearance of the weld requires very little post treatment. The drawbacks are the relatively slow welding speed and the need for skilled welding personnel, which increases the costs compared to MIG/MAG welding process [2], and [15].

Plasma welding

Similar to TIG, plasma arc welding (PAW) also uses a non consumable tungsten electrode. The main difference lies in the fact that the electrode is positioned within the torch, and two separate gas orifices are provided for the plasma and the shielding gas. The plasma gas and the shielding gas are usually identical, but can be of different composition for certain applications. As the plasma arc is more concentrated than a TIG arc, advantages such as higher welding speeds, smaller distortion rates and heat affected zones, as well as higher metallurgical quality compared with TIG welds exist. The PAW welding is less sensitive to arc length variations, enables deep penetration, and can be used for very thin and thick materials. On the contrary, the equipment for PAW is more complex, expensive, and bulkier compared to a TIG welding set up [2] and [15].

2.1.3 Power beam welding

Processes that employ a source of high-intensity electromagnetic radiation to cause fusion and produce welds are called power beam welding processes. The better known of these are the high-energy-density beam processes, including electron-beam welding (EBW) and laser-beam welding (LBW). These processes are employed, when the density of the energy source is more important than the total energy input into the weld, for example when deep penetration is needed. Another advantage of power beam welding processes is their relatively fast welding velocity. Laser beam welding can reach speeds of up to 50 m/min, when welding thin materials [15].

Laser-beam welding

The rays of the laser light are parallel and highly concentrated, which enables them to be conducted by mirrors or glass fibers to a welding position that is remote from the laser unit. During the welding process, the beam is focused by a lens or mirrors to a point with a diameter of few tenths of a millimeter, resulting in high energy density. This enables small heat-affected-zones and high heating- and cooling rates. The focus point is arranged to fall on, or slightly below, the surface of the workpiece. The base material is immediately melted and to some extent evaporated. The metal vapor forms a plasma, which is a good absorber of incident light. When appropriate process parameters are used, energy-absorption and efficiency are improved. A shielding gas is used in order to prevent air from reacting with the melted metal and protect the lens from spatter and vapor. The most common types of lasers used for laser-beam welding are the CO₂ laser and the Nd:YAG laser. Diode lasers are rapidly evolving, to reach the high outputs needed for most industrial applications [15]. A schematic view of the LBW process can be seen in *Figure 2-7*. The main advantages of laser-beam welding are deep and narrow penetration, high welding speeds, supreme quality of welds, and the low distortion levels of the workpiece. The LBW process is also very clean and quiet during operation. The drawbacks include the increased danger of thermal

2 WELDING

cracking and unwanted local hardening due to the low width/depth ratio of the weld geometry and rapid cooling rates. The LBW process is very tolerance-sensitive, and hence requires high precision of the welding equipment and fixtures. Investment costs are high and require skilled personnel for operation. Additional care must be taken to protect the operator from laser light [2], [15] and [19].

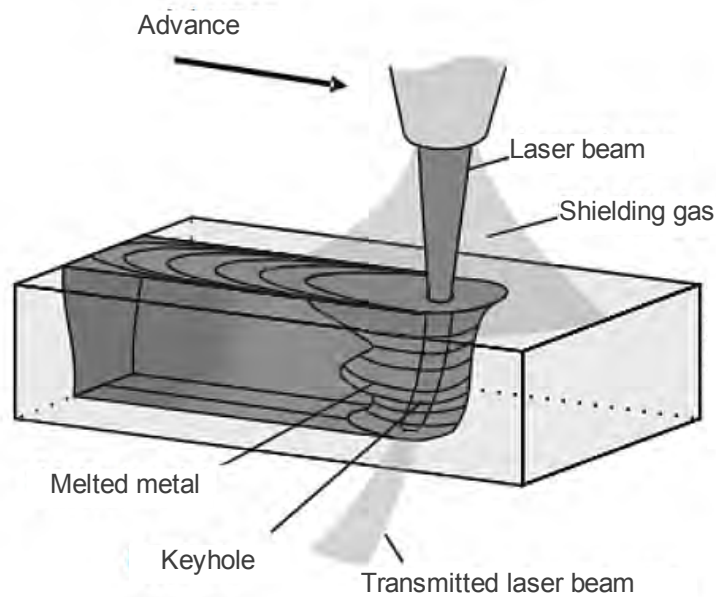


Figure 2-7: Schematic view of laser-beam welding [19]

Hybrid welding

Hybrid welding refers to a combination of two welding methods, usually laser welding and an arc welding method, such as MIG or plasma welding. The filler wire from the MIG/MAG welding process provides molten material for filling the joint gap and thus reducing the requirements for workpiece and fixture tolerances. When welding fillet joints, this combination provides reinforcement of the joint, and also reduces the risk of undercutting, which seriously reduces fatigue strength. In comparison with ordinary MIG/MAG welding, the welding speed is considerably higher, due to use of the laser [15].

Electron-beam welding

Electron-beam welding (EBW) uses a high-energy electron beam to produce the deepest and most narrow weld penetration among all known welding technologies, as can be seen in *Figure 2-8*. Compared to the LBW, the energy content and density is higher, resulting in very low distortion levels of the workpiece. Electron beam welding is used for advanced materials, complicated, critical parts, such as turbine rotors, and is particularly competitive for welding thick welds up to 250 mm, but is limited to materials with a low vapor pressure at melting point (this constraint excludes zinc, magnesium, and most non-metals), and nonmagnetic materials, as interference with the electron beam may occur [15].

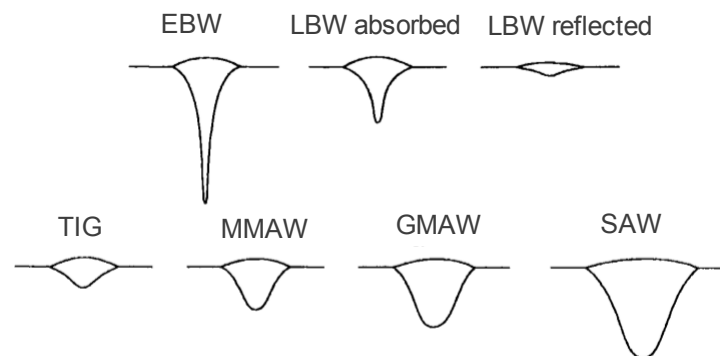


Figure 2-8: Schematic comparison of penetration of various welding processes [2]

In the EBW process, the electrons are supplied from a high-voltage power source (30 – 175 kV), with a low current (less than 1 A). Magnetic coils accelerate and focus the electrons in a similar manner, as used in older cathode ray tube displays. As the electron beam interferes with air, the welding needs to be carried out in a vacuum environment and the vacuum chamber needs to be opened, closed, and evacuated with each new workpiece. As the electron beam hits the workpiece, energy in form of x-rays is emitted. For most of the applications, the electron gun is stationary and the workpiece is moved according to the weld geometry. Similar to LBW, the EBW equipment needs to operate with extreme precision, due to the narrow nature of the electron beam [15].

2.2 Pressure welding processes

Pressure welding accomplishes material continuity, forming atomic bonds by applying pressure and temperature below the melting point of the base materials. This is achieved either by pressure and gross deformation, by friction and microscopic deformation or by the means of diffusion.

The major advantages of pressure welding methods in comparison to fusion welding processes include the retainment of the structure of the workpiece, as no melting and solidification takes place. Furthermore, a lower heat input results in a smaller HAZ, and the micro-structure of the workpiece material is much less affected. A wide variety of pressure welding processes exist, which can be used to weld materials of different material classes. The general shortcomings are extensive joint preparation and the complicated, elaborate, and very specialized tooling required for some processes. Additional drawbacks are the challenging inspection of joint quality, as well as the difficult, or even impossible repairing processes of pressure- welded joints [2].

2.2.1 Friction welding

Friction welding (FRW) processes convert mechanical energy into heat at the joint to be welded. As two contacting surfaces move relative to each other, atoms at the interface are set into motion, resulting into heat. The heat causes the temperature of the material to rise, having a softening effect on the material. The Young modulus decreases, making it easier for the material to be deformed. Friction welding processes use this physical characteristic to deform and forge the workpieces together, creating material continuity and, hence, a weld. FRW processes are usually designed to function without any melting of the workpieces and, therefore, are called solid-state processes. The friction welding technology has been further developed, so that the necessary friction can be applied by an external tool, as in friction stir welding.

Orbital friction welding

During the orbital friction welding one part is rotated against another, while an axial force is applied. As the heat, resulting from friction, softens the workpieces to desired extent, the axial force is increased in order to form a solid-state joint [15]. Orbital friction welding is the conventional form of friction welding and is schematically shown in *Figure 2-9*. The main process parameters are:

- Rotational speed,
- Duration of rotation or friction burn-off distance for direct drive processes,
- The moment of inertia of flywheel for inertia-drive processes, and
- Axial force.

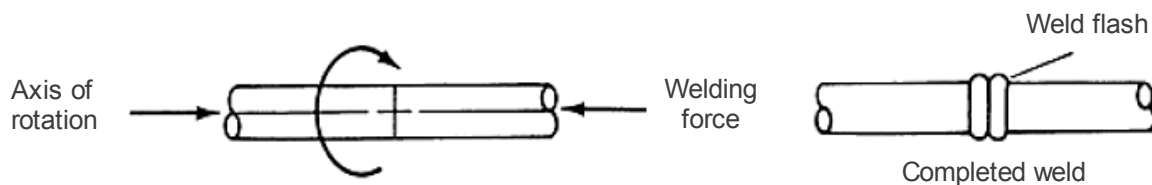


Figure 2-9: Principle of the orbital friction welding process [15]

Advantages of orbital friction welding include the excellent weld quality and reproductivity, with low requirements for operating personnel, as the process is highly mechanized. For large series of production, the FRW process is very cost-effective. Little preparation of workpieces prior to welding is needed, as FRW disrupts and removes surface films. Wide range of similar and dissimilar metal combinations are weldable and no filler material is required. Last but not least, no fumes, spatter or radiation are produced during welding process. The limitations of friction welding are that at least one part of the workpiece needs to be rotationally symmetrical and it must be of plastically deformable material.

Radial friction welding

Faced with the challenge, to successfully weld hollow sections, such as tubes or pipes, in 1975 a new FRW process, known as radial friction welding, was devel-

oped. The radial friction welding process adopts the principle of rotating and compressing a solid ring around two stationary pipe ends. The pipes to be welded are butted together and then securely clamped, to prevent axial and rotational movement. A solid, internally beveled ring of compatible material is positioned around the pipe ends with a supporting mandrel positioned inside the pipes at the weld position to prevent both the flow of metal into the bore and the collapse of the pipe ends. The ring is then rotated and subjected to radial compressive loading, in order to obtain the friction between the rubbing surfaces. After a predetermined heating duration, the ring rotation is terminated. The level of compressive load is then either maintained or increased to consolidate the bond. After the welding, the ring remains as a part of the weld [15].

Linear friction welding

Unlike the formerly described FRW processes, linear friction welding (LFW) uses linear motion to generate heat from friction. As one part is securely clamped and fixed stationary, the second is rubbed against it in an oscillating manner. As soon as the desired temperature has been reached, the oscillation is decayed to zero and the axial force is then increased in order to forge the workpiece together. As with FRW and radial friction welding, LFW welds usually expel a flash, which secures the quality of the weld, as contaminations are pushed outside of the weld. In recent years, the LFW process has been introduced in the production of aerospace engines. Gas turbine blades are attached to disks using the LFW process enabling longer life cycles, as well as lowering the overall weight of the construction [15].

2.2.2 Ultrasonic welding

Ultrasonic welding (USW) is a quasi-solid-state process that produces a weld by introducing high frequency vibration into the weld area, as it is held together by suitable clamping. The USW does not require any filler material and is commonly used for joining plastics and especially dissimilar materials.

An ultrasonic welding system consists of an ultrasonic stack, a fixture to hold the workpieces under pressure, a nest or anvil, where the parts are placed, an electronic ultrasonic generator, delivering a high power AC signal with frequency matching the resonance frequency of the stack, and a controller, which monitors and sets the movement of the press, as well as delivers the ultrasonic energy.

The weld is produced by oscillating shear forces at the interface between the workpieces. The resulting internal stresses cause elastoplastic deformation while the highly localized slip at the interface tends to break up oxides and surface films, permitting a metal-to-metal contact at many points. As the oscillation continues, the points are smoothened out and the contact area grows, enabling diffusion processes to take place. The finished weld has similar structure to that of a diffusion weld. USW is used for spot-, line-, seam-, and ring welds. The USW process has many advantages. The joining of thin and thick materials of dissimilar nature is possible. The weld preparation is fairly simple, because welding through the oxide layer is possible. USW joints generally have a good thermal and electrical conductivity. Ultrasonic welding is environmentally friendly, as it is energy efficient, and no arc, sparks, gases, or fumes are produced during the process. No filler material, or shielding atmosphere is needed. As the process is mechanized, the required skill level of the personnel is comparatively low.

The UWS process is relatively new, yet numerous applications in the automotive, electrical, aerospace, and military industries, exist [20].

2.2.3 Cold pressure welding

Cold pressure welding is carried out, entirely without the heating of the workpieces at ambient temperatures. As pressure is applied at the interface of the workpieces, severe deformation causes any residual oxides or contaminants to be expelled from the weld area. A metallic bond is created across the interface, producing the weld, without requiring any further recrystallisation or diffusion processes. For most cold pressure welding applications, degreasing and cleaning of the interface surfaces is needed, prior to welding. Cold pressure welding is

frequently used for welding nonferrous metals and is suitable for cold-formable metals with a brittle cover layer, such as aluminum. Cold pressure welding is an excellent method to join copper terminals to aluminum conductors, as fusion welding processes would produce brittle intermetallic compounds. Further dissimilar metal combinations include aluminum-titanium, aluminum-nickel, copper-titanium, copper-zinc, and many other. Different process variations of cold pressure welding exist, as welds can be carried out as lap or butt welds. Some applications involve cold pressure welding during drawing, extrusion, and rolling processes. In general, cold pressure welds are best examined by destructive techniques, as nondestructive testing methods fail to generate reliable results [15].

3 ALUMINUM AND ALUMINUM ALLOYS

3 ALUMINUM AND ALUMINUM ALLOYS

Aluminum is the third most abundant element and the most abundant metal in the earth's crust. The low density and ability to resist corrosion, as well as advances in the research of aluminum metallurgy, have made it the material of choice for uncountable applications, from the food container to aerospace industry. In the pure state, aluminum is a relatively soft, ductile, malleable metal, with an appearance ranging from silvery to dull gray. Its density and stiffness is approximately one third of the one of steel [21]. Further chemical and physical properties of pure aluminum are summarized in *Table 3-1*.

Properties of elementary aluminum			
Phase	Solid	Electrical resistivity (20°C)	28.2 nΩ·m
Density	2.7 g/cm ³	Thermal conductivity	237 W/(m·K)
Melting point	660.32 °C	Thermal expansion (25°C)	23.1 μm/(m·K)
Boiling point	2519 °C	Young's modulus	70 GPa
Heat of fusion	10.71 kJ/mol	Shear modulus	26 GPa
Heat of vaporisation	294.0 kJ/mol	Bulk modulus	76 GPa
Molar heat capacity	24.2 kJ/(mol·K)	Poisson ratio	0.35
Electronegativity Pauling	1.61	Mohs hardness	2.75
Crystal structure	Face-centered-cubic	Vickers hardness	167 MPa
Magnetic ordering	Paramagnetic	Brinell hardness	245 MPa

Table 3-1 Properties of elementary aluminum [9]

In the pure state, aluminum is too chemically reactive to occur in its native form. In the earth's crust it is found combined in over 270 minerals. The main ore, from which aluminum is extracted, is bauxite, which usually contains 40 to 60% of hydrated alumina, together with impurities, such as iron oxides, silica, and titania. Currently, China, Russia, Australia, Canada and the United States are among the major suppliers of primary aluminum. It is foreseeable, that high grade bauxite reserves will be depleted in near future, which will evoke the need for new refining methods, as well as increase the importance of recycling of this valuable commodity.

3.1 Production of Aluminum

Aluminum forms strong chemical bonds with oxygen. It is very difficult to extract from ore, due to the high reactivity and the high melting point of most of its ores. The first commercial preparation of Aluminum occurred in France, in 1855, when H. Sainte-Claire Deville reduced aluminum-chloride with sodium. However, this process was not efficient, as the purity of aluminum was below 95% and the huge costs of production made it more expensive than gold at that time. Due to its light weight and good mechanical performance, further investigations in the production of aluminum were made, and by the end of the century two subsequent processes, known as the Bayer- and Hall–Heroult process, were established. These production methods still are the only ones, used for aluminum smelting on an industrial scale today.

The first step of production, in which alumina (aluminum-oxide) is produced from bauxite, is known as the Bayer process. It was invented and patented by Karl Josef Bayer in Austria, in 1888. In the Bayer process, bauxite is crushed and digested in strong sodium hydroxide solution at temperatures as high as 240°C. Most of the alumina is dissolved, leaving an insoluble residue, known as 'red mud', which mainly comprises iron oxides and silica, and is removed by filtration. This first stage of the Bayer process can be expressed by equation (3.1):



In the second, decomposition stage, conditions are adjusted, so that the reaction is reversed, as can be seen in equation (3-2):



Decomposition is achieved by cooling the liquor to a temperature around 50°C and seeding it with crystals of the trihydrate $\text{Al}_2\text{O}_3 \cdot 3\text{H}_2\text{O}$, to promote precipitation. This step may take up to 30 hours, and afterwards the alumina is obtained by

calcining the trihydrate in rotatory kilns or fluidized beds. Calcination is carried out in two steps, with most of the water being removed, at temperatures between 400°C and 600°C. The product is alumina in the chemically more active γ -form. The alumina is then converted to the relatively inert α -alumina, at temperatures as high as 1200°C. The white, chemically inert powder is now ready for the next production step, known as the Hall–Heroult process.

Due to its high melting point and poor electrical conductivity, the key to a successful production of aluminum lies in dissolving the oxide in molten cryolite (Na_3AlF_6) and then running of an electrical current through the cryolite/alumina mixture. A direct current with a voltage of just 5.25 V and a very high amperage, around 250 kA, is needed. An electrolytic reduction cell is shown in the *Figure 3-1*. It consists

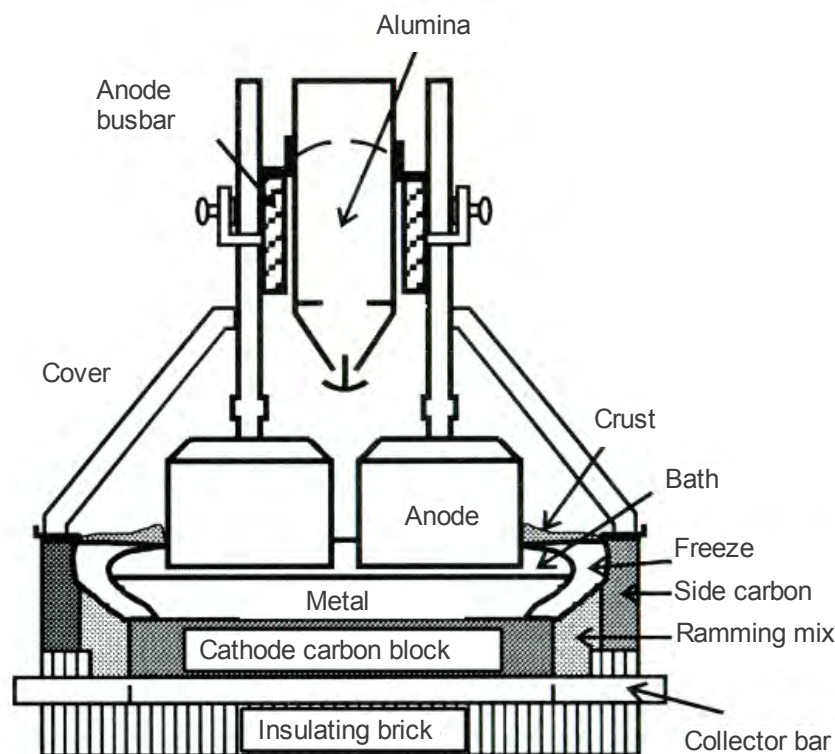


Figure 3-1: Hall-Heroult cell for production of Aluminum [22]

of consumable baked carbon anodes, the molten cryolite/alumina electrolyte, a pool of liquid aluminum, a carbon-lined container to hold the metal and a electro-

lyte- and gas collection system, to prevent fumes from the cell escaping into atmosphere [21]. The overall reaction can be summarized in the following equation (3.3):



Some 1800 kg of aluminum are produced by a single cell, on a daily basis. Usually around 150 cells are connected in a series, to make up a potline. The production of aluminum is very energy- and cost intensive, so alternative methods of aluminum production have been researched. A chloride-based smelting process was introduced by the US based company Alcoa, in 1976, with a potential to achieve 30% cost savings. However, it was discontinued after 10 years, as the aggressive chlorine, involved in the production process, proved to be too big a challenge for the construction materials, over a large period of time [21]. Several other companies have investigated carbothermic methods for producing aluminum with cost-saving potential, yet, no commercially viable process so far has been introduced on a industrial scale. The long range research efforts focus on increasing the current efficiency (currently at 95% in modern cells) and reducing the distance between the cathode and anode, which is the major component of ohmic resistance [23].

The secondary production of aluminum is a key factor to reduce costs, both for raw materials and especially energy. The production of one ton of aluminum from bauxite requires about 17.000 kWh of electricity. Modern state of the art cells achieve 13.000 kWh energy per ton [23]. The same amount of recycled aluminum consumes approximately 750 kWh, therefore, resulting in a net gain of 95% [24]. Even though some high performance aluminum alloys, still need pure aluminum as a source material, aluminum can be recycled repeatedly, without losing its mechanical properties [25]. Recycled aluminum offers obvious energy and environmental benefits, as it only requires 5 % of the energy consumed and emissions, associated with primary production [23].

3.2 Aluminum alloys

For most technical applications, pure aluminum is too soft to be of practical use, so instead, alloys are used. Most aluminum alloys contain 90% to 96% aluminum, with one or more other elements added, to provide a specific combination of properties and characteristics. The typical alloying elements are copper, magnesium, manganese, silicon and zinc. Two principal classifications of aluminum alloys exist namely the wrought aluminum alloys and cast aluminum alloys [26].

3.2.1 Wrought aluminum alloys

The term wrought aluminum alloys is applied to alloys, which are primarily produced in ingot or billet form and are further worked by other processes, such as rolling, extruding, forging, and drawing, in order to get semi-finished products [26].

The basic characteristics of wrought aluminum alloys are listed below:

- Corrosion resistance: Aluminum is very eager to react with oxygen in order to produce aluminum oxide according to the equation (3-4):



Even though, oxidation is usually an unwanted process, in aluminum a very thin oxide film is produced, which then provides a shield for further oxidation, without harming the material. This process is known as passivation [21]. Alloys of the 1xxx, 3xxx, 5xxx, and 6xxx systems are especially favorable in this respect.

- Thermal conductivity: Aluminum and its alloys are good conductors of heat and slowly reach high temperatures during fire exposure.
- Electrical conductivity: Pure aluminum and some aluminum alloys have an exceptionally high electrical conductivity.
- Strength to weight ratio: Its relatively high strength and low density has made aluminum the popular material, it is today. It is used for light weight

structures, especially for transportation means.

- Fracture toughness and energy absorption capacity: Some special alloys, such as 2124, 7050, and 7475, are exceptionally tough and make excellent choices for applications, where resistance to brittle fracture and unstable crack growth are necessary, such as in aircraft applications.
- Cryogenic toughness: Aluminum alloys of the 3xxx, 5xxx, and 6xxx series have the remarkable feature that their strength, ductility, and toughness are higher at subzero temperatures than at room temperature.
- Workability: Wrought aluminum alloys are workable by a great variety of metalworking technologies. This property enables aluminum to be produced in a wide range of geometries and shapes.
- Ease of joining: Soldering, brazing, welding, riveting, bolting, and even nailing are just a few possibilities to join of aluminum parts with aluminum or other materials. When joining aluminum to other materials, galvanic corrosion properties must be considered. Special care needs to be taken, when dealing with carbon fiber reinforced construction materials [27], and [28].
- Recyclability: Aluminum can be easily and efficiently recycled [9].

Among other standards, the Aluminum Alloy and Temper Designation System of the Aluminum Association is the most widely applied system for aluminum alloys. It enables the user to understand the chemical composition, characteristics, as well as the way, in which the alloy has been fabricated. The Aluminum Association Wrought Alloy Designation System uses four numerical digits, sometimes including alphabetical prefixes or suffixes [29]:

- The first digit defines the major alloying element of the series starting with that number (see *Table 3-2*).
- The second digit defines variations in the original basic alloy, which are typically defined by differences in one or more alloying elements of 0.15 – 0.50% or more. A zero indicates the original composition, a one the first

variation, and so forth.

- The third and fourth digits designate the specific alloy in the series.

Wrought aluminum alloy systems	
Alloy	Main alloying element
1xxx	Pure aluminum, no major additions
2xxx	Copper
3xxx	Manganese
4xxx	Silicon
5xxx	Magnesium
6xxx	Magnesium and silicone
7xxx	Zinc
8xxx	Other (iron, tin, titan,...)
9xxx	Unassigned

Table 3-2: Wrought aluminum alloying elements according to Aluminum Association [29]

- The 1xxx series are pure aluminum and its variations. The last two of the four digits indicate the minimum aluminum percentage, specified for the designation. The second digit indicates modifications in the impurity limits or intentionally added elements. Compositions of the 1xxx series do not respond to any solution heat treatment, but may be modestly strengthened by strain hardening.
- 2xxx series alloys have copper as their main alloying element and respond well to heat treatment, as copper is soluble in aluminum. The alloys of this series are often referred to as heat treatable.
- 3xxx series alloys are based on manganese and are strain hardenable. They do not respond to solution heat treatment.
- 4xxx series alloys are based on silicon. Depending on the silicon content, heat treatment may be applied.
- 5xxx series alloys are based on magnesium. Strain hardening is possible, while heat treatment is not.
- 6xxx series alloys, having both magnesium and silicon as their main alloying elements, are heat treatable. Magnesium silicide (Mg_2Si) will go in

3 ALUMINUM AND ALUMINUM ALLOYS

solid solution with aluminum.

- 7xxx series alloys have zinc as their main alloying element, often with significant amounts of other elements, such as copper and magnesium. The alloys of this series are heat treatable.
- 8xxx series alloys have other alloying elements, such as iron or tin in their composition. The characteristics largely depend on the major alloying component [26].

The chemical composition of selected wrought aluminum alloys according to the Aluminum Association Designation System is listed in the following *Table 3-3*.

Wrought aluminum alloys: percent of alloying elements Aluminum and normal impurities constitute remainder								
Alloy	Si	Cu	Mn	Mg	Cr	Ni	Zn	Ti
1050	99.50% min Aluminum			
1060	99.60% min Aluminum			
1100	...	0.12	99.0% min Aluminum			
1175	99.75% min Aluminum			
2014	0.8	4.4	0.8	0.5
2018	...	4.0	...	0.7	...	2.0
2124	...	4.4	0.6	1.5
3003	...	0.1	1.2
3105	...	0.6	0.5
4032	12.2	0.9	...	1.0	...	0.9
4145	10.0	4.0
5005	0.8
5056	0.1	5.0	0.1
5356	0.1	5.0	0.1	0.1
5556	0.1	5.1	0.1	0.1
5654	3.5	0.3	0.1
6003	0.7	1.2
6053	0.7	1.2	0.3
6101	0.5	0.6
6253	0.7	1.2	0.3	...	2.0	...
7008	1.0	0.2	...	5.0	...
7049	...	1.6	...	2.4	0.2	...	7.7	...
7178	...	2.0	...	2.8	0.2	...	6.8	...
7475	...	1.6	...	2.2	0.2	...	5.7	...
8017	...	0.2	...	0.0	...	*Iron 0.7		...
8030	...	0.2	*Boron 0.02		...

Table 3-3: Wrought aluminum alloys [28]

3.2.2 Cast aluminum alloys

The designation system for cast aluminum alloys is in some respect similar to the one for wrought aluminum alloys, yet some important differences exist. The cast alloy designation system has also four digits and the first digit indicates the major alloying constituent(s), as can be seen in *Table 3-4*. A decimal point is introduced between the third and fourth digit, to indicate that these are designations used to identify alloys in the form of castings and foundry ingot.

- The first digit indicates the alloy system, as shown in *Table 3-4*. Note that the 6xx.x series is designated as the unused series.
- The second and third digits for the 1xx.x series indicate the aluminum purity, and for the other alloys, they identify the specific alloy.
- The fourth digit indicates the product form: 0 is used for castings, 1 is used for ingots, and rarely a 2 indicates, that the use of tighter limits on certain impurities apply [26].

Cast aluminum alloying systems	
Alloy	Main alloying element
1xx.x	Pure Aluminum
2xx.x	Copper
3xx.x	Silicon, with added Copper and/or Magnesium
4xx.x	Silicon
5xx.x	Magnesium
7xx.x	Zinc
8xx.x	Tin
9xx.x	Other elements
0xx.x	Unassigned

Table 3-4: Cast aluminum alloying elements according to Aluminum Association [29]

The characteristics of the wrought aluminum alloys can also, generally, be applied to the cast alloys. The three following properties play an additional role, which determine the limits of cast aluminum alloy application:

- Ease of casting: The alloys of the 3xx.x series feature good flow and mold-filling capability, due to their high silicon content. Consequently, the alloys

of the 3xx.x series are chosen for large and very complex castings.

- **Strength:** The 2xx.x alloys offer the highest strength, which comes at the cost of ease of casting and usually lacks good surface characteristics. The alloys of the 2xx.x series are used in applications, where expert casting techniques can be applied and strength and toughness are a priority, such as in the aerospace industry.
- **Finish:** The 5xx.x, 7xx.x and 8xx.x series offer fine finish, but are more difficult to cast than the 3xx.x series. Their use is limited to applications, where surface quality is paramount [26].

3.3 Temper designations of aluminum alloys

Besides the chemical composition, it is the condition, which determines the mechanical properties of aluminum alloys. There are five basic designations, identified by a single letter, which may be followed by one or more numbers to identify the precise condition [26]:

- **F :** as fabricated. Applies to wrought products, where there is no special control of the amount of strain hardening or the thermal treatments. No mechanical properties are specified for this condition.
- **O :** annealed. This is used for products, which are annealed to produce the lowest strength (and improved ductility for cast alloys).
- **H :** strain hardened. Applies to products that have their strength increased through cold working. The H is always followed by two digits, which indicate the amount of cold working or a specific heat treatment.
- **W :** solution heat treated. This is applied to alloys, which precipitation-harden at room temperature (natural aging) after a solution heat treatment. It is followed by a time, indicating the natural aging period, e.g. W 1h.
- **T :** thermally treated. Applies to products, which are thermally treated to produce stable tempers, other than F, O or H. The 'T' is always followed by one or more numbers to indicate the specific heat treatment.

The following digit(s) after the letter represent the specific condition **[26]**:

- H1 : strain hardened only.
- H2 : strain hardened and partially annealed to reduce the strength back to the desired level.
- H3 : strain hardened and stabilized. Stabilization is a low temperature heat treatment, applied during or on completion of fabrication. Ductility is improved and unstable strain hardened alloys are artificially aged to a stable condition.
- H4 : strain hardened and painted or lacquered. This indicates a low-temperature heat treatment, as part of paint baking or adhesive curing operation.

A second digit after 'H' represents the amount of strain hardening in the alloy. The digit 8 as in 'HX8' is used for the hardest available temper, resulting from the most heavily cold worked condition. A temper with the designation 'HX4' has a strength halfway between the fully hard HX8 and the fully annealed condition, the 'HX2' halfway the strength between 'HX4' and fully annealed and so on.

The 'T' designations are applied to those alloys, which are age hardened, with the first digit identifying the condition **[26]**:

- T1 : cooled from elevated temperature shaping process and naturally aged to a substantially stable condition,
- T2 : cooled from elevated temperature shaping process, cold worked and naturally aged to a substantially stable condition,
- T3 : solution heat treated, cold worked and naturally aged to a substantially stable condition,
- T4 : solution heat treated and naturally aged to a substantially stable condition,
- T5 : cooled from elevated temperature shaping process and artificially aged,
- T6 : solution heat treated and artificially aged,

- T7 : solution heat treated and overaged or stabilized,
- T8 : solution heat treated, cold worked and artificially aged, and
- T9 : solution heat treated, artificially aged and cold worked.

3.4 Strengthening mechanisms for aluminum alloys

Five general strengthening mechanisms may be applied to aluminum and its alloys, namely grain size control, solid solution strengthening, second phase formation, strain hardening, and precipitation hardening [28].

3.4.1 Grain size control

The role of grain size control is not as essential for the general strength of aluminum alloys, as it is for reducing the risk of hot cracking during welding applications [28]. Generally, increased grain size leads to reduced yield- and ultimate tensile strength, as can be seen in *Figure 3-2*. The relationship between grain size and yield strength is described in the Hall-Petch equation (3-5):

$$\sigma_y = \sigma_0 + \frac{k_y}{\sqrt{d}} \quad (3-5)$$

with:

σ_y ...	actual yield strength
σ_0, k_y ...	metal constants
d ...	grain size

As grain growth occurs in the heat affected zone (HAZ), toughness and strength are reduced. Larger grains are also more subtle to hot cracking. To avoid this, titanium, zirconium, and scandium may be introduced in the base or filler material, acting as nuclei for a fine grain growth [26].

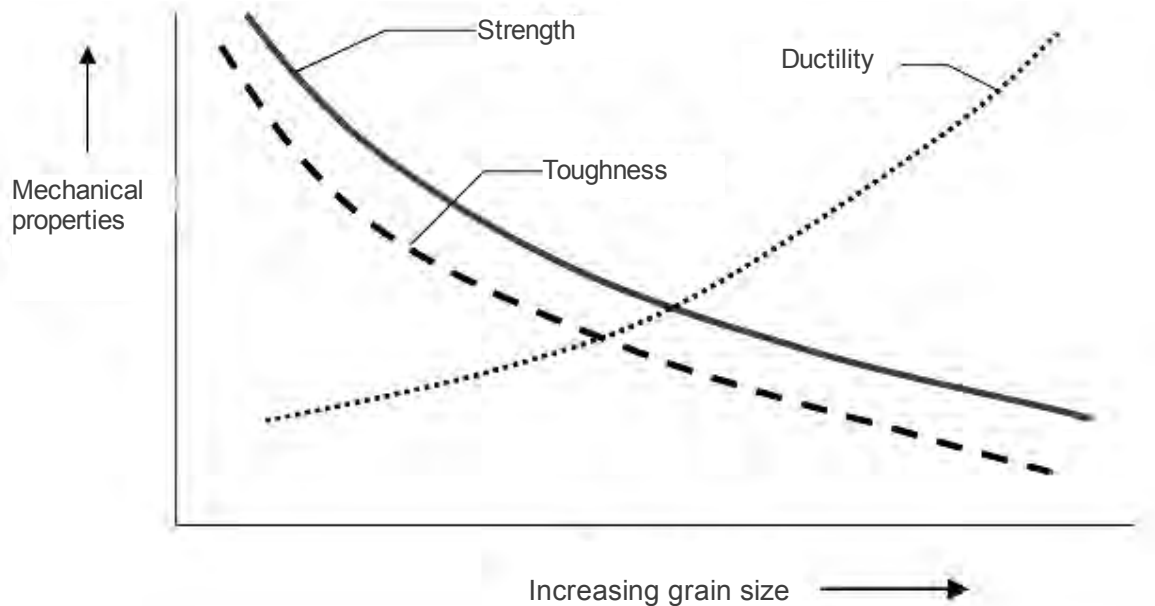


Figure 3-2: The influence of grain size on mechanical properties [26]

3.4.2 Solid solution strengthening

Metals in their pure state are very rarely used, as their strength is insufficient for the most engineering purposes, which is the reason, why they are alloyed. An alloy is a metallic solid, formed by dissolving in the liquid state, one or more solute metals – the alloying elements, in the bulk metal – the solvent [28]. A limit of solid solubility, which depends on the elements involved, exists and determines, whether the solution is homogeneous (single phase). If the solubility limit is reached, a second phase emerges. This second phase may be a secondary solid solution, an inter-metallic compound or the pure alloying element. In solid solution alloying, the alloy element is completely dissolved in the bulk metal and, depending on the ratio of the atom size of the elements involved, an alloying element may be an interstitial or a substitutional alloying element (see Figure 3-3) [30]. Both, the substitutional and interstitial, alloying atoms distort the lattice, due to atom size differences. The resulting strain increases the tensile strength, but reduces the ductility. The most important alloying elements for aluminum in this respect are si-licone, which increases strength and fluidity. Copper and

magnesium also improve

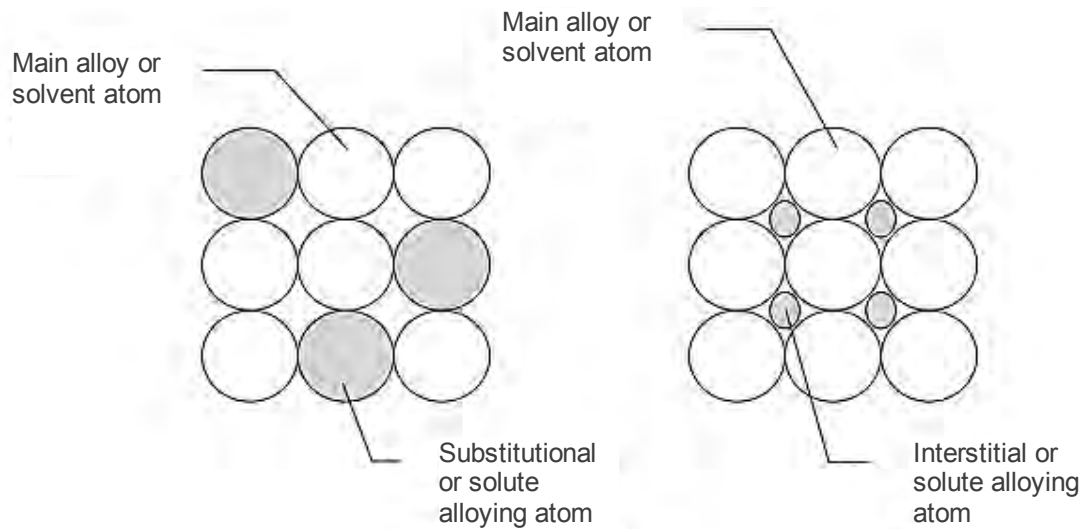


Figure 3-3: Substitutional and interstitial alloying elements [26]

corrosion resistance. Manganese increases the strength and ductility, whereas zinc assists in regaining some strength lost during welding [26].

3.4.3 Strain hardening

Also known as cold working, strain hardening is a mechanism, which increases the strength and hardness of metals. Deformation of the metal structure is provoked by input of mechanical energy during processes, such as forging or rolling, resulting in a stronger and harder metal, but a loss of ductility has to be accepted in most cases. The cold working can be done, until the metal has become so brittle that further additional deformation leads to fracture. Another side effect of strain hardening is the elongation and orientation of the grains, which leads to a high level of internal stress. Further effects include a small decrease in density, a decrease in electrical conductivity, an increase in the coefficient of thermal expansion and a decrease in corrosion resistance, particularly corrosion stress resistance [26].

A counter-mechanism of strain hardening can be achieved through heat treat-

ment. Depending on the temperature and heating time, it can provoke recovery, recrystallisation and grain growth. Recovery starts to take place at lower temperatures. The deformations and dislocations are reorganized, resulting in a reduction of the internal stresses, but retaining the original grain structure. If the temperature is elevated, recrystallisation begins. Recrystallisation is a process, during which the old cold worked and deformed grains are replaced by a new set of strain free crystals. An increase of ductility but a decrease in strength is observed. At temperatures, above the recrystallisation temperature, grain growth is initiated. The new grains begin to grow in size, by absorbing each other and resulting in a coarse grain structure, which is not desired regarding its mechanical properties and weldability.

3.4.4 Precipitation (age) hardening

Precipitation hardening is based on the principle of increased solubility of one phase into another at elevated temperatures. To precipitation harden an alloy, the temperature is raised, making the second phase go into solution. A rapid cooling of the metal, which can be achieved by quenching the alloy in water, oil bath or air, results into retention in solution. A metastable, super-saturated solution is obtained. A controlled heating to a low temperature of the metal then acts as activation energy for a diffusion process of the second phase. A very fine precipitate begins to form, resulting into a very distorted lattice with extremely high strength, but a poorer ductility. If the heating is continued, over-aging might take place. Over-aging is undesired, as the fine precipitate recrystallises back into coarse grain, matching the properties of the annealed structure.

A summary of mechanical properties for some aluminum alloys with varying condition is shown in *Table 3-5*.

Mechanical properties of aluminum alloys				
Alloy	Condition	R _{0.2}	R _m	ε
		[N/mm ²]	[N/mm ²]	[%]
1060	O	28	68	43
1060	H18	121	130	6
5083	O	155	260	14
5083	H34	255	325	5
6063	O	48	89	32
6063	TB (T4)	100	155	15
6063	TF (T6)	180	200	8
2024	O	75	186	20
2024	TB (T4)	323	468	20

Table 3-5: Mechanical properties of selected aluminum alloys [26]
 (R_{0.2} : proof strength; R_m : ultimate tensile strength; ε : maximum strain)

3.5 Problems associated with welding of aluminum

3.5.1 Porosity

Porosity in aluminum welds occurs, when hydrogen gas is entrapped during solidification of the molten pool. This is due to the solubility differences of hydrogen in aluminum in the liquid and the solid state. The solubility of hydrogen in aluminum is shown in *Figure 3-4*. Upon solidification, hydrogen forms gas bubbles in the molten pool, resulting in extremely fine pores, causing micro-porosity to coarse pores with a diameter of 3 – 4 mm. The porosity of an aluminum weld depends on the following factors:

- **Welding velocity:** If the solidification front is moving at a lower velocity than the pore's buoyancy velocity, gas pores may escape. Lower welding velocities result in slower solidification fronts and are beneficial for a pore-free weld.
- **Welding position:** In general, vertical up welding of aluminum produces the least porosity, as the solidifying pool provides easy escape of gas pores. Overhead welding produces the largest amount of pores as the gas bubbles are entrapped in the root weld.
- **Amount of hydrogen present:** Sources of hydrogen can be of different

origin. It can be present in the base metal, the filler metal or within the shielding gas. Regarding the filler material of the conventional fusion welding processes, TIG has lower levels of porosity than MIG, due to possible hydrogen contamination of the MIG wire. The shielding gas plays an important role, as for low porosity levels shielding gas with a high purity is to be used. Ideally, a gas with a low dew point, of less than -50°C (39 ppm water), should be used, guaranteeing low levels of moisture contamination. Another source of moisture can be porous gas hoses [28], and [31].

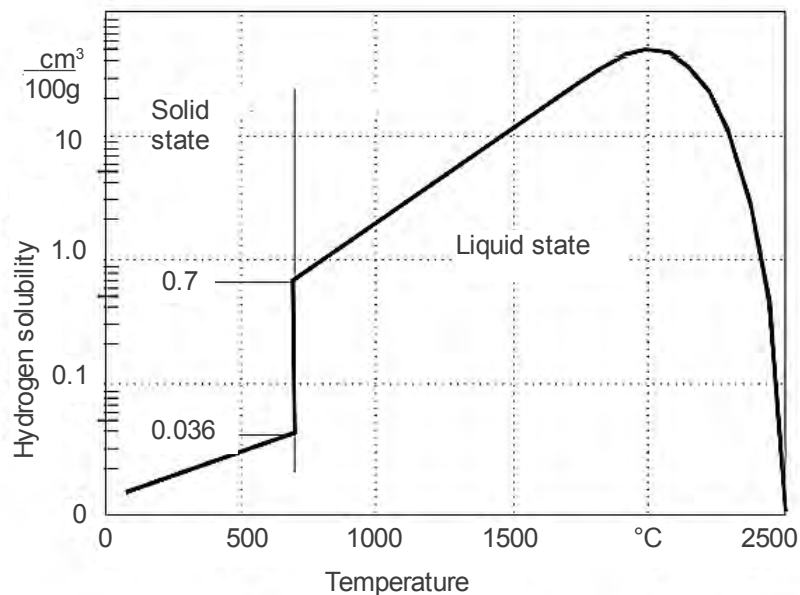


Figure 3-4: Hydrogen solubility in pure aluminum [19]

3.5.2 Crack Sensitivity during Welding

Due to aluminum's relatively high thermal expansion, large change in volume upon solidification, and wide solidification-temperature range weld cracking is a major issue, when welding aluminum and aluminum alloys. Because of the detrimental effect of weld cracks on joint properties, the weldability of aluminum alloys is defined as its resistance to weld cracking. Weld cracking in aluminum alloys may be classified into two primary categories based on the cracking mechanism

and location:

- Solidification cracking: Also known as hot tearing. It takes place within the weld fusion zone and typically appears along the center of the weld or at termination craters. These types of cracks occur, when high levels of thermal stress and solidification shrinkage are present, while the molten pool is undergoing the solidification process. Hot tearing is affected by weld-metal composition and welding parameters, such as heat input and the joint geometry. The primary method for eliminating hot tearing is through filler alloy additions, which are determined experimentally. The crack sensitivity of the AL-Mg system is shown in *Figure 3-5*. Another mean to reduce hot cracking is, obtaining a fine grain structure by adding titanium, zirconium, or scandium to the filler material. These act as forming nuclei for the new grains [28].
- Liquiation cracks: These occur adjacent to the fusion zone in the partially melted region. This region is produced, when eutectic phases or constituents with a lower melting point melt at grain boundaries during welding and, accompanied by thermal stresses, may tear. Higher heat input enlargens the partially melted region and increases the risk of liquiation cracks.

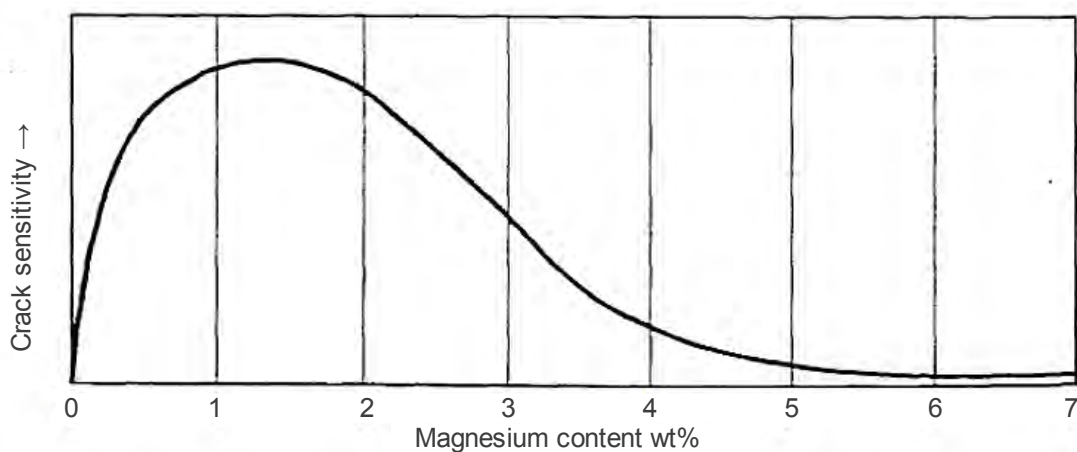


Figure 3-5: Crack sensitivity of Al-Mg alloys versus magnesium content [31]

3.5.3 Oxide film entrapment

Aluminum oxide (Al_2O_3) is a very tenacious, rapidly forming layer, acting as a shield to corrosion. The high melting point of Al_2O_3 (2060°C) compared to aluminum (660°C) cause difficulties for the welder, if the aluminum oxide layer is not removed, prior to welding, by mechanical, chemical or physical means. The molten aluminum is enclosed in a thin skin of oxide, which eventually bursts and ruins the weld. During welding, the strategies differ among the conventional welding processes. Processes using flux material, such as brazing or soldering, use a very aggressive flux, which is needed to dissolve the oxide layer. The flux material has to be thoroughly removed after welding, as corrosion and porosity might occur. The gas shielded welding processes, such as MIG, use the phenomenon of cathodic cleaning. Basically, this means, connecting the electrode to the positive pole and using direct current. The electrons flow from the workpiece to the electrode and ions travel the opposite direction, bombarding the workpiece surface, , breaking it up, and dispersing the oxide layer. TIG welding, however, uses alternating current with one half of the cycle used for oxide removal and the other for electrode cooling, as the positive pole generates 60 – 70% of the total heat [28].

3.5.4 Degradation of the heat affected zone (HAZ)

The heat affected zone (HAZ) is created during welding, adjacent to the fusion zone. Elevated temperatures can cause degradation of the material properties and are associated with micro-structural modifications of the base material. The impact of welding on the HAZ very much depends on the history of the material. The cold worked aluminum alloys experience a loss in strength, as recrystallisation begins to take place, when the temperature in the HAZ exceeds 200°C . Full annealing can be expected at 300°C . Within heat-treatable aluminum alloys, the HAZ can be distinguished, due to the dissolution or growth of precipitates. A common method for determining the width of the HAZ is measuring the hardness

3 ALUMINUM AND ALUMINUM ALLOYS

across the weld, which is proportional to the strength of the material [30]. The effect of welding on strength in a cold worked alloy can be seen in *Figure 3-7*.

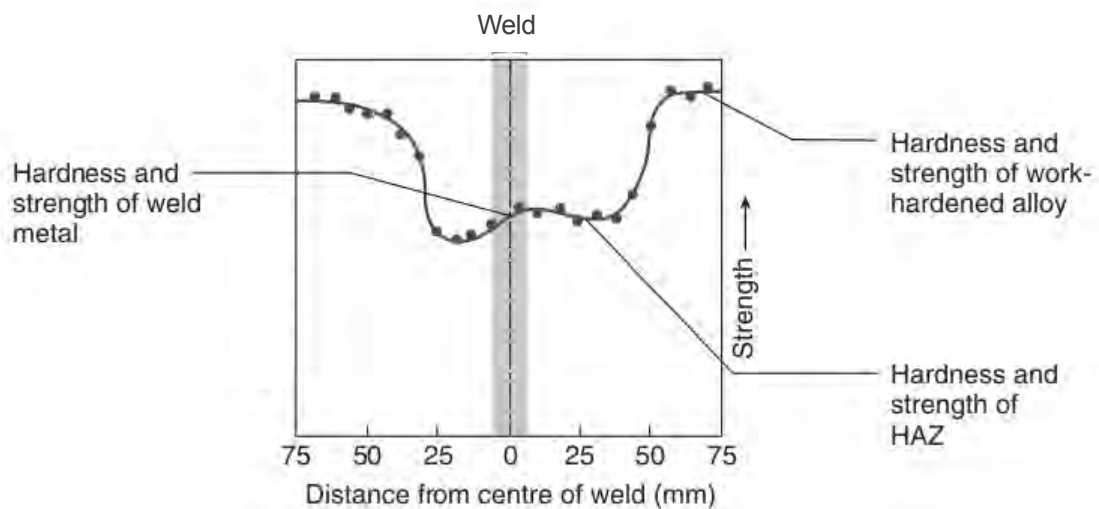


Figure 3-7: Effect of welding on strength in a cold worked alloy [28]

4 FRICTION STIR WELDING (FSW)

4 FRICTION STIR WELDING

4.1 Description of the friction stir welding process

Friction stir welding (FSW) is a solid-state process, of the non-fusion welding processes. Non-fusion welding can be defined as the process of joining materials through plastic deformation, due to the application of pressure, at temperatures below the melting point of the base material(s), with the assistance of solid-state diffusion. FSW was invented and developed at The Welding Institute (TWI) in Cambridge, UK. It allows metals, including aluminum, lead, magnesium, steel, and copper, to be welded without melting of the workpieces. Essentially, the pin of the rotating tool is plunged into the abutting faces of the workpieces, while the tool propagates along the joint generating frictional heat. The heat creates a softened, plasticized region around the immersed probe and at the interface between the shoulder of the tool and the workpiece. The shoulder provides additional frictional treatment of the workpiece and prevents plasticized material from being expelled from the weld region. As the temperature rises, the strength of the workpiece material falls below the shear stress. Plasticized material is extruded from the leading side to the trailing side of the tool. The tool is then steadily moved along the joint line, resulting in a continuous weld [32]. The basic principle of FSW is shown in *Figure 4-1*.

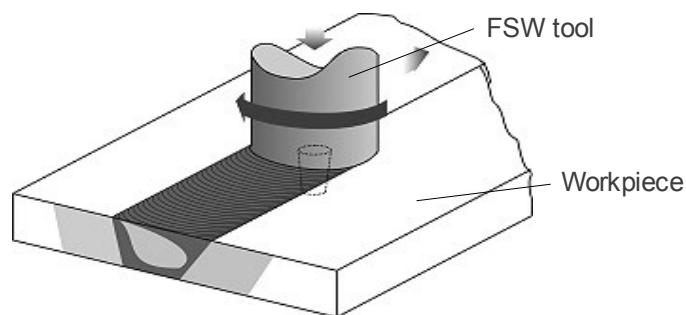


Figure 4-1 Principle of FSW [32]

4 FRICTION STIR WELDING (FSW)

The following lists the key advantages and disadvantages of the FSW process at present [32], [33], and [34]:

- Technological advantages:
 - The process is semi-automatic or fully automated, and is user friendly.
 - High integrity welds are produced for an increasing range of materials.
 - Welding can be carried out in all positions, including vertical and overhead position.
 - Plain low carbon steel and 12% chromium alloy steel can be welded in a single pass with thickness ranging from 3 to 12 mm. Steel with a thickness up to 25 mm can be welded from two sides.
 - The surface appearance approaches to that of a rough machined surface. Costs for post-processing and finishing are reduced.
 - No special edge preparation is required (only nominally square edged abutting plates are needed for a butt joint), so it saves consumable material, time, and money.
 - Distortion levels are comparatively low.
 - Equipment is simple with relatively low running costs.
 - Once established, optimized process conditions can be preset, and subsequent in-process monitoring can be used as a first line check of weld quality maintenance.
 - The workpiece can be loaded right after welding and is cooler in comparison to fusion weldments.
 - Like most friction techniques, FSW can be operated underwater.
- Metallurgical advantages:
 - The process is solid-phase. Problems, associated with the liquid phase, such as alloy segregation, porosity, and cracking, are avoided.
 - Welding of dissimilar alloys and materials is possible.
 - FSW results in fine, recrystallized microstructure.
 - Parent metal chemistry is retained without any gross segregation of al-

loying elements.

- No loss of alloying elements takes place.
- Environmental advantages:
 - Welding is carried out without spatter, ozone formation, or visual radiation, associated with fusion welding techniques.
 - Low energy input required: compared to a laser weld only around 2.5% of the energy is needed for a weld.
 - FSW is relatively quiet.
 - For most materials, the process does not require a shielding gas.
 - No harmful emissions are produced.
 - No solvents are needed for degreasing the workpieces.
 - FSW is associated with lightweight applications, leading to decreased fuel consumption in transportation applications.

Disadvantages:

- During welding, it is necessary to clamp and fix the workpieces materials firmly. Suitable jiggling and backing bars are needed to prevent the abutting plates moving apart, or material breaking out of the root of the joint.
- At the end of the weld a keyhole is left as the probe is withdrawn, which can serve as the starting point of crack propagation.
- The costs of the FSW equipment and licensing are relatively high.
- At present, no complete set of norms, covering the FSW specifications, exist in the EU, which is why the application of the FSW process is limited.

4.2 FSW variables

In order to achieve a weld that suffices the requirements set, certain parameters need to be looked at and inspected, during the FSW process. The joining of two parts involves the transport of material of one side to another. Regarding the specifications of the FSW process, the terms advancing side and retreating side have emerged. They describe the tool rotation direction, compared with the tool

travel direction (see *Figure 4-2*).

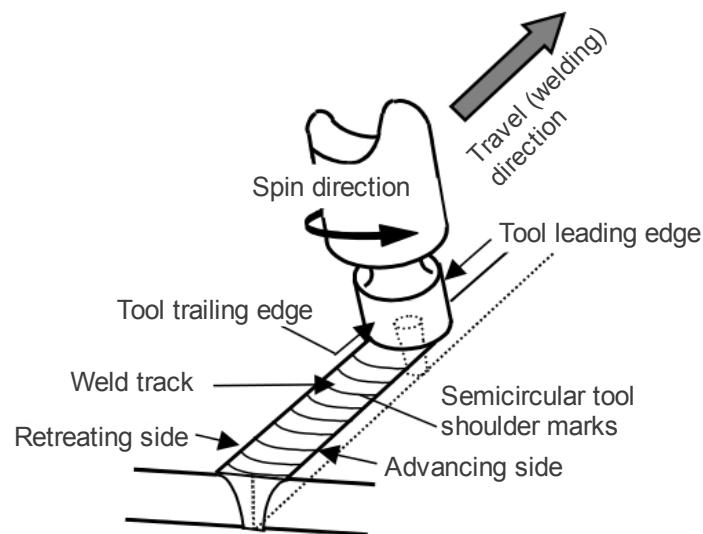


Figure 4-2: Schematic drawing and terminology of the FSW process [35]

The following parameters influence the FSW process [32]:

- Welding tool geometry and material,
- Welding velocity: can be split up in tool travel velocity and tool rotation (angular velocity),
- Tool tilt angle, and
- Downward force of the tool.

4.3 Friction stir tools

The FSW process is not possible without a non-consumable tool. The tool produces the thermo-mechanical energy and consists of a pin and a shoulder. Both can have a wide variety of geometries, optimized for the specific weld type. The typical sequence of steps, which a tool undergoes in order to produce a weld, are as follows: during the tool plunge, the rotating tool is forced into the workpiece. Contact of the pin with the workpiece creates frictional and deformational heating and softens the workpiece material. As soon as the shoulder touches the work-

piece, heat generation increases, and the zone of softened material expands. Typically the tool dwells (undergoes only rotational movement) at the starting point of the weld, in order to expand the softened volume of the workpiece. After the dwell period the tool begins the advance along the predetermined path, leaving a fine-grained recrystallized microstructure behind [32].

4.3.1 Tool materials

During the FSW process, the tool is loaded with a normal and a transversal force and its temperature approaches the solidus temperature of the workpiece. Regarding such conditions, the right selection of the tool material is essential, in order to produce a high quality weld. The tool material should have the following characteristics [32]:

- Ambient- and elevated-temperature strength: The tool material has to withstand the compressive loads during tool plunge, as well as it has to have sufficient compressive- and shear strength at elevated temperatures, to prevent tool fracture or distortion during the friction stir welding process.
- Elevated-temperature stability: The tool must maintain its dimensional and strength stability during the time of its use. Material creep has to be considered for long weld lengths. Tool materials that have been precipitation-, work- or transformation-hardened, experience a loss of their mechanical properties, if used above their maximum-use-temperatures. This is due to overaging, annealing, and recovery of dislocations or reversion to a weaker phase.
- Wear resistance: Excessive tool wear changes the tool shape, thus changing the weld quality and increasing the probability of defects. During the FSW process, tool wear can occur by adhesive, abrasive or chemical wear, or by a combination of those.
- Tool reactivity: Tool materials should be inert with the workpiece and the environment, in order to prevent a change of the surface properties of the tool. Especially, when welding titanium, which is reactive at elevated tem-

peratures, a shielding environment needs to be considered in order to prevent oxidation of the workpiece or the tool.

- Fracture toughness: The tool material should have sufficient fracture toughness, in order to withstand the loads during tool plunge and dwell time, which are considered to produce the most damage to the tool.
- Coefficient of thermal expansion: Especially, when using bi-metal tools, large differences of the coefficient of thermal expansion between the shoulder and pin material should be avoided, as elevated temperatures might cause internal stresses, which could lead to tool failure.
- Last but not least, the tool material should be machinable, in order to achieve the required or desired design.

At present, depending on the workpiece, different materials are used for FSW tooling. A summary of current friction stir welding tool materials is shown in *Table 4-1*. The most common tool material are tool steels. This is due to the fact that, at present most of the FSW welds are performed on aluminum and its alloys, which are easily friction stirred with tool steels. The advantages of tool steels include low cost, availability and machinability, as well as established material characteristics. The most cited tool material of the tool steel group is AISI H13, which is a chromium-molybdenum hot worked air-hardening steel, known for good elevated temperature strength and wear resistance. Besides welding aluminum alloys, tools made of H13 tool steel have proved themselves in friction stirring copper alloys. The maximum temperature of use of tool steels is between 500°C (oil- and water-hardened tool steels) and 600°C (secondary-hardened tool steels) [32].

The second group of tool materials are nickel- and cobalt-base alloys, which were developed to have high strength, ductility, creep resistance, and corrosion resistance. As these alloys derive their properties from precipitates, the temperature applied must be kept below the precipitation temperature, which typically lies between 600 and 800°C.

When stirring materials, such as titanium and steels, working temperatures above 1000°C occur and demand tool materials, which still perform well at such condi-

FSW tool materials		
Alloy	t [mm]	Tool material
Aluminum alloys	<12 <26	Tool steel, WC-Co MP159
Magnesium alloys	<6	Tool steel, WC
Copper and copper alloys	<50	Nickel alloys, PCBN tungsten alloys
	<11	Tool steel, WC
Titanium alloys	<6	Tungsten
Stainless steels	<6	PCBN, tungsten alloys
Low-alloy steel	<10	WC, PCBN
Nickel alloys	<6	PCBN

Table 4-1: Currently used FSW tool materials (t - thickness of the base material; WC – tungsten carbide; Co – cobalt; MP 159 – cobalt-nickel-based super alloy ; PCBN - polycrystalline cubic boron nitride) [32]

tions. Refractory metals including tungsten, molybdenum, niobium, and tantalum are used for their high-temperature capabilities. Many of these alloys are produced as a single phase, so strength is maintained to nearly melting point temperature. Disadvantages of refractory metals include high solubility of oxygen at elevated temperatures (especially for niobium and tantalum [32]), which quickly degrades ductility. Also, powder processing is the primary production method for refractory metals, which can result in density differences within the tool, leading to premature failure. Furthermore, high costs, limited material availability, and difficult machining limit the application of refractory metal tools.

A whole different group of FSW tool materials are the carbides and metal-matrix composites. Carbides, such as tungsten carbide (WC), offer superior wear resistance and reasonable fracture toughness at ambient temperatures and are often used as machining tools. Metal-matrix composites with TiC as the reinforcing phase are used for stirring copper alloys. However, the brittle nature of this material is reported to have caused fracture during the tool plunge [32].

Polycrystalline cubic boron nitride (PCBN) was originally developed for the machining of tool steels, cast irons and superalloys. The excellent properties of

PCBN have led to the introduction of this material for FSW tools, especially for high-temperature alloys. As the size of producible PCBN is limited, by the extremely high temperatures and pressures applied in the manufacturing process, PCBN is only used for the pin and the shoulder. The tool shank is made from tungsten carbide. Both phases are held together by a superalloy locking collar. Besides the high tool costs, the relatively low fracture toughness of PCBN demands for special care, when using PCBN tools. A spindle with low eccentricity is required to minimize tool fracture. Among other base materials, PBCN tools have been successfully applied in the welding of ferritic-, austenitic-, and dual-phase steels, nickel-base alloys, ultrafine-grained steels, as well as nitinol [32].

4.3.2 Tool geometry

Each of the friction tool parts (pin and shoulder) has a different function. Therefore, the best tool design may consist of the shoulder and pin constructed with different materials. When selecting the shoulder and pin design, workpiece and tool materials, joint configuration (butt or lap, plate or extrusion), welding parameters (tool rotation, travel speeds, and tool loading), and the user's own experience and preferences are factors to consider. New designs of FSW tools emerge constantly, as new applications and challenges drive the innovation [32].

Design of tool shoulder

Tool shoulder is designed to produce heat through friction and material deformation to the surface- and subsurface regions of the workpiece. The tool shoulder produces most of the frictional- and deformational heating in thin sheets, while the influence of the pin is increasing with the thickness of the workpieces. Furthermore, the shoulder produces the downward forging action necessary for weld consolidation. The first shoulder design was the concave shoulder, and still is the most common shoulder type, used in FSW applications. The simple design is easily machined, as a small angle, usually between 6° and 10°, is milled between the edge of the shoulder and pin. The cavity, which emerges from this design,

serves as a reservoir for the displaced material during tool plunge. Forward movement of the tool forces new material into the cavity of the shoulder, pushing the existing material into the flow of the pin. Proper operation of this shoulder design requires tilting the tool 2 to 4° from the normal of the workpiece, away from the direction of travel. The tool tilt is necessary, in order to maintain the material reservoir and enable the trailing edge of the shoulder to produce a compressive forging force upon the weld. When dealing with non-linear welds, a multi-axial FSW machine is needed to obtain satisfactory results at the turning points of the weld. For certain applications a convex shoulder geometry is preferred. The first attempts, using convex shaped tools, were not successful, as material was pushed away from the pin. The solution to this problem was achieved, as a scroll feature was added to the convex shape, which moves material from the outside of the shoulder towards the pin. The advantage of the convex shape is that the outer edge of the tool needs not be in contact with the workpiece. Thus, a sound weld is produced, when any part of the scroll is engaged with the workpiece, moving material toward the pin. This shoulder design allows for a larger flexibility in the contact area between the shoulder and workpiece, improves the joint mismatch tolerance, increases the ease of joining workpieces with different thickness, and improves the ability to weld complex curvatures. Depending on the application, a flat shoulder geometry is also possible, but similar aspects, as with the convex form, need to be taken into account [32].

For higher-quality FSW welds the shoulder may contain features in order to increase the amount of material deformation. Such features include scrolls, ridges, grooves or concentric circles and result in increased workpiece mixing (see *Figure 4-3* and *Figure 4-4*). The choice of the correct diameter of the shoulder is essential, as the shoulder generates most of the heat, and its grip on the plasticized materials establishes the material flow field. The heat is generated by both, sliding and slipping, while the material flow is caused only from sticking [32].

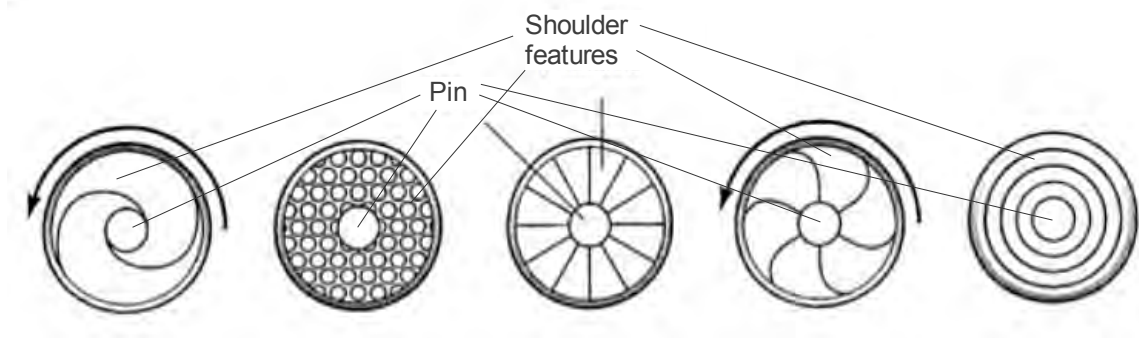


Figure 4-3: Different shoulder features used to improve material flow [32]

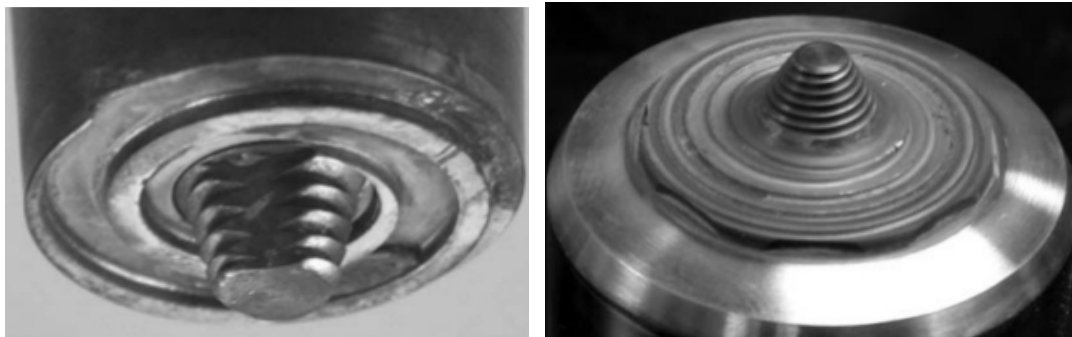


Figure 4-4: Scrolled shoulder tool on the left and convex shoulder with curved features on the right [32]

Experimental investigations have shown, that the sliding torque increases with the tool diameter, while the sticking torque experiences a maximum at a certain diameter, and then decreases, due to the decreasing flow stress with rising temperatures. Therefore an optimal shoulder diameter can be obtained by calculating the maximum torque [36].

Design of tool pin

Friction stirring pins are responsible for the heat generation within the workpiece along the joint surfaces. Additionally the pin is designed to disrupt the faying, or contacting, surfaces of the workpiece, shear material in front of the tool, and move material behind the tool. The design of the pin largely influences the depth of the deformation, as well as the achievable travel speed of the tool. The most simple pin design is a cylindric shape, yet in the original FSW patent by TWI a threaded

cylindrical pin was used. The threads are used for material transport from the shoulder down to the bottom of the pin [32]. A clockwise tool rotation requires left-handed threads and vice-versa. When operating under extreme conditions, such as high temperatures or highly abrasive composite alloys, the threads are subjected to excessive tool wear, so a threadless tool geometry with a simple design and robust features needs to be chosen. Furthermore, investigations have shown that a round or domed end of the pin reduces the tool wear during tool plunge and increases the quality of the weld root directly underneath the pin [32]. On the contrary a flat bottomed pin increases the ability of the pin to affect and deform the metal right underneath the pin, due to larger maximum velocity. Both designs are shown in *Figure 4-5*.

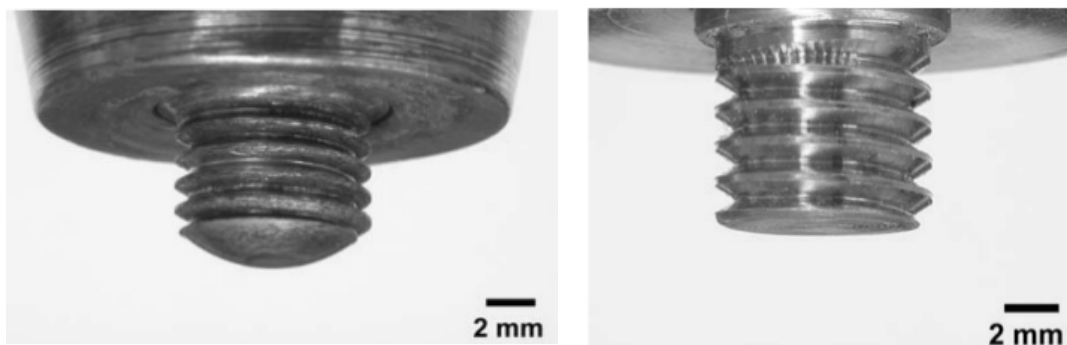


Figure 4-5: Cylindrical threaded pin with a round tip on the left and a flat tip on the right [32]

In order to increase the travel speed of the tool, as well as the thickness of weldable workpieces, truncated cone pins were introduced. When compared to a cylindrical pin, truncated cone pins have lower transverse loads, and the largest moment load on a truncated cone is at the base of the cone, where it is the strongest. A variation of the truncated pin is the stepped spiral pin (see *Figure 4-6*), which enables friction stir welding at elevated temperatures, where threaded pins suffered from excessive tool wear, and threadless tools do not produce sufficient material flow. A threaded design is not possible, when using ceramic tools, such as PCBN. A stepped spiral design offers a solution, in order to increase the volume of material deformed and moved by the pin, as the spiral steps

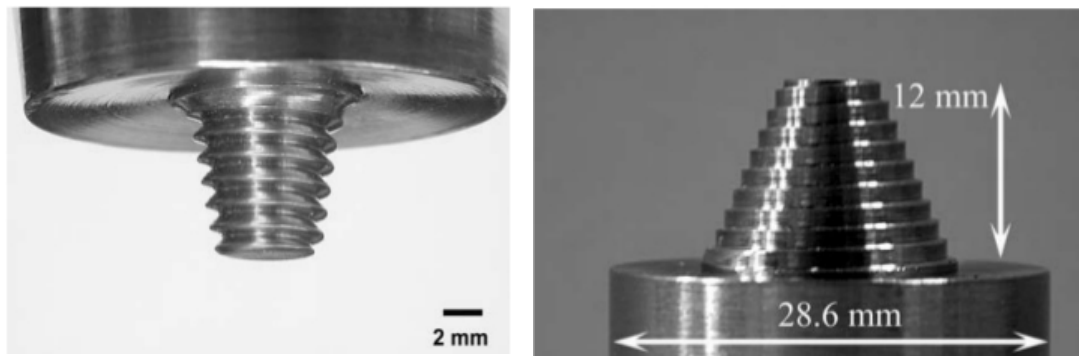


Figure 4-6: Threaded truncated cone pin with concave shoulder on the left, and a stepped spiral pin design on the right [32]

can be ground into the tool material. Further innovations in FSW tools include the addition of machined flats on the edges of the pin (see *Figure 4-8 a and 4-8 b*), which act as 'paddles' and create a local turbulent flow of the plasticized material, increasing the size of the weld nugget area. Further functions of the machined flats are reduced transversal and torque on the FSW tool. An extreme of this particular de-sign is the triangular tool, which can be seen in *Figure 4-8 c*.

The Whorl™ pin is the next generation of friction stir welding pin geometries. It reduces the displaced volume of a cylindrical pin of the same diameter by 60%. Reducing the displaced volume, decreases the trans-verse loads, which enables faster tool travel speeds. The downward material flow is achieved by the helical ridge, which is more effective than a thread (see *Figure 4-7*) [32].

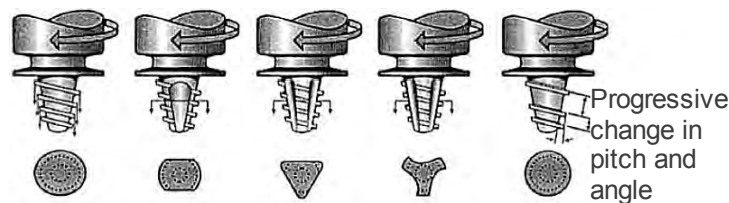


Figure 4-7: Variations of the Whorl™ pin [32]

New tool designs are introduced (and patented) constantly, so in this thesis only a fraction of them are presented. Aiming for higher welding speeds, scientists at the TWI used two-dimensional computational fluid dynamics simulations to examine material flow and to determine the profile that produced the minimum transversal

force. The result was the Trivex™ tool (see *Figure 4-8 d*). The Triflute™ (schematic drawing is shown in *Figure 4-8 f*) pin, also developed by the TWI, proved to be suitable for lap joint configuration, as the flow pattern around the bottom of the pin changes, improving the lap joint quality.

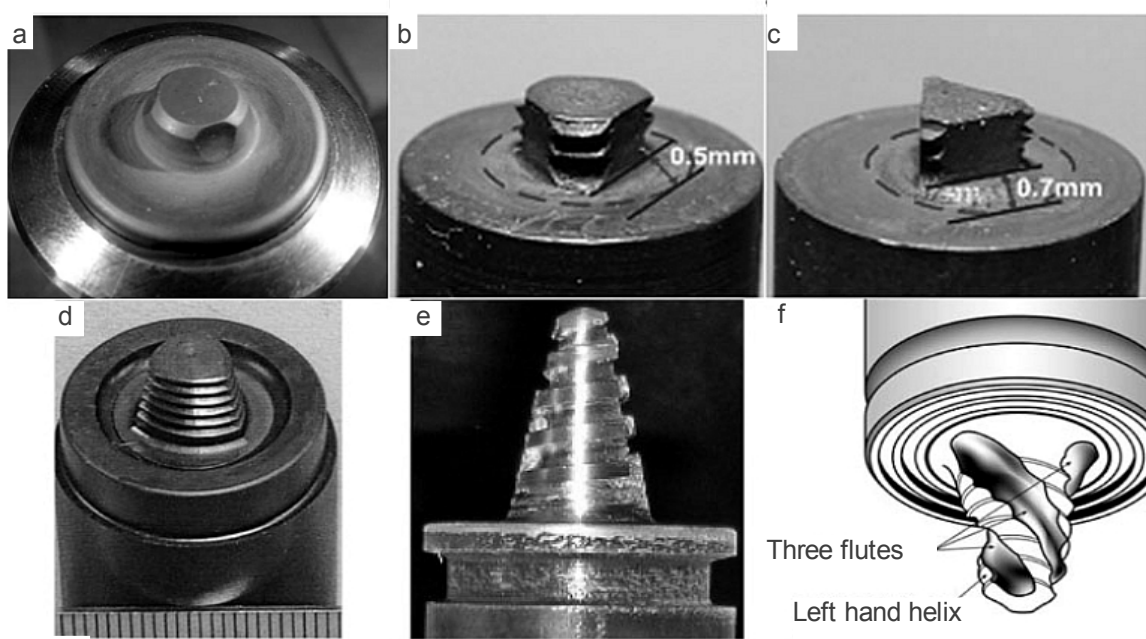


Figure 4-8: Commonly used tool pin geometries: a ... pin with machined flats; b ... three flat threaded; c ... triangular; d ... Trivex™; e ... threaded conical; e ... Triflute™ [36]

The pin length is determined by the workpiece thickness, the tool tilt, and the desired clearance between the tip of the pin and the bottom plate. The diameter of the pin needs to be sufficiently large to avoid failure by fracture, being subjected to the welding forces during tool plunge (axial pressure), rotation in the workpiece (torque), and transversal tool motion (transversal forces). On the contrary, the pin diameter needs to be sufficiently small to allow consolidation of the workpiece material behind the tool before the material cools. With increasing thickness the workpiece, less thermal energy from the shoulder-workpiece interaction is reaching the lower layer of the weld. Thus a larger pin diameter needs to be chosen. There is no such thing as a universal FSW tool, as different materials and process parameters demand specific tool designs [32].

4.3.3 Special tool designs

Complex motion tools

Recent research at TWI has focused on tools that increase the tool travel speed, the volume of material swept, and enhance the weld symmetry. The result of the investigation were the complex motion tools. Complex motion tools focus on tool motion, rather than on tool design, and mostly require specialized machinery or specially machined tools. As an example the Skew-Stir™ tool is shown in *Figure 4-9*. The axis of the pin is offset from the axis of the spindle, producing an orbital motion, and increasing the volume of material swept by pin-to-pin volume ratio. As a result, the weld nugget produced by the Skew-Stir™ tool is greater than the pin diameter.

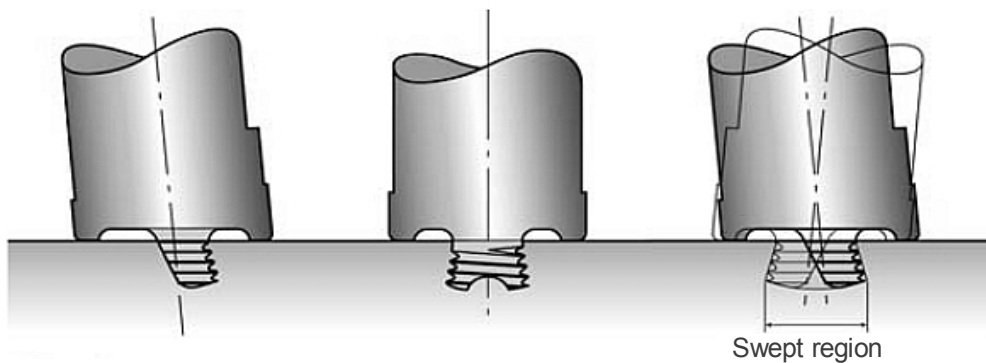


Figure 4-9: Principle of Skew-Stir™ FSW tool [37]

A symmetrical weld is achieved by using the Re-Stir™ tools. By constantly changing the tool rotation, alternating regions of advancing and retreating sides are achieved. Asymmetrical issues, such as lack of deformation on the retreating side, associated with rotatory FSW welds, are thus eliminated. The principle of this technology is shown in *Figure 4-10 [38]*. The Dual-Rotation™ tool allows different rotation speeds and directions of the tool shoulder and the pin. Using this technology enables to influence the thermal energy, induced by the shoulder and pin separately, as workpiece overheating due to too high shoulder velocity proved to be a problem within certain applications. In order to increase the speed and efficiency of the FSW process, variations, using two or more FSW tools simul-

taneously, have emerged. These tools can be arranged on the opposite (see *Figure 4-11* left) or same side of the workpiece, rotating in the same or different directions, and can be arranged in a parallel-, in-line- or overlapping direction. Counter-rotating tools reduce the forces needed to fix the workpieces, while parallelly arranged tools increase the material stirred, which is of significant importance for lap joints. Currently, the two-FSW-tool concept is being developed at TWI in several variations and is referred to as Twin-Stir™ (see *Figure 4-11* right) [37].

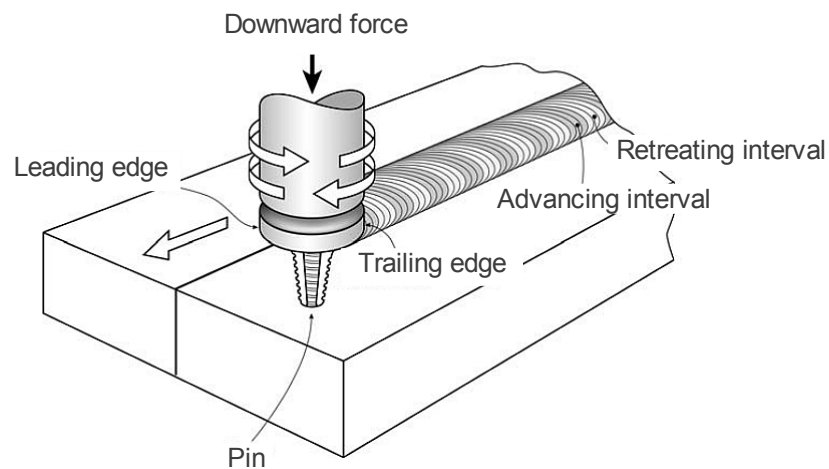


Figure 4-10: Principle of Re-Stir™ FSW tool [38]

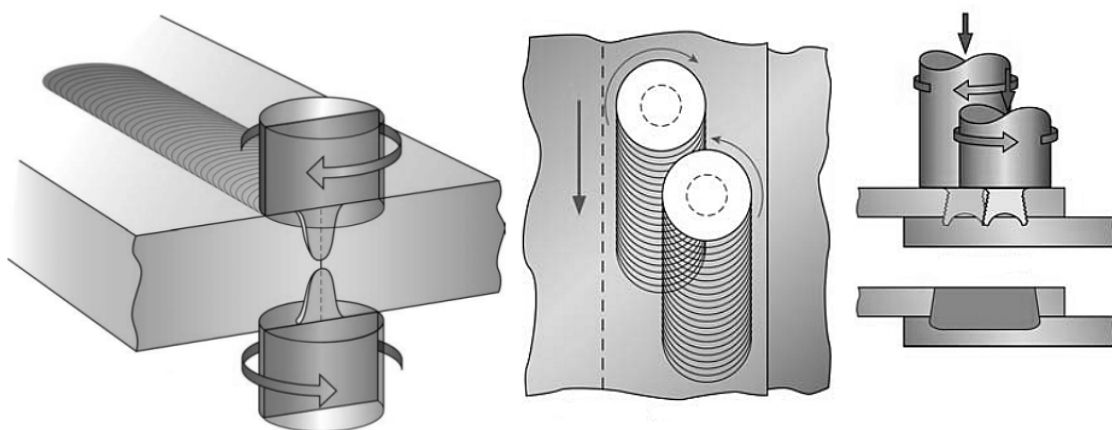


Figure 4-11: Principle of FSW using two tools: both-sided friction stir welding on the left and Twin-Stir™ technology, applied on lap joints, on the right [38]

Bobbin tools

Bobbin tools consist of two shoulders, one on the top surface and one on the bottom surface of the workpiece, connected by a pin, which is fully contained within the workpiece. The principle of the bobbin tool is shown in *Figure 4-12*. The main advantage of this tool is eased fixturing of the workpieces (no bottom-plate is needed), elimination of root flaws, and increased travel speeds, as the heat is generated by two shoulders. Two concepts of the bobbin tool have emerged. The first is a fixed shoulder-to-shoulder distance bobbin tool. In this design both shoulders and the pin are fixed to each other, and no relative movement is possible. Hence, a specific tool is needed for a specific application, and thermal stresses, occurring during welding, need to be taken into account, in order to prevent tool fracture. When using the fixed shoulder-to-shoulder distance tool, convex and scrolled shoulders are necessary, so the tool needs not to be tilted. The second concept is the retractable pin technology. The second shoulder is attached to the retractable pin, and the bottom shoulder is drawn toward the top shoulder, until the desired downward force is reached. When using the bobbin tool technology, the heat cannot escape as easily, as using conventional FSW tools, where the bottom plate acts as a heat sink. Also, the forging forces need to be less than with conventional FSW tools [32].

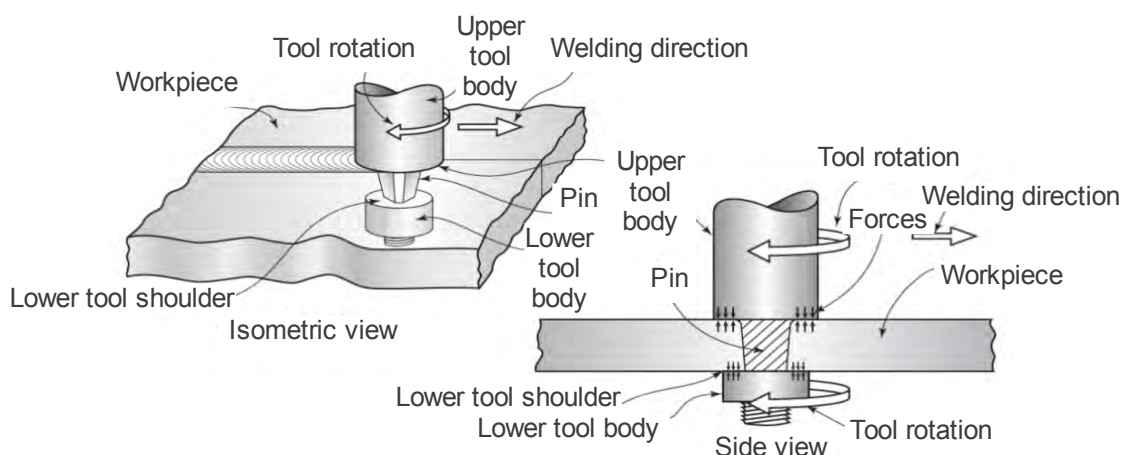


Figure 4-12: Principle of the bobbin tool technology [39]

Retractable pin tools

As with the Dual-Rotation™ tool, the retractable pin tool also consists of a shoulder and pin that can move relatively to each other. The main function of this tool configuration is to adjust the pin length during the friction stir process. This enables to retract the pin, at a prescribed rate, in order to close the exit hole, which is at the end of each conventional FSW weld. The exit hole proves to be the weakest part of the weld at certain applications. Another feature is the possibility to control and ensure full penetration welds, in workpieces with known thickness variations. A schematic overview of this technology is depicted in *Figure 4-13*.

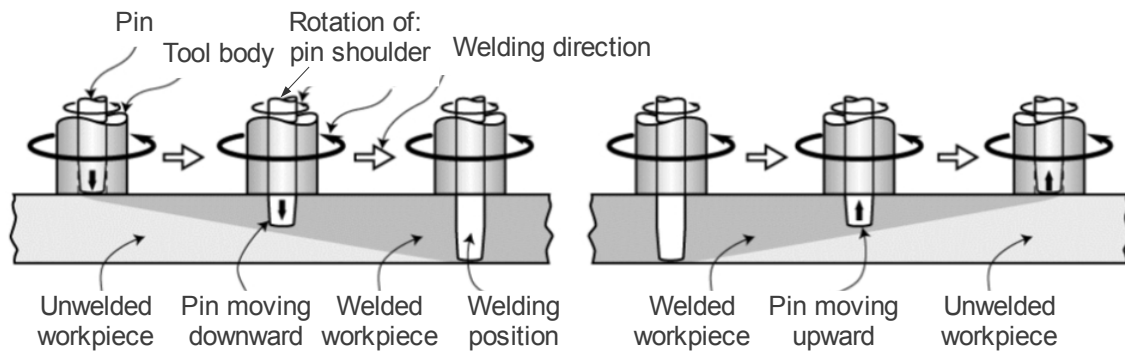


Figure 4-13: Retractable Pin tool [39]

4.4 Influence of FSW welding parameters

Friction stir welding presents a multiphysics modeling challenge. Closely coupled heat flow characteristics, plastic deformation at high temperatures, as well as microstructure and property evolution contribute to the processability of a material and to the subsequent properties of the weld. During the early stages of development, the main focus of FSW studies was on the heat generation from the tool into the workpiece. As the FSW tools evolved, increased attention was given to the metal flow properties of the various configurations. At present numerical methods dominate the research field, due to the power and ease of use of modern workstations [32].

4 FRICTION STIR WELDING (FSW)

In order to understand the basics of the FSW process, equation (4.1) expresses a value for welding energy per length unit. Welding energy per weld length is a value, which is widely used for process analysis of conventional welding methods, such as arc welding. Equation (4.1) includes all important FSW parameters, such as the tool geometry, welding velocity and the downward force. When using suitable machinery, these parameters can be adjusted, measured, and serve as the main reference, when welding specifications are introduced [39]. The equation is applicable for simple tools with a cylindrical pin geometry.

$$E^w = \frac{4}{3} \frac{\pi \times r_s \times n \times F_z}{v} \times \mu \times \left(1 + 3 \times \left(\frac{r_p^2 \times l_p}{r_s^3}\right)\right) \quad (4.1)$$

with:

E^w ... Welding energy

r_s ... Radius of tool shoulder

n ... Rotation per minute

F_z ... Downward force

v ... Advance speed [m/min]

μ ... Coefficient of friction between tool and workpieces

r_p ... Radius of pin

l_p ... Length of pin

Several studies have examined the effects of variation of welding parameters on the mechanical properties of the finished welds. The results show that the welding energy has a major impact upon the quality of the weld. Yet it is not possible to specify any general limits on the welding velocity or the downward force, as the effects vary among the different material groups. Within the material groups major differences occur among the different alloy systems. Among similar alloys, the history of the material also has an impact on the effect of the mechanical properties of the finished weld [32]. This is due to the specific nature of each material, which is unique in its chemical composition and treatment history, which, when subjected to FSW processing, may undergo microstructural changes, such as annealing, hardening, solution-strengthening, and other. On general terms, the welding energy has to be sufficiently high, as to produce a sound weld, yet not too high in order to prevent local material melting.

4.5 Microstructure of FSW welds

For all material types, the microstructure has three distinct zones, which result from the FSW welding process. The area, which contains all three zones and is modified by the stirring, is called the weld affected zone (WAZ). The center of the weld seam is the dynamically recrystallized zone (DXZ), and, due to its round shape and layer-like structure, often is referred to as the weld nugget. This zone is bordered on both sides by the thermo-mechanically affected zone (TMAZ) and the heat affected zone (HAZ). The WAZ with its constituents is shown in *Figure 4-14*.

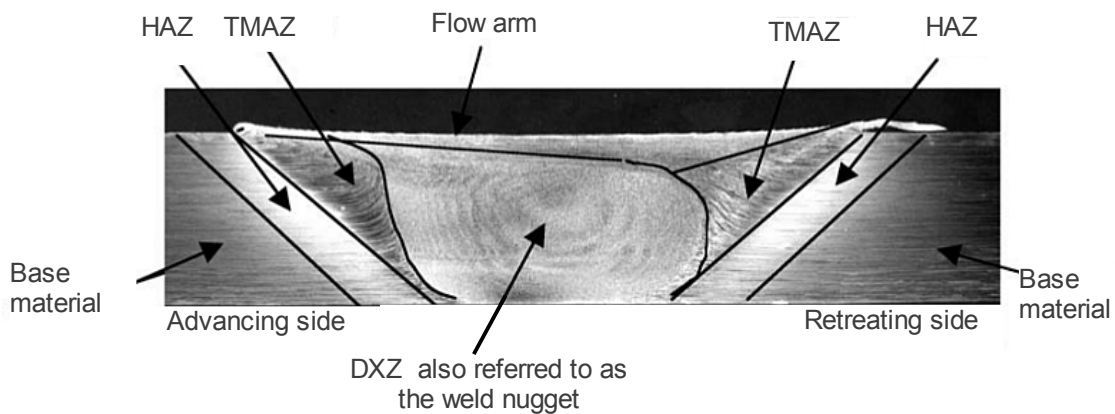


Figure 4-14: Macroscopic view of weld affected zones [32]
(HAZ: heat affected zone; TMAZ: thermo-mechanically affected zone;
DXZ: dynamically recrystallized zone)

Dynamically recrystallized zone (DXZ)

The DXZ is directly affected by the stirring action of the revolving pin. The extreme strain and elevated temperature cause recrystallisation of the weld material and result in fine, equiaxed grains in this area. Low stirring results in less dynamic recrystallization and, therefore, larger grains. Excessive stirring may also cause large grains, due to grain growth. Depending on the material, the DXZ can have properties that differ from the base material. Due to the elevated temperatures, secondary phases may occur, as solution-strengthened alloys may dissolve the strengthening particles. Generally, a fine grain structure is preferred, due to its superior mechanical properties [32].

Thermo-mechanically affected zone (TMAZ)

The TMAZ is subjected to severe plastic deformation, as well as elevated temperatures. Recrystallization does not occur, however the resulting grains differ from the base material, due to the deformation by the FSW tool. The temperatures can be high enough, as to dissolve precipitates, and thus weaken this particular area of the weld [32].

Heat affected zone (HAZ)

The HAZ is not plastically deformed, but is still affected by the thermal energy of the FSW process. Precipitation strengthened alloys might experience a degradation of their mechanical properties, due to overaging. The size of the HAZ depends on the total thermal energy input into the workpiece and can be measured using thermocouples to mark temperature boundaries [32].

4.6 Possible welding flaws during FSW process

If the welding parameters are not set correctly, welding flaws are indispensable. Welding flaws can be of purely optical nature (surface finish) or flaws that deteriorate the weld performance (such as cracks). For industrial application, it is important to analyze the occurring welding flaws, detect their origin, and adjust the welding parameters accordingly to avoid them. Following is a summary of welding flaws that can be found in friction stir welded joints [40].

Voids

Voids are hollows that occur on the advancing side, at the edge of the weld nugget. Voids often occur directly beneath the surface of the weld, which makes them particularly dangerous, as they cannot be detected by visual testing. The hollow represents a weak point of the weld and can cause failure due to strain peaks. Possible causes for voids are insufficient welding force or a momentary variation of the downward force during welding. Voids are also the result of an excessively high advance speed, which prevents sufficient material flow. A third possible

cause for voids is the failure of workpiece clamping. If the plates are not clamped close enough together or slip apart during welding process, hollows may occur [40]. A surface breaking void, which was caused by insufficient clamping, is shown in *Figure 4-15*.

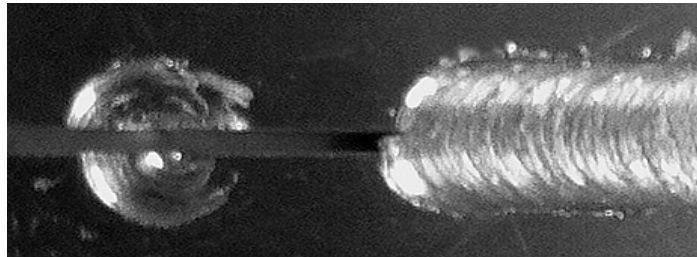


Figure 4-15: Void caused by insufficient clamping

Joint line remnants

Joint line remnants are produced, when the oxide layer is not removed prior to welding. The result is finely dispersed oxide particles along a wave-like path around the center of the seam. Joint line remnants cannot be detected by non destructive testing methods and can serve as the starting points of crack propagation. Even tough studies show that the mechanical properties are only slightly affected by joint line remnants, thorough machining of workpieces is advised, to avoid these. Excessive welding speed and tool shoulder diameter may also be the cause of this kind of welding flaw [40]. An example of a joint line remnant in a FSW weld of AW5754 is shown in *Figure 4-16*.



Figure 4-16: Joint line remnant in an FSW weld

Root flaws

A root flaw is the result of insufficient penetration or misalignment of the FSW tool. Root flaws occur at the root of the weld and run into the weld nugget. Similarly to joint line remnants, root flaws are very hard to detect with NDT methods and are dangerous, as they serve as starting points for crack initiation. The main reason for root flaws is the use of a too short tool pin or incorrect tool plunge depth adjustment. As a result the tensile strength is reduced, as well as a loss in fatigue strength is observed. The best method to detect root flaws is a destructive bend test with the root on the tension side [40].

4.7 Applications of FSW

Ever since its introduction in 1991, FSW has evolved rapidly and is used in various applications. An overview of the possible joint types is shown in *Table 4-2*.

FSW in maritime applications

The first commercial application of the FSW process was introduced in 1995 by Marine Aluminum, Norway. FSW welds were applied on 6xxx aluminum extrusions to make large panels for decking of fast ferries [10]. The cost per mass of material rises and the tolerance quality decreases with increasing size of the extrusion [41]. FSW process allows smaller extrusions to be joined to generate larger extrusions, resulting in lower distortion rates, and the ability to prefabricate the panels outside the shipyard. This reduces the required amount of manual arc welding, saves labor costs, decreases fume pollution in the shipyard, and enables faster ship production rates. Also the smooth surface of the root side of the weld eliminates post-treatment to surfaces, which are exposed to view [42].

FSW in the aeronautic industry

The first company to implement FSW in aeronautic industry was Boeing. They used this process for their Delta II and Delta IV space launch vehicles, to apply longitudinal and circumferential welds to the fuel tanks. In 1993, NASA challenged

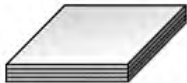
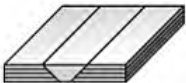
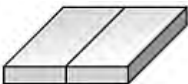
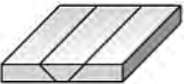
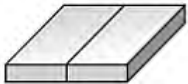
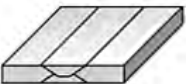


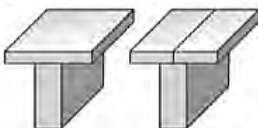

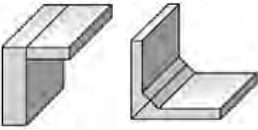
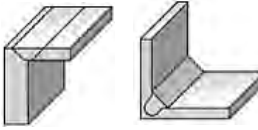


Various weld joint designs possible using the FSW process		
Joint type	Before welding	After welding
Lap joint		
Butt joint single pass		
Butt joint double pass		
Combination of a butt joint and lap joint		
T-joint		
Corner joint		
But joint performed on a tube		

Table 4-2: Various examples of weld joint designs before and after FSW processing [08627]

the Lockheed Martin Laboratories to find a better performing alloy for the external fuel tanks of the Space Shuttle program. The solution was found in the aluminum-lithium alloy Al-Li 2195, which proved to be unweldable with fusion welding techniques. The use of FSW resulted in a net weight loss of 3.402 kg and proved to produce stronger joints than previous fusion arc welded joints. The first friction stir welded tank flew into space in 2009, and further research was done to implement the process in the next generation spacecraft [1]. Eclipse Aviation used

FSW lap welds to replace riveting, for joining longitudinal and circumferential internal stiffeners to the aft fuselage section of their Eclipse 500 business-class jet. With welding speeds exceeding 0.5 m per minute, the FSW technology reduced the production cycle time significantly and resulted in lighter and stronger welds [32].

FSW in the automotive industry

Ford Motor introduced FSW in several thousand Ford GT cars, where FSW welds ensured a rigid and stiff assembly of the central tunnel. An improved dimensional accuracy, as well as 30% stronger joints, compared to GMAW were achieved. Mazda used friction stir spot welding technology for the rear door structure for the Mazda RX-8 model. Production costs were reduced significantly, and since 2003 more than 100.000 vehicles were manufactured using this technique [32]. The Japanese company Hitachi applied FSW welds in their new high speed A-Train concept, using aluminum extrusions to form a double skin vehicle car body. The aluminum extrusions were joined by the FSW process resulting in smaller distortion rates, stronger joints and remarkably increased fracture strength, compared with the previously used MIG technology [43] and [44]. FSW has gained importance in the production of tailored blanks, which nowadays are increasingly used in the automotive industry. A tailored blank is a sheet of steel or aluminum, that combines several alloy types with various thicknesses, different coatings or a combination of the former. The different constituents can be joined using the FSW process [41], and [45].

Other FSW applications and future outlook

In 2004, MegaStir Inc. completed a prototype oil field pipeline FSW demonstration program. X-65 steel pipe segments with a diameter of 32 cm and a wall thickness of 6 mm, were successfully joined using an automated internal mandrel and an external FSW tooling system [46]. Other research groups have produced full-thickness, single-pass welds in 19.1 mm thick steel, with portable machines being

developed for field applications **[47]**. The implementation of the FSW process in the pipeline construction still awaits ASME qualification requirements, before it can be used in field operations. FSW applications have been also considered in the nuclear energy field. Nuclear fuel plates, consisting of an low enriched uranium in monolithic uranium-molybdenum alloy plates, coated with an aluminum 6061-T6 alloy, can be bonded together using FSW technology **[48]**.

5 LASER HYBRID WELDING

5 LASER HYBRID WELDING

Laser-hybrid welding (LHW) combines a high-energy laser beam with a conventional GMAW process, usually MIG, to create an optimal welding pool. The main function of the laser is to provide deep weld penetration and stabilize the GMAW arc, by the means of cathodic stabilization. The GMAW process provides filler material and excellent gap-bridging capability, which is a major shortcoming of LBW processes. Combining the laser and the GMAW process results in advantages, such as higher welding speeds, lower distortion rates, and single-pass welding of large thicknesses [15]. A hybrid welding head, developed by Fronius International, can be seen in *Figure 5.1*.

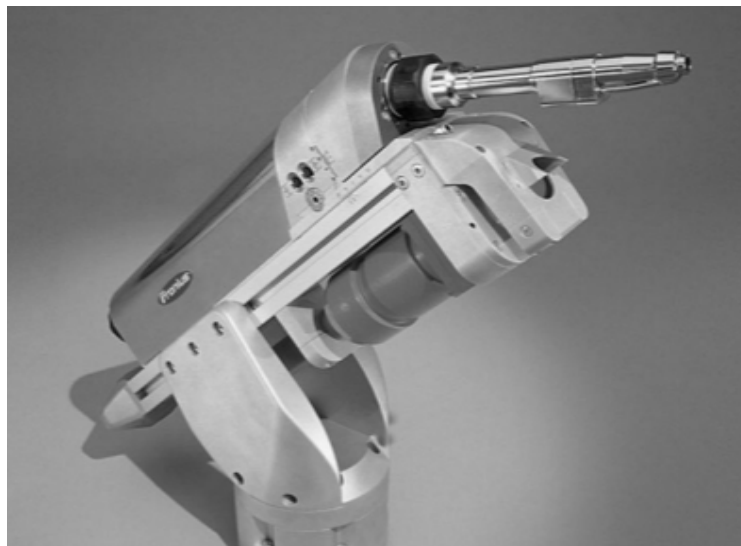


Figure 5.1: A LHW welding head developed by Fronius International [49]

5.1 LHW process

Along with a MIG or MAG welding torch, a laser head is introduced either ahead or behind the torch. The CO₂ laser and the Nd:YAG laser are the most commonly used lasers for LHW applications. A schematic view of the LHW process can be seen in *Figure 5.2*.

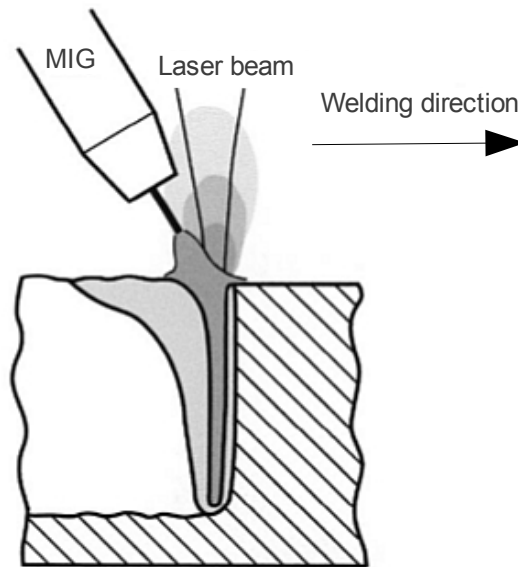


Figure 5.2: Schematic view of laser-hybrid welding process [15]

The CO₂ laser

The CO₂ laser generates its light in a tube, through which a mixture of gases, including CO₂ flows, producing a wavelength of 10.6 μm . The energy input is achieved by means of an electric discharge through the gas. It can produce a high power output and, therefore, is popular for welding and cutting applications. The light is usually conveyed to the welding head and focused by mirrors. A shielding gas, usually helium, is used to protect the lens and the weld. It helps to control the amount of energy-absorbing plasma, formed above the surface of the joint.

CO₂ lasers, available today, have much higher powers than Nd:YAG lasers. As welding speed is proportional to output power, CO₂ lasers offer higher welding speeds. However, one problem is that a considerable portion of the beam energy is reflected by certain materials, which makes laser-welding of aluminum, magnesium, and copper rather difficult [15].

The Nd:YAG laser

The active substance in this laser is neodymium. It is provided in the form of a dopant in a transparent rod of yttrium aluminum garnet. The energy is supplied by

a flash tube as can be seen in *Figure 5.3*. The light output wavelength is $1.06\ \mu\text{m}$, which is considerably shorter than that of the CO_2 laser, but still within the invisible infra-red section of the spectrum. An important difference is that the shorter wavelength enables the light to be carried by fiber optics, and focused with ordinary lenses. This enables the use the laser for robot welding. Nd:YAG laser is particularly suitable for welding otherwise poorly weldable materials, such as tantalum, titanium, and zirconium. The main drawback of the laser is that it is not available with such high power outputs, as the CO_2 laser, and so tends to be limited to metal thicknesses up to 6 mm [15].

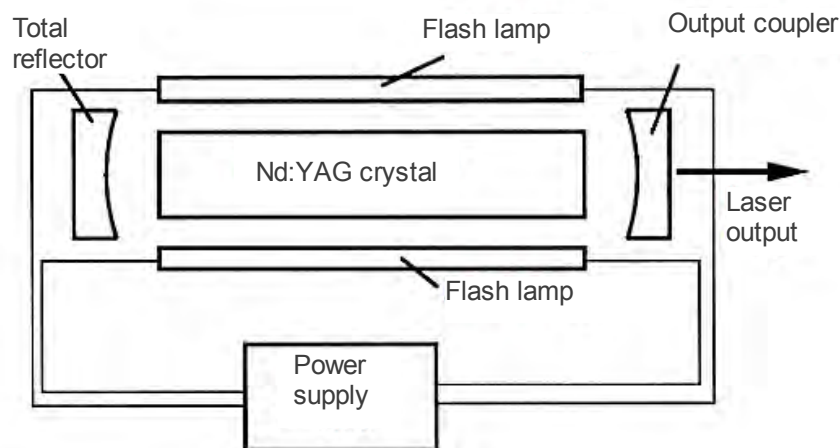


Figure 5.3: The functional principle of the Nd:YAG laser [2]

5.1.1 LHW process parameters

Laser power

Nowadays, the power of lasers is in the range of 5-10 kW (25 kW for certain applications) for CO_2 lasers, and 0.3-3 kW for Nd:YAG lasers. The energy is very concentrated, resulting in welds with a very high depth-width ratio. An increase in laser power will, generally, increase the weld penetration. This effect further enhanced, when coupled with an electric arc, as the reflectivity of the workpiece metal is generally reduced, when melting occurs [50].

Welding speed

The welding speed determines the power input into the weld. Slower welding speeds result in higher power input, increased penetration and better gap-filling capabilities of the process. The wire feeding speed has to be carefully adjusted to the welding speed in order to achieve good process stability [50].

Relative arrangement of the laser and the MIG torch

To get the maximum weld penetration, the laser is positioned perpendicularly to the direction of welding. The leading or trailing position of the arc torch is a determining factor for the weld characteristics. For mild steels the arc leading configuration is preferred, since an increase in penetration is obtained in this way. Also, the distance between the laser and the wire tip is one of major importance, when controlling hybrid laser-arc welding performance. A short distance, typically 2 mm between the laser spot and the filler wire tip has been shown to be favorable for a steady keyhole and for maximum penetration [50].

Focal point position

To achieve the maximum weld penetration, the focal point of the laser needs to be adjusted below the top sheet surface. Values between 0.5 and 4 mm have been shown to yield the best results [50].

Angle of the electrode

The penetration of the weld increases with the angle of the electrode to the workpiece surface up to 50 degrees. The gas flow along the welding direction, provided by the MIG torch, deflects the plasma induced by the laser and reduces the absorption of the laser beam by its plasma, when CO₂ lasers are employed. Therefore, the angle of electrode to the top surface of the workpiece is often set at around 40-50 degrees [50].

Shield gas composition

The shielding gas prevents the weld pool from reacting with the surrounding atmosphere. The choice of the shielding gas also has an impact on the metal transfer, arc length, chemical composition of the weld pool, weld energy input, as well as the weld penetration geometry. The main constituent of the shielding gases, used in the LHW process, are inert gases. Helium is preferred to argon due to its higher ionization potential, which causes less interference with the laser beam, compared with argon. The addition of reactive gases, such as oxygen and carbon dioxide, has an influence on the weld pool wetting characteristics and bead smoothness [51].

Power source of the MIG/MAG welding unit

For LHW applications, the arc welding source uses a DC mode, rather than an AC mode. The energy input and density are higher in the first case. The arc source is often operated in a pulsed mode, since this reduces the amount of spatter, whilst maintaining a deep penetration of the weld. The welding voltage does not influence the weld penetration depth greatly, which mostly depends on the laser power. However, the weld bead gets wider if the welding voltage increases, giving a lower depth to width ratio for a same laser power. The welding current is generally matched to the filler wire diameter (higher welding current for higher wire diameter). Considering a given wire diameter and voltage settings, it has been shown that an increase in welding current will give a deeper weld, with a higher depth to width ratio [52].

Weld geometry and preparation

The additional use of the MIG/MAG unit allows the welding gap to increase from 0.2 mm to 1 mm without weld defects, such as incomplete weld bead, and undercut being observed. This enables higher tolerances for joint edge preparation and decreases thermal distortion rates of the workpiece during welding. For material thicknesses higher than 8 mm, a groove is usually machined, prior to welding. The

LHW process is less sensitive to the presence of oxides at the joint edges compared to the LBW process, yet a removing of the oxides result in higher quality welds [53].

5.1.2 LHW advantages and applications

Ever since its introduction, the LHW process has been implemented in various industrial applications. The main advantages of LHW, compared to laser welding, are [15], [50], [52], and [54]:

- Lower capital costs, compared to laser alone, due to reduction in laser power requirement,
- Higher welding speeds,
- Larger tolerances of edge preparation,
- Control of seam width,
- Control over metallurgical variables by addition of filler material,
- Less material hardening,
- Higher process reliability and stability, and
- Higher energy efficiency.

The advantages of LHW compared with GMAW are [54]:

- Higher welding speeds,
- Deeper penetration at higher welding speeds,
- Higher energy intensity, resulting in lower total energy input,
- Lower distortion rates, and
- Narrower weld joints possible.

Currently the limiting factors of LHW for a wider use in the industry are [15], and [19]:

- The high investment costs and
- High complexity of the process due to the large amount of process variables. Skilled personnel needed to set up a LHW unit and determine the correct process parameters.

LHW in the automotive industry

The German car manufacturers, Volkswagen, Audi, and Daimler, have introduced LHW in the production lines of their high-end vehicles. The doors of Volkswagens limousine, Phateon, have 48 LHW welds each, with a total length of 3570 mm. The use of LHW has enabled a stiffer structure, with a lower mass [54]. Audi uses the method, for the spaceframe design of the Audi A8 model, to join materials of different thicknesses. Daimler has implemented laser-hybrid welds in the axles of their C-Class vehicles. In these applications, lasers from 2 to 4 kW are used and welding speeds, exceeding 4 m/min, are possible [55].

LHW in the maritime industry

Similar to FSW, LHW welds are applied to join stiffeners to large panels, which make up the hull and body of modern ships. The LHW process has replaced SAW in several shipyards around the world. The production line at MEYER Werft, Germany, includes 4 CO₂ lasers with 12 kW power output each, combined with MIG welding heads, producing around 400 km of weld length per year. Hybrid welding permits significant time and cost savings, by the elimination of multi-pass requirements [56]. Also, valuable post-treatment labor hours can be saved, due to the smaller distortion rates of the welded structures [57].

LHW in pipeline construction

Laser-hybrid welding has been investigated to improve weld quality and reduce manufacturing costs of pipelines. Higher welding speeds and a reduced number of passes make LHW a prospective alternative to the currently used GMAW technologies. The amount of filler material needed, per day of operation, can be reduced from 780 kg, when using the conventional GMAW process, and to 60 kg, when laser hybrid welding is implemented [58]. Stainless steel pipe lines are now welded with a pore free structure and no significant hardness increase, at a welding speed of up to 1.2 m/min, for a wall thickness of 5 to 8 mm [59]. The LHW process can also be used for the root pass of longitudinal welds of large pipelines

[58]. Another study on the economical factors of using the LHW method on pipeline construction, determined that the cost of the equipment pays back after 1.5 years of operation. Also, it was shown that using the LHW technology results in a time saving factor of 6.6 compared with the conventional arc welding method **[60]**.

6 WELDING OF THE SPECIMENS

6 WELDING OF THE SPECIMENS

6.1 Welding of the FSW specimens

The welding and the testing of the specimens were carried out in the laboratories of TGM in Vienna. The scope of the project included a feasibility analysis, manufacturing of FSW tools, and manufacturing of FSW welds, while varying the welding parameters. Testing of the welding samples using both, non-destructive and destructive, methods was also performed.

6.1.1 Selection of the workpiece material

Due to the wide application possibilities and knowledge base of existing studies, it was clear that an aluminum alloy would be chosen for carrying out the FSW experiments. Most studies of the FSW technology, focus on the heat treatable aluminum alloys of the 2xxx, 6xxx, and the 7xxx series, which mainly have poor weldability characteristics [32]. With a comparison of weld characteristics of FSW and LHW welds in mind, a compromise was found in the AW-5754 alloy. AW-5754 is widely used in shipbuilding applications and the automotive industry. Its excellent corrosion resistance enables the use of AW-5754 in food processing applications, as well as in chemical and nuclear structures. The chemical composition of this alloy is shown in *Table 6-1*. The temper of the base material plate is H26, which means that after the strain hardening process by rolling, partial annealing is imposed by thermal treatment, in order to soften the material, so that further processing is possible. AW-5754 has excellent weldability properties, as it can be welded by both arc and gas processes.

Chemical composition of AW-5754									
Si	Fe	Cu	Mn	Mg	Cr	Zn	Ti	Other	Al
0.4	0.4	0.1	0.5	2.6-3.6	0.3	0.2	0.15	0.15	Balance

Table 6-1: Chemical composition of AW-5754 [61]

6.1.2 Selection of the FSW welding equipment

As no special FSW welding equipment was available, the universal milling machine GUK-260, by Prvomajska, was chosen for carrying out the FSW welds. The technical data of the machine can be taken from *Supplement S-1*. The advantages of a universal milling machine are the wide range of welding velocities adjustable, the sufficient machine power for generating a FSW weld, as well as the availability, which reduced the costs of the experiments. The main drawback was the lack of measuring equipment to determine the downward forging force during welding.

6.1.3 Designing and manufacturing of FSW tools

The shoulder diameter has a major impact on the total energy input into the weld, so it was designed to be one of the process parameters. Comparing values from literature [32], shoulders with 10 mm, 12 mm, and 16 mm diameter were chosen. Due to the reasons explained in tool design section in Chapter 4, a concave form of tool shoulder was implemented. Keeping simplicity and machinability in mind, no features were added on the shoulder surface.

The length of the pin was designed to be 3.8 mm long, being slightly shorter than the thickness of the workpiece material with 4 mm. This was to ensure thorough penetration, without the danger of the pin eroding the backing plate. A truncated conical pin was chosen, as truncated pins are less sensible to transversal loads and enable the welding of thick workpieces as well as the application of high welding speeds. The pin was designed with a flat threadless surface. Three FSW tools were used in the experimental procedure with the shoulder diameter varying from 10 to 16 mm. The FSW tools, as well as the blueprints, are shown in *Appendix A-1 to A-4*. The tool material 1.2080 is an oil hardening, high carbon/chromium type tool steel with very high wear resistance. It hardens with a marginal change in dimension. The alloy possesses very high compressive strength and is deep hardening [63]. The relevant technical data, chemical composition, heat treatment, and applications of tool steel 1.2080 are summarized in the *Sup-*

plement S-2. The tools were machined using the CNC lathe CTX 210 by Gilde-meister AG. The relevant technical data of the lathe are summarized in *Supplement S-3*. The machining of the tools is shown in *Appendix A-5*. The hardening of the FSW tools was carried out by a heat treatment procedure, which is explained in *Supplement S-2*. In order to get a smooth surface, the tools were polished after the heat treatment.

6.1.4 Experimental setup

Prior to welding, a small hole was introduced, using a file, on either side of the joint edge of the workpieces. The hole served as the starting point for the welding procedure and was positioned directly beneath the plunge spot of the FSW tool pin. The cavity strongly decreased the stress on the tool tip, as it penetrated the cold and hard workpiece. The aluminum plates were put upon a backing plate, made of steel, in order to prevent damage to the milling machine's table during welding. The workpieces were fixed using clamping equipment, as can be seen in *Appendix A-6*. The secure clamping of the specimens was very important, in order to prevent the aluminum plates from drifting apart during the welding process, and resulted in welding flaws. In order to secure the path of the pin protruding along the joint edge, the plates were aligned parallel to the advance direction of the milling machine. The tool tilt angle, between the rotational axis of the FSW and the perpendicular of the plates, was set to 3° in a leaning backward position. Combined with the concave shoulder this setting enabled the material to be pushed into the stirring area. The plunge depth, the rotation rate, and the travel speed of the FSW tool were adjusted on the panel of the milling machine. The dwell time at the start of the weld was varied between 15 and 30 seconds. During the dwell time, the FSW tool was introduced into the weld with full forging force, yet no advance took place. The heat, produced by shoulder-workpiece friction, softened the material and eased the advance of the pin, as the welding set off. A picture of the welding process can be seen in *Appendix A-7*. The specimens were marked right after welding.

6.1.5 Variation of FSW parameters

The parameters, which were varied during the experimental set-up, were:

- Advance speed: Using the knowledge, obtained by the literature study, the advance speed was varied between 90 mm/min and 200 mm/min. The interval was predetermined by the capabilities of the milling machine, so the values 90, 112.5, 160, and 200 mm/min were chosen.
- Rotation rate: The rotation rate was set with the values 1000, 1250, as well as 1600 rpm.
- Shoulder diameter of the FSW tool: All three FSW tools with the differing shoulder diameters of 10, 12 and 16 mm were used in the experimental process.
- Dwell time at start of weld: The dwell time was chosen either to be 15 or 30 seconds.

A total of 7 specimens were welded using the previously described setup. A summary of the parameters used for the specific specimen can be seen in *Table 6-2*.

Variation of the FSW parameters during experimental setup						
Rotation rate	t _D	d _s	Advance speed [mm/min]			
[rpm]	[sec]	[mm]	90	112.5	160	200
1000	15	10		1		
1250		12	2			
		16	4			
	30	12	5	3		
1600		12			6	7

Table 6-2: Variation of the FSW parameters during experimental setup
(t_D : dwell time before start of welding; d_s : shoulder diameter;
1...7 : specimen number)

The *Supplements S.4* to *S.10* summarize the experimental data and include pictures of the specimens. The specimens were welded in three batches. Specimen **1** was welded to make sure, that the experimental set up was adequate. After revising and adjusting the clamping device, specimens **2**, **3**, and **4** were welded. Tensile tests were performed, to determine weld performance. Afterwards, specimens **5**, **6**, and **7** were welded. For the specimens **5** and **6**, the joint edges were cleaned prior to welding, with a grinding paper, in order to remove the oxide layer. After welding, test samples, for the non-destructive as well as destructive testing, were prepared from the specimens.

6.2 Welding of the LHW specimen

Welding of the LHW specimen was carried out by Matthias Michl at the Austrian based Fronius International research laboratories. 4 Workpiece plates of the same charge, as the FSW specimens, were sent to Fronius. After adjusting the welding parameters on the first test plate, the welding was carried out using a laser-MAG hybrid welding unit, developed by Fronius. A Nd:YAG laser with an output power of 3200 W was used in the process. The focus of the laser beam was adjusted to lie 1.5 mm beneath the surface of the base material. The advance speed was set to 25 mm/sec, which is 1.5 m/min and approximately 10 times as fast as the welding velocity of the FSW specimens. The welds were performed in the flat position. The MAG unit operated with a current of 142 A and the potential was set to 19.5 V. The filler material used in the LHW process was an AlMg4.5Mn wire with a diameter of 1.2 mm. The chemical composition, as well as the mechanical properties of the filler material are listed in the *Supplement S-11*. The feed rate of the filler material was adjusted to the welding current and was set to 8 m/min. The welding parameters are summarized in the *Table 6-3*.

6 WELDING OF THE SPECIMENS

Welding parameters for LHW welding	
Laser power L_P	3200 W
Laser focus L_f	+ 1.5 mm
Welding velocity	25 mm/sec
Welding current	142 A
Welding potential	19.5 V
Filler material	AlMg4.5Mn, Ø 1.5 mm
Feed rate	8 m/min

Table 6-3: LHW welding parameters

7 TESTING OF THE SPECIMENS

7 TESTING OF THE SPECIMENS

In order to evaluate the quality of welds, standardized systems of tests were introduced by the responsible regulatory bodies. In the United States of America, the American standard, ASME code, is applied, whereas in the European Union the European standard (EN) provides rules and guidelines for welding procedure specifications (WPS), as well as the relevant testing methods.

7.1 Testing methods for FSW and LHW welds

The testing can be classified in non-destructive testing (NDT) and destructive testing (DT) methods, depending on the fact, whether the specimen is usable without any loss of function, after the method being applied. An example of an NDT procedure would be visual testing (VT). After a visual inspection and measurements taken, the specimen or the welded part can be used to fulfill its original purpose. DT methods often involve the preparation of specimens, usually by cutting, which then are subjected to the DT testing. An example of a DT method is the Charpy pendulum impact test, which involves the measurement of impact energy, absorbed by a standardized specimen during a fracture test. It is obvious, that the workpiece will no longer be able to fulfill its original designation after such a test had taken place [17].

7.1.1 Non destructive testing (NDT) methods

Visual testing (VT)

Visual testing is one of the most common and powerful means of non-destructive testing. It requires qualified personnel, with adequate knowledge about the product, the welding process, anticipated service conditions, acceptance criteria, and record keeping. Additional equipment to ensure proper lighting, to enable remote inspection, such as mirrors, boroscopes or cameras, and instrumentation to take measurements may be applied in the process [65]. VT starts prior to welding with an examination of the joint preparation. The shape and dimensions of the weld,

7 TESTING OF THE SPECIMENS

the condition of the joint surfaces, and the fixturing of the workpieces have to be examined and compared with the WPS or other product standards. During the welding process, VT has to ensure that correct process parameters are used. For fusion welding processes, special care needs to be taken, when inspecting the weld condition and cleanness, in between the weld passes. After the welding process, the condition of the weld needs to be checked to fulfill the requirements, specified by the corresponding standard.

For fusion welds, imperfections detected by eyesight may be as follows **[17]**, and **[65]**:

- Slag remnants,
- Tool impressions or blow marks,
- Grinding marks from cleaning process,
- Excessive or insufficient height of the weld, irregular welding pattern,
- Inconsistent width of weld,
- Incomplete penetration, burn-through or shrinkage grooves, excessive root concavity,
- Undercuts, and
- Cracks or porosity on the surface.

According to EN ISO 25239 draft for friction stir welding of aluminum alloys, part 5 quality and inspection requirements **[66]**, VT has to be performed as described in ISO 17637, Non-destructive testing of welds: VT of fusion-welded joints. However, the standard does not provide a specific guideline for FSW welds. Therefore the VT was performed according to a guide for approval of friction stir welding in aluminum, by the American Bureau of Shipping, from October 2011 **[67]**. It has to be noted, that the FSW technology still is very new, and, hence, there is a lack of available and thorough welding procedure specifications and testing standards in the European Union.

7.1.2 Destructive testing (DT) methods

Destructive testing methods are used to determine the mechanical properties of welds. Depending on the test strength, toughness, hardness, the microstructure, as well as cyclical toughness features can be examined using a wide variety of tests available. Destructive testing methods are best suited for products, designed for mass production, as well as when a certain repetitive production process is examined for approval, as for example, when examining a welder [17], and [30].

Tensile testing

The tensile test is one of the most widely used tests to determine the technical capabilities of a material. It is of major importance for an engineer, to know the strength of a material, when considering its use for any possible application, in order to avoid over- or under-dimensioning. In engineering terms, the strength of a material is described as a value of stress, which a material can withstand, before irreversible damage occurs. Stress is a measurement of density of forces, defined as force per unit area of the cross-section, as can be seen in Formula (7.1). The unit of stress is N/mm² or MPa.

$$\sigma = \frac{F}{A} \quad (7.1)$$

with:

σ ... stress [N/mm²]

F ... force [N]

A ... area of cross-section [mm²]

Another important value obtained by a tensile test is the strain. Strain is a value, which describes the deformation of a material under influence of stress. It is measured as an increase of length of a material, referred to its original length, as can be seen in Formula (7.2).

$$\epsilon = \frac{\Delta l}{l_0} \quad (7.2)$$

with:

ϵ ... strain

Δl ... elongation

l_0 ... original length

Strain may be reversible or irreversible. The engineering terms are elastic and plastic. Elastic strain disappears when the stress is removed. Stress and strain are determined by a tensile test, and are usually displayed together in a stress-strain curve, as can be seen in *Figure 7-1*. The stress-strain curve is individual for each material, and provides the engineer with useful information about its mechanical properties. Exemplary stress-strain curves of various material types are depicted in *Figure 7-2*. The maximum strength of a material attained in a tensile test is called tensile strength, and is represented with the abbreviation R_m . Tensile strength usually is of subordinate importance to an engineer, as the material may already be undergoing plastic deformation, which may cause a failure in repetitive loading cycles at lower loads than the tensile strength. Therefore the yield strength is taken into account. Yield strength is the maximum stress, which a material can withstand without undergoing any plastic deformation, and is marked as R_e . For materials of ductile nature, which do not have a well defined elastic limit, a substitute value called the proof strength (R_p) is given. Proof strength indicates the stress level sustained by the tested material, which leads to a plastic elongation of 1%, 0.1 % or 0.2% [17], and [30].

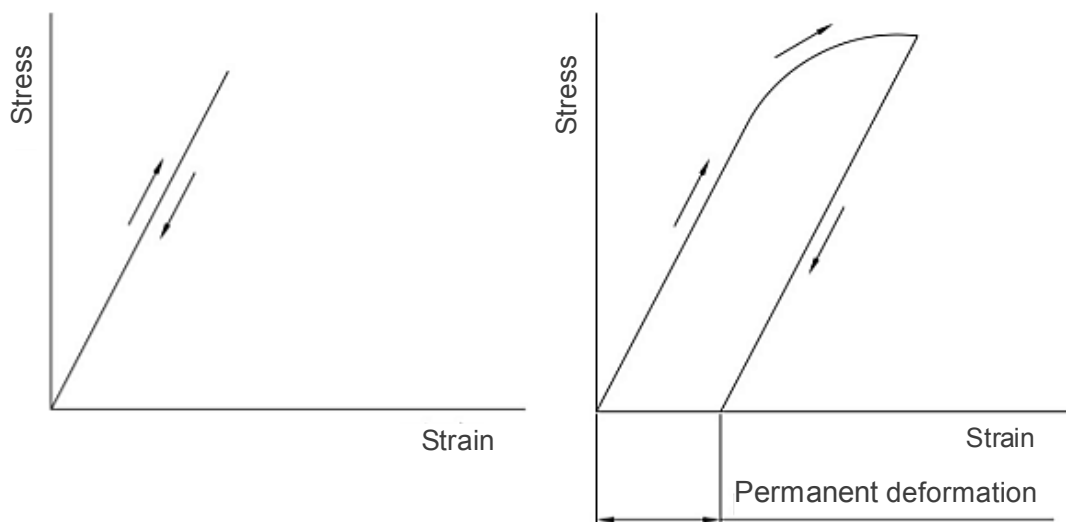


Figure 7-1: stress-strain curves of elastic strain (left) and plastic strain [30]

In order to perform a tensile test, a standardized specimen needs to be fabricated from the existing material. Depending on the type of product, different specimen geometries exist. For welded plates a specimen is cut and prepared according to the relevant standard. A blueprint of a specimen geometry for a FSW weld tensile test can be seen in *Appendix A-8*. The specimen is then elongated very slowly until fracture, using a tensile test machine. Technical data of a universal testing machine can be taken from *Supplement S-12*. During the process, a record of the force and the elongation is kept. The according stress and strain pairs can be then used to plot a stress strain curve [17], and [30].

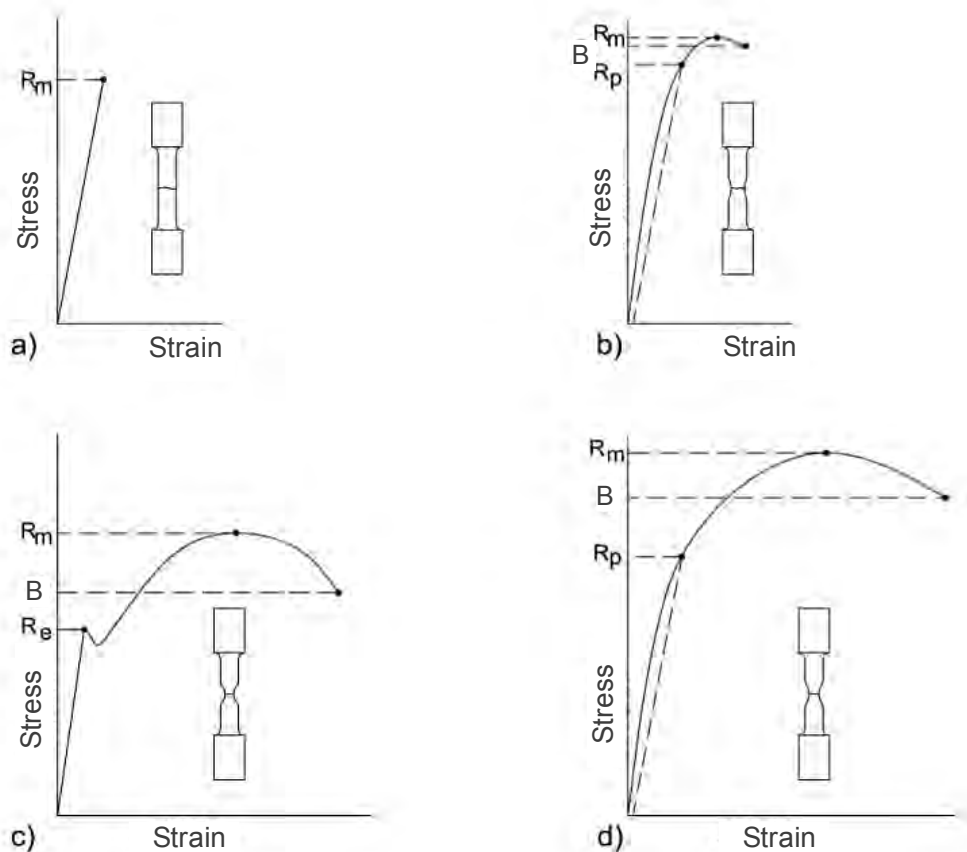


Figure 7-2: Representative stress-strain curves for various types of materials. a) non-ductile material; b) semi-ductile material; c) and d) ductile materials [30] (R_m : tensile strength; B : breaking strength; R_e : yield strength; R_p : proof stress)

Metallography and macroscopic examination

In order to examine the physical structure and components of metals and welds, metallography is an almost indispensable tool, to enable a view inside the material. After preparation of the specimens, an etching method is applied to provide the contrast needed for microscopic analysis. Light optical microscopes (LOM) are most commonly used, yet for higher resolution rates scanning electron microscopes (SEM), and transmission electron microscopes (TEM) can be applied [68]. The first step of metallography is to distinguish the area of interest, which is to be examined. For welds, this usually is in the region of the weld pool or the area of the heat affected zone (HAZ). Comparative examples of unaffected base material may also be taken for reference purposes. The specimens are obtained by the means of abrasive cutting. It is important to limit the heat input into the base material during cutting, as this could affect the base material and result in false conclusions. Low cutting speeds or water cooling can be applied. The specimens are then mounted using a hot thermosetting resin, such as epoxy. Mounting a specimen provides a safe, standardized, and ergonomic way for further handling of the specimens. The cutting delivers an uneven edge, usually marked with scratches from the cutting equipment, which is of little use for microscopical analysis. In order to remove the cutting marks and obtain a planar edge, the surface of the specimen is grinded, polished, and etched prior to examination. Successively finer abrasive particles from the surface of a silicone carbide abrasive paper or a diamond grit suspension are used for grinding, until the desired surface quality is reached. The next step is to polish the surface. A suspension, containing fine alumina, silica or diamond particles, is used with a polishing cloth to remove the grinding marks, drag or pull-outs still present at the specimens surface [68].

After polishing, certain microstructural constituents, such as inclusions, pores, and secondary phases, may be already seen using a microscope. Yet to distinguish grain boundaries, phase differences, and most metallurgical features, etching is indispensable to create a contrast between the elements of the metals micro-

structure. Chemical solutions, known as etchants, are used to selectively corrode some of those elements, which show up as darker regions. Differences in the composition, structure or phase of a metal will create electrochemical potentials that alter the relative rates of corrosion, when exposed to an etchant [68]. The resulting surface can then be inspected with a microscope in order to analyze:

- The grain size,
- Grain direction and deformation,
- Grain growth features,
- Inclusions and hollows,
- Phase segregations, and
- Welding flaws.

7.2 Testing of the FSW specimens

VT of FSW Specimens

The guideline for the VT of the FSW specimens was taken from the guide for approval of friction stir welding in aluminum, by the American Bureau of Shipping, from October 2011 [67].

Inspection before welding

Before welding, it was made sure, that the machinery, the tool, the process parameters, the base material, the joint design, the fixture of the joint, and the joint pretreatment were adjusted according to the provided WPS. It has to be noted, that specimens **1**, **2**, **3**, **4** and **7** were not subjected to a joint edge preparation. For specimens **5**, and **6**, the oxide layer was removed using abrasive paper.

Inspection during welding

During welding, a continuous in-process monitoring was carried out. Due to the limited capabilities of the milling machine, no data of the actuating welding forces could be measured. The fixture of specimen **1** was not sufficient to withstand the

welding forces. As a result, the base material plates slipped apart, resulting in a welding gap. No other discrepancies, during welding of the remaining specimens, were noted.

Inspection after welding

The guide for approval of friction stir welding in aluminum, by the American Bureau of Shipping, defines the following quality criteria for VT of FSW joints [67]:

- Exit hole uniformity: The exit hole is to be examined and the uniformity has to be more than 75% complete.
- Herring bone or chevron marking: This is occasionally observed when welding aluminum alloys of the 5xxx series. These markings have not reported to affect the mechanical or corrosional behavior of FSW welds, yet they shall be noted and, eventually, removed prior to DT [69].
- Flash: Prior to removal of flashes, regions within friction stir welds containing excessive flashes shall be marked on the plate, and these areas shall be inspected for dimensional conformance.
- Dimensional requirements: It has to be verified that the thickness of the weld and its adjacent base metal are to the satisfaction of the surveyor. Weld concavity depth (face or root) shall not exceed 0.8 mm or 10 percent of the adjacent base metal thickness, whichever is less.
- Butt joint alignment: Height offset misalignment, extrusion to extrusion, is to be less than or equal to 0.2 times the base material thickness or 2 mm, whichever is less, unless specifically qualified.
- Irregular width: Width variation of the welded assembly is to be within the limits of the design specification.
- Root reinforcement: Root reinforcement is to be less or equal to 10% of the base material thickness.
- Cracks, porosity, lack of penetration: No cracks, porosity, or lack of penetration are allowed.

The quality criteria are listed in *Supplement S-13*. The results of the VT are summarized in *Table 7.1*. The measurements can be taken from *Supplement S-14*.

FSW specimens: summary of VT testing results							
Specimen	1	2	3	4	5	6	7
Exit hole uniformity	✓	✓	✓	✓	✓	✓	✓
Chevron marking	✓	✓	✓	✓	✓	✓	✓
Flash	✓	✓	✓	✗ ³	✗ ³	✗ ³	✓
Thickness variation	✗ ¹	✓	✓	✓	✓	✓	✓
Joint alignment	✗ ¹	✓	✓	✓	✓	✓	✓
Irregular width	✗ ¹	✓	✓	✓	✓	✓	✓
Root reinforcement	---	---	---	---	---	---	---
Cracks, porosity, lack of penetration	✗ ¹	✗ ²	✗ ²	✗ ⁴	✓	✗ ²	✗ ^{2;5}
Result of VT	✗ ¹	✗ ⁶	✗ ⁶	✗ ⁶	✓	✗ ⁶	✗ ⁷

Table 7.1: Summary of VT results of the FSW specimens

(✓ : test passed; ✗ : test not passed (notes see below); --- : not relevant for specific weld)

Notes:

- ✗¹: The fixture of specimen 1 was not sufficient to withstand the welding forces during welding. The base material plates slipped apart, resulting in a welding gap, which did not produce a continuous weld (see *Appendix A-9*).
- ✗²: The first couple of centimeters of the weld were characterized, by irregular welding pattern on the face side. On the root side material discontinuity was visible (see *Appendix A-10, and A-11*).
- ✗³: Excessive flash alongside the weld (see *Appendix A-12*). The analysis of dimensional requirements did not provide any reason for quality inferiority.
- ✗⁴: The first couple of centimeters of the weld were characterized, by irregular welding pattern on the face side. Also a very small crack-like disruption was visible at the start of the weld (see *Appendix A-13*).
- ✗⁵: A cavity could be observed 38 mm after weld start. Cavity was on both – face and root side (see *Appendix A-14 and A-15*). The cavity resulted from a previously existing hollow, which was filed into the edge of the specimen, to ease the tool plunge.
- ✗⁶: The defects were only found at the start of the weld. Further testing methods have to determine the effects of the quality of the remaining weld.
- ✗⁷: The cavity could be ignored for the further tests, as it was a foreseen defect, is localized, and did not depend on the welding parameters examined.

Tensile tests of FSW specimens

As the FSW specimen **1** clearly did not pass VT, one tensile specimen was fabricated from FSW welds **2** to **7** each. For reference purposes, a specimen of the base material was also tested. According to the existing ISO 25239, draft for friction stir welding of aluminum and aluminum alloys, the position of the tensile specimen needed to be sufficiently far away from the start and finish of the weld **[72]**. The position of the tensile specimen can be seen in *Figure 7-3*.

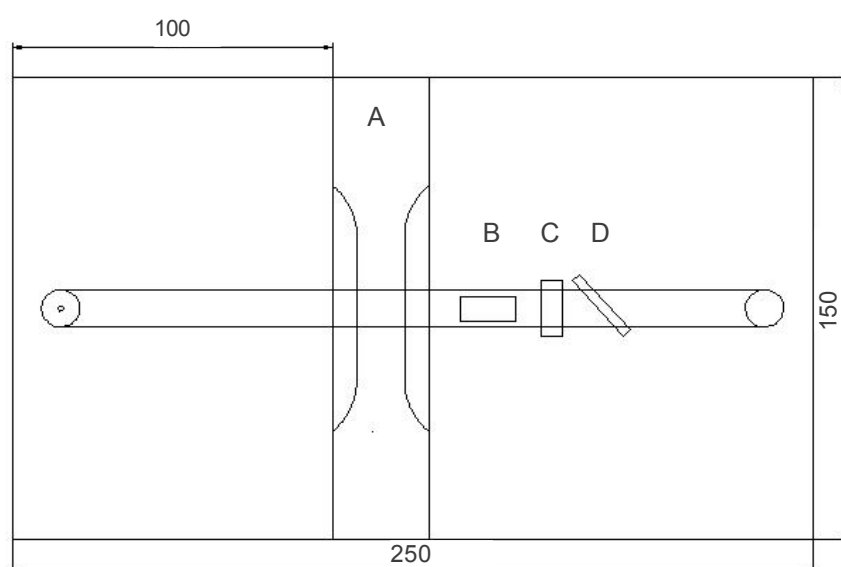


Figure 7-3: FSW weld; (A: tensile specimen, B: longitudinal macroscopic specimen, C: transversal macroscopic specimen, D: diagonal macroscopic specimen)

The specimens were tested using a Wolpert universal testing machine. The technical data of the tensile machine are summarized in *Supplement S-12*. All specimens were tested until fracture. The maximum force, as well as the maximum strain, were noted and are summarized in *Table 7-2*. A picture of a tested specimen is shown in *Appendix A-16*.

FSW specimens: summary of tensile test results							
Specimen	AlMg3	2	3	4	5	6	7
R_m [N/mm ²]	291.4	224.2	222.2	165.3	241.3	208.3	242.3
ϵ %	7.70%	3.70%	3.5%	3.20%	3.53%	3.00%	5.30%
Necking	Yes	No	No	No	Minimal	Minimal	Yes
Location of fracture	Middle	Along the joint	Along the joint	Along the joint	Slightly offset to joint	Along the joint	Slightly offset to joint

Table 7-2: Summary of tensile test results
(R_m : tensile strength; ϵ : maximum strain)

Macroscopic examination of FSW specimens

The specimens were cut out of the FSW samples **2**, **3**, and **4**, according to *Figure 7-3*. In order to obtain a flat surface, the specimens were wet-grinded using abrasive paper with the the grit steps varying successively from 500, 800, 1000 to 1200. The water served as a heat sink and helped to transport the abraded material away from the specimen surface. The mounting was done using an epoxy by the name ClaroCit™. ClaroCit™ is a two component curing system, developed by Struers, which is suited for universal applications and cures at room temperature [73]. The specimens were positioned in the mounting caps, filled with resin, and left to cure for 24 hours prior to further action (see *Appendix A-17*). The specimens were then polished, using a suspension of fine alumina in alcohol, for approximately 10 minutes.

The chemical etchant, chosen for preparing the specimens, was Duralumin, which is a mixture of water, hydrofluoric acid (HF), and phosphoric acid (H₂PO₄). After a reaction time of 4 minutes the specimens were cleansed with running water.

The setup for the macroscopic analysis of the specimens consisted of a microscope by Reichelt, type 363.716, and a Canon EOS 550D SLR camera. Two different objectives were used on the microscope, enabling two different magnification levels. The setup is shown in *Appendix A-18*.

Specimen 2

For specimen **2**, three macro-etches were prepared. The combination of a longitudinal, a transversal, and a diagonal sample, as shown in *Figure 7-3*, enabled observing the effects of the stirring action, performed by the FSW tool. The longitudinal specimen was examined using the 0.08 objective. An exemplary picture is displayed in *Appendix A-19*. The transversal macro-etches were examined using two levels of magnification. The results can be observed in *Appendix A-20*. The macroetch of the diagonal specimen is shown in *Appendix A-21*.

The images reveal that the FSW process resulted in a fine grain structure. No weld nugget could be observed from any angle of examination. All three perspectives showed material discontinuity by inclusion of phases. Through the process of etching, the phases appeared as dark regions. Comparing the images with examples from literature [69] and [74] led to an assumption that the phase resulted from oxide particles from the edges of the joint, which were dispersed in a wave-like pattern by the stirring action of the pin. *Appendix A-21* showed a gap, which can be interpreted as a root flaw [69] and [74].

Specimen 3

Two macroetches were produced of specimen **3**. A transversal and a diagonal specimen were taken and examined using the 0.08 objective. *Appendices A-22 and A-23* show the transversal probe. An example of the examination of the diagonal macroetch is depicted in *Appendix A-24*.

Similarly to the results of specimen **2**, the etches revealed a wavelike inter-phase, which could be interpreted as oxide particles. A root flaw can be seen in *Appendices A-22, and A-24*.

Specimen 4

A transversal and a diagonal specimen were prepared of specimen **4**. The transversal macroetch is shown in *Appendix A-25*. The macroetch of the diagonal probe can be seen in *Appendix A-26*.

Appendix A-26 revealed a distinct brighter region, which could be interpreted as the dynamically recrystallized zone DXZ [32] and [69]. Similar to specimens 2 and 3, a wavelike inter-phase could be observed. A root flaw was also present, as shown in *Appendix A-26*.

7.3 Testing of the LHW specimen

The laser hybrid welded specimen is shown in *Appendix A-27*. The welded plate had a length of 220 mm a width of 200 mm, with the weld extending for 200 mm. The bright region along the side of the weld represented the heat affected zone. The root side of the weld is depicted in *Appendix A-28*. A close-up of the root is shown in *Appendix A-29*.

VT of the LHW specimen

When taking a first look at the LHW weld, the distortion of the specimen caught the eye. Due to the high energy input, the workpiece was deformed by the action of thermal stresses [17], as can be seen in *Appendices A-30*, and *A-31*. According to EN ISO 15614, specification and qualification of welding procedures for metallic materials - part 2: arc welding of aluminum and its alloys [74], visual testing was carried out following the guideline specified in EN ISO 17637, non-destructive testing of welds: VT of fusion-welded joints [65] and [74]. As the welding procedure was carried out at the laboratories of Fronius Int., the visual testing was limited to post weld inspection. It has to be noted, that EN ISO 17637, does not provide any specific quality criteria but merely provides a guideline for VT. The recommended standard to use is EN ISO 10042, welding - arc-welded joints in aluminum and its alloys - quality levels for imperfections [71]. This guideline was used, next to EN ISO 13919-2 electron and laser beam welded joints, guidance on quality levels for imperfections, part 2: aluminum and its weldable alloys, for visual inspection [70]. Within both standards three sets of quality levels are given: D for moderate, C for intermediate, and D for stringent quality levels. The *Supplement S-13* shows the specific quality criteria alongside the figures for the

7 TESTING OF THE SPECIMENS

quality criteria for both standards. As can be seen in *Supplement S-13*, the tolerance levels decrease, as a higher quality level is attempted. The results of VT of the LHW specimen are summarized in *Table 7-3*. The protocol of the exact measurements can be found in *Supplement S-14*.

VT of LHW specimen						
Quality criteria	ISO 10042			ISO 13919		
	Quality level			Quality level		
	D	C	B	D	C	B
Cracks	✓	✓	✓	✓	✓	✓
Crater cracks	✓	✗	✗	✓	✓	✗
Porosity	---			---		
Surface pore	✓	✗	✗	---		
Shrinkage cavity	✓	✓	✓	✓	✓	✓
Crater pipe	✗	✗	✗	✗	✗	✗
Lack of fusion	✓	✓	✓	✓	✓	✓
Incomplete root penetration	✓	✓	✓	✓	✓	✓
Undercut	✓	✓	✗	✓	✓	✗
Excess weld metal	✓	✓	✓	✓	✗	✗
Excessive penetration	✓	✓	✓	✓	✗	✗
Overlap	✓	✓	✓	✓	✓	✓
Sagging	✓	✓	✓	✓	✓	✓
Linear misalignment	✓	✓	✓	✓	✓	✓
Shrinkage groove	✓	✓	✓	✓	✓	✓
Test result	✗	✗	✗	✗	✗	✗

Table 7-3: Summary of VT of LHW specimen

(D: moderate quality criteria; C: intermediate quality criteria; B: stringent quality criteria; ✓ : test passed; ✗ : test not passed; --- : not relevant for specific standard or not detectable with VT methods)

8 SUMMARY AND DISCUSSION OF THE RESULTS

8 SUMMARY AND DISCUSSION OF THE RESULTS

8.1 FSW results

The aim of this thesis was to study the friction stir welding process and determine the influence of variation in FSW parameters. A total of seven welds were produced, each one using a different set of parameters. The NDT, as well as the DT methods, served as a basis for judgment for the evaluation of the tests.

8.1.1 Influence of the welding tool shoulder diameter

The amount of welding energy, which is used to produce a FSW weld, is proportional to the tool shoulder diameter Formula (4.1). Three different shoulder diameters were tested in this study: 10 mm, 12 mm, and 16 mm. The first welding attempt, using a 10 mm tool, was a failure, as the fixtures of the base material did not withstand the welding forces and let the plates slip apart. The 12 mm tool was used for specimens **2**, **3**, **5**, **6**, and **7**. Specimen **4** was welded using the 16 mm tool. The VT results showed, that the 12 mm tool did produce better results than the other tools, as it produced the only specimen, which passed VT. *Appendix A.13* shows the start of the weld of specimen **4**. The irregular welding pattern might be caused because of increased sticking of the tool upon the workpieces surface, yet other welds also displayed such pattern. The tensile tests delivered a clear result in favor of the 12 mm tool, as specimens **2**, **4**, and **5** were welded using similar welding speeds. The tensile strength of specimen **4** was 26% lower than the tensile strength of specimen **2** and 32% lower than the tensile strength of specimen **5** (see *Figure 8-1*). A possible cause for these significant differences could be insufficient welding pressure, when using a large shoulder tool. Pressure is calculated by dividing force by area, so the pressure decreases proportionally to the square of the shoulder radius, when the same force is applied. Unfortunately, the universal milling machine was not equipped with a force-measuring device, so no certain conclusions could be made at this point.

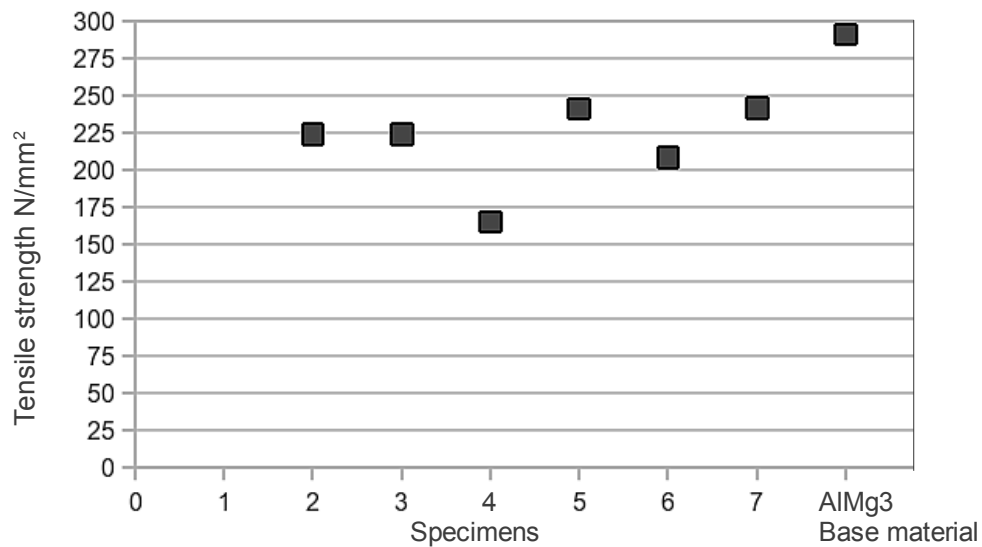


Figure 8-1: Summary of results of tensile tests of FSW specimens

8.1.2 Influence of the edge preparation

Although, it is stated in literature [32], [33], and [35] that no specific plate preparation is required prior to welding, the oxide particles, visible in the macro-etches, did prove the contrary. Specimens **1**, **2**, **3**, **4**, and **7** were welded without any edge preparation. The plates for weldments **5** and **6** were cleaned prior to welding, using abrasive paper and a file. The oxide particles formed a distinct phase, and prevent material continuity, as can be seen in the macroetches in Appendices A-19 to A-20, as well as A-22 to A-26. The effects on the mechanical properties could be distinguished, when the specimens **2**, **4**, and **5** were compared, as these specimens were welded applying similar welding speeds. The ultimate tensile strength of specimen **5** was 8% higher than the ultimate tensile strength of specimen **2**, and 47% higher than the ultimate tensile strength of specimen **4**. Contrary to specimens **2**, and **4**, specimen **5** also showed a minimal necking during the tensile test, and the fracture was slightly offset to the joint, which was a sign of ductility. It could be assumed that the oxide layer caused material discontinuity and was the main reason for the brittle nature of fracture.

8.1.3 Influence of the dwell time prior to welding advance

The dwell time t_D is the time, during which the tool has already penetrated the base material, yet does not advance along the joint. The main reason for t_D is to cause energy input in form of friction heat into the workpiece. The heat softens the base material, easing the following advance, the material flow, and avoiding the danger of tool fracture [32]. During the welding experiments two different t_D were applied. Specimens **1**, **2**, and **4** experienced 15 seconds of “welding on the spot” prior to welding. For specimens **3**, **5**, **6**, and **7**, t_D was set to 30 seconds. The close-up pictures of the welds in *Supplements S-4 to S-11* show that a longer t_D , yielded a better weld finish. The welding pattern was more regular and the starting effects were less distinct, as with the shorter t_D . Especially when combined with high welding speeds, as in the case of specimens **6** and **7**, a shiny surface emerged throughout the weld. Looking at the tensile test results revealed, that the specimens with a dwell time of 30 seconds yielded the highest results, and necking was observed, while testing specimens **5**, **6**, and **7**.

8.1.4 Influence of the welding speed

The welding speed consists of two components, the rotational rate and the advance of the FSW tool. During welding of the FSW specimens, 3 different rotational rates were applied: 1000, 1250, and 1600 rotations per minute. The advance speed was varied in 4 steps: 90, 112.5, 160, and 200 mm per minute. The limited amount of FSW trials only allowed the parameter study of the advance speed among the specimens **3** and **5** and among the specimens **6** and **7**, which were welded at similar rotational rates but differing advance velocities. Specimens **3** and **5** were processed using a rotation rate of 1250 rpm. Specimen **5** was welded using the slowest advance rate and performed better in VT, as well as the tensile test, than specimen **3**, which was welded at 112.5 mm per minute. A contrary effect could be observed among specimens **6** and **7**. Specimen **7**, which was welded with the highest overall welding speed, achieved the highest tensile test result, as well as the biggest elongation. A possible explanation could be the

influence of other parameters, such as the welding force, which could not be adjusted or measured during the experiments. Also, the fact that the edges of specimen 7 were not cleaned prior to welding posed the question, whether the test results might have even be improved, if such action had taken place. Higher welding speeds also resulted in a regular welding pattern and a shiny surface finish.

8.1.5 Conclusions of the FSW parameter study

Although, certain patterns could be distinguished after the evaluation of the tests, the conclusions were based on a very small number of specimens. To get a better understanding of the FSW process, a wider parameter study should be carried out. The equipment used for the FSW welds was limited in its capabilities to reproduce results. The milling machine did not have a possibility to adjust and measure the welding force, which is one of the most important FSW welding parameters. The variance of the remaining welding parameters was increased, while the informative value of the results suffered. The fact that only 82% of the tensile strength of the base material was achieved with the best-performing FSW specimen, posed the question, whether better results could be achieved using a completely different set of parameters. Nevertheless following conclusions could be made:

- It was possible to produce FSW welds with a common milling machine, yet the reproducibility of weld performance was affected by missing welding force setting and measuring devices.
- Tool diameter had a profound influence on the FSW weld quality.
- The removal of oxide layers prior to welding led to better results, as oxides were not sufficiently dispersed by the FSW action during the process.
- A sufficiently long dwell time prior to welding led to higher weld quality and a better surface finish.
- The existing VT guidelines did not prove to predict the weld performance, as subsurface defects remained undetected.

8.2 LHW results

Only one LHW specimen was produced, for study purposes of this thesis. The specimen was tested using only VT testing methods. The first distinct conclusion was, that the LHW process resulted in a much higher heat input into the weld. As a result, thermal stresses caused both, longitudinal and lateral distortion. Such deformed workpieces would require a lot of post-weld treatment, which is expensive. The second conclusion was that the base material AW-5754 could be welded by both, pressure- and fusion welding processes. LHW proved to be a much faster welding technology than FSW. The welding rate was 10 times as high as the highest welding speed, achieved in the FSW trials. The LHM specimen performed poorly in the visual testing, as the crater pipe height and the height of the root of the weld proved to be too big for the applied VT guidelines. Nevertheless, one has to mention, that no specific LHW guideline has yet been set up, so the results have to be judged with care. It would have been informative to perform further tests, both NDT and DT, to examine the weld performance of the LHW weld, yet it was off the scope of this thesis.

8.3 Comparison of FSW and LHW test results

Direct comparison of both welding methods, performed on the AW-5754 alloy was difficult, as a different sets of guidelines applied for the visual testing. For the LHW specimen the weld performance was judged looking at the geometrical aspects of the solidified weld pool, whereas for the FSW specimens, characteristic features, such as excessive flash, and exit hole uniformity were taken into account. Nevertheless, the only weld sample to pass the VT was the FSW specimen **5**. If both welding methods were to applied on an industrial scale, friction stir welding would be advantageous regarding the post treatment of the weld. The fine surface finish, would not require any further processing, whereas for the LHW welds, excessive weld and crater height would have to be evened out and polished. The main advantage of the LHW specimen is the welding velocity, which was 10 times as high, as the highest welding velocity achieved by a FSW sample. However, the

distortion of the LHW sample, due to thermal stresses, would require extensive post-treatment.

To make a direct comparison of both welding technologies possible, it would be necessary to perform further tests regarding the strength of the welds, and take a closer look at the inside of the LHW weld using macro-etches.

8.4 Comparison of FSW and LHW technologies

Both, the FSW and LHW processes, are relatively new and still have a marginal share of the whole welding sector today. A major advantage of FSW, is the ability to weld alloys, which are not fusion-weldable. The LHW technology is used, where single pass welds, welded at high speeds is desired. Both technologies compete in the automotive, as well as maritime, applications. FSW and LHW are highly automated processes, which require skilled labor to set up the devices and adjust the welding parameters. During the implemented process, the FSW technology is less labor intensive, as operating a FSW device is just slightly more complex than using a CNC milling machine. Also, no special enclosure of the FSW environment is necessary, as no radiation, gases or fumes result from the welding. The application of laser hybrid welding demands special precautions, regarding the laser safety aspects [75], as well as the general hazards, resulting from fusion welding processes, such as spatters and fumes. Regarding post-treatment of the weldments, the FSW technology is more efficient, as no slag or spatter are involved. Also, the distortion rates are smaller. Regarding the costs of both processes, it is difficult to make an estimate, as the applications usually are specific, and the machines are custom-designed for the demands of the customer. A study, regarding the costs of FSW in comparison to MIG welding [76], notes the investment to be as high as 160.000 €, adding licensing costs of 43.000 € per year. A different study puts the machinery costs as high as 800.000 \$. During welding, the expenses of FSW processing are relatively low, as the process is very energy efficient. Depending on the base material, the tool cost must be considered. First it has to be noted, that there is no such thing as a universal FSW tool. Each base

material and weld geometry bring about considerations, which demand for specific tool designs. For hard materials, such as steel and titanium, the tool costs and excessive tool wear may result in significant expenditure [33]. However, resources are saved, as no filler material or shielding gases are needed. Also, for 'simple' repetitive tasks low-cost solutions exist. The latter consist of a FSW welding head, which can be introduced in a standard milling machine and is capable of monitoring the relevant welding parameters [77]. The size of investment for a LHW unit largely depends on the desired output power. A Laser beam apparatus costs approximately 100.000 € per kW of laser output [78]. Adding are the costs for a MIG unit and the integration of both systems in one automated welding head. Also significant amount of money has to be spent on the running costs for filler material, electrical energy, and shielding gases. The cost saving potential of LHW arises, when the welding velocity is considered. Welding speeds, exceeding 8 m per minute, can be achieved, which can result in economies, in large production series or when long welds are desired [49].

For the moment, it is difficult to foresee, whether the technologies described in this thesis, will remain exotic, rarely used applications. However, the increasing amount of publications and patents show an exponential upward trend, which paves the path for new process variations and a more widespread use. In my personal opinion, the use of FSW related technologies will gain increasing importance in the non-fusion weldable material section. Also, when the costs of the machinery will decrease, and the portability of equipment will be enhanced, the sky will certainly not be the limit, as can be seen in the example of the NASA spacecraft program.

R REFERENCES

R REFERENCES

- [1] Friction Stir Welded Spin-Formed Dome
<http://www.nasa.gov/exploration/multimedia/highlights/2010-15C.html>
Accessed on 4.11.2012.
- [2] Robert W. Messler Jr.: Principles of Welding Processes, Physics, Chemistry and Metallurgy. WILEY-VCH Verlag, 2004.
- [3] A History of Welding & Brazing, <http://www.weldinghistory.org/>
Accessed on 10.05.2012.
- [4] History of Aluminum, <http://www.historyofaluminum.com>,
Accessed on 12.06.2012.
- [5] Aluminum, <http://nautilus.fis.uc.pt/st2.5/scenes-e/elem/e01310.html>
Accessed on 12.06.2012.
- [6] The first successful Airplane
<http://airandspace.si.edu/wrightbrothers/fly/1903/index.cfm>
Accessed on 12.06.2012.
- [7] Aluminium in aircraft construction
<http://www.aluminiumleader.com/en/around/transport/aircraft>
Accessed on 12.06.2012.
- [8] M. Peters and C. Leyens: Aerospace and Space Materials, Materials Science and Engineering – Vol III, published 2011 EOLSS; Institute of Materials Research, DLR, German Aerospace Center, Cologne, Germany.
- [9] <http://en.wikipedia.org/wiki/Aluminium>. Accessed on 12.06.2012.
- [10] Bruce Halverson et al: Friction Stir Welding (FSW) of Littoral Combat Ship Deckhouse Structure; Marine Corporation and Friction Stir Link 06.01.2006.

R REFERENCES

- [11]** Proven Friction Stir Welding Technology Brings Together Reliability and Affordability for NASA's Space Launch System
<http://www.sciencedaily.com/releases/2012/05/120521153524.htm>
Accessed on 13.06.2012.
- [12]** Marc Wouters: Hybrid Laser-MIG welding: An Investigation of geometrical considerations, Litentiate Thesis Luleå University of Technology 2005.
- [13]** Paul Denney: Hybrid Laser Arc Welding – Has its time finally arrived?
Internet Publication by Lincoln Electric Corporation.
- [14]** Jens Klaestrup Kristensen: State of Art in Shipbuilding applications of hybrid Laser-arc welding; Force Technology.
- [15]** Klas Weman: Welding Processes handbook, Woodhead Publishing Ltd, Abington Hall, Abington 2003.
- [16]** Oxyacetylene Gas Welding <http://www.solidmetals.net/2011/02/20/oxyacetylene-welding/>, Accessed on 6.11.2012.
- [17]** Felber, S: Schweiss- und Verbindungstechnik, Skriptum zur Vorlesung: 206.176 WS2011, TU Wien, Wien 2010
- [18]** <http://www.weldguru.com/tig-welding.html>, Accessed on 6.11.2012
- [19]** Andreas Otto: Laserbearbeitungstechnik 311.126 2012S Lecture notes, TU Wien.
- [20]** Janet Devine: Ultrasonic Welding ASM Metals Handbook Vol 6, p 900 – 910, 1993.
- [21]** I. J. Polmear: Light Alloys: Metallurgy of the light metals. J. Wiley & Sons, 1995.
- [22]** I. J. Polmear: Light Alloys: From Traditional Alloys to Nanocrystals Butterworth Heinemann, 2004.
- [23]** Aluminum Industry Technology Roadmap, February 2003.
- [24]** George E. Totten, D. Scott Mackenzie, Marcel Dekker: Handbook of Alumin-

- um: Alloy Production and Materials Manufacturing. CRC Press, 2003.
- [25] Dr. Subodh K Das: Emerging Trends in Aluminum Recycling: Reasons and Responses. Light Metals. TMS (The Minerals, Metals & Materials Society) 2006.
- [26] J. Gilbert Kaufman: Introduction to Aluminum Alloys and Tempers. ASM International, 2000.
- [27] Dr. I.C. Skrna–Jakl: Skriptum zur Vorlesung: Leichtbau mit Faserverstärkten Werkstoffen. ISLB 2011.
- [28] Gene Mathers: The welding of aluminum and its alloys. Woodhead Publishing 2002.
- [29] Alloy Designation Systems for Aluminum and Aluminum Alloys
<http://www.keytometals.com/page.aspxID=CheckArticle&site=ktn&NM=1>
 Accessed on 6.11.2012
- [30] Felber, S: Metallische Werkstoffe, Skriptum zur Vorlesung. TU Wien, Wien 2010.
- [31] Richard P. Martukanitz: Selection and Weldability of Heat-Treatable Aluminum Alloys, 1995.
- [32] Rajiv S. Mishra, Murray W. Mahoney: Friction Stir Welding and Processing.
- [33] Jean Pierre Bergmann: Thermische Fügeverfahren Werkstoff- und Prozesstechnik für das Fügen bei niedrigen Temperaturen; TU Ilmenau, 2008, p 49-54, p 95 – 103.
- [34] Friction Stir Welding: Technical Handbook, ESAB.
- [35] Terry Khaled: An outsider looks at Friction Stir Welding; REPORT #: ANM-112N-05-06; Federal Aviation Administration, January 2005.
- [36] R. Rai, A. De, H. Bhadeshia: Review: friction stir welding tools, Science and Technology of Welding and Joining 2011 Vol 16 No 325.

R REFERENCES

- [37]** W. M. Thomas, I M Norris et al: Friction Stir Welding – Process Developments and Variant Techniques; The SME Summit 2005 Oconomowoc, Milwaukee, USA, August 2005.
- [38]** C.E.D.Rowe, W. Thomas: Advances in tooling Materials for Friction Stir Welding, Publication by TWI and Cedar Metals Limited, 2009.
- [39]** EN ISO 25239-1 Friction stir welding — Aluminium, 2. Draft, 2009.
- [40]** A J Leonard and S A Lockyer: Flaws in Friction Stir Welds, TWI Ltd, Granta Park, Great Abington, Cambridge, CB1 6AL, UK, 4th International Symposium on Friction Stir Welding, Park City, Utah, USA, 14-16 May 2003.
- [41]** Christopher B. Smith, Wade Crusan et al: Friction Stir welding in the automotive industry, Tower Automotive – Technology Application.
- [42]** Kevin J. Collign: Friction Stir Welding for Ship Construction, Concurrent Technologies Corporation.
- [43]** Hitachi A-Train, http://en.wikipedia.org/wiki/Hitachi_A-train, Accessed on 13.01.2013.
- [44]** FSW <http://www.hitachirail.com/> Accessed on 13.01.2013.
- [45]** Christopher B. Smith: Robotic Friction Stir Welding using a Standard Industrial Robot; Tower Automotive, Milwaukee, WI.
- [46]** Zhili Feng, Russel Steel et al: Friction Stir Welding of API Grade X65 Steel pipes, Oak Ridge National Library, Oak Ridge, TN, Mega Stir Technologies, Provo, UT, April 2005
- [47]** Matt Boring, Brian Thompson and Brad Nagy: Advanced pipeline welding technologies boost productivity; Edison Welding Institute, Columbus, OH Pipeline and Gas Journal February 2011 Vol 238 No. 2.
- [48]** Douglas Burkes, Pavel Medvedev, Michael Chapple et al: The role of Friction Stir Welding in nuclear fuel plate fabrication, TMS 2009 Annual Meeting, February 2009.

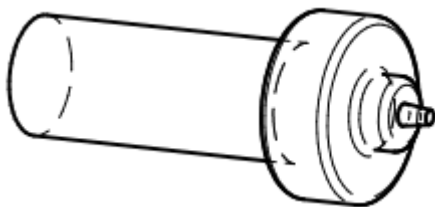
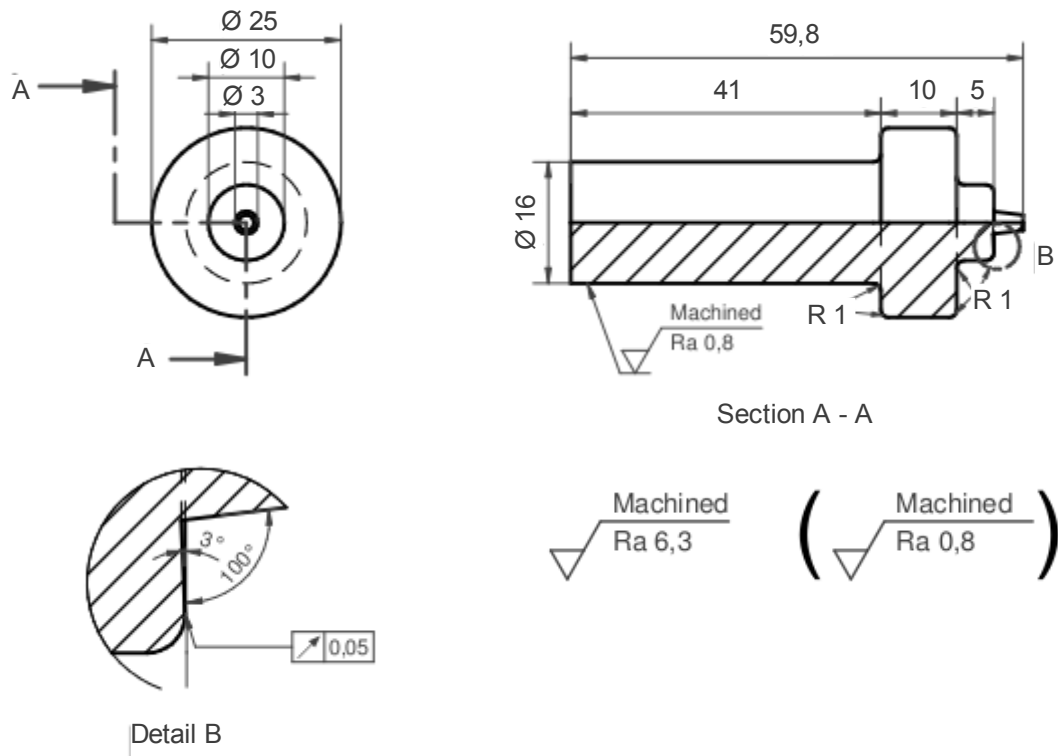
- [49] H. Staufer: LaserHybrid Welding: State of Art and Applications, Fronius International GmbH, Presentation at the ÖGS Workshop Laser Hybrid Schweißen on 21.06.2013.
- [50] M. El Rayes, C. Walz, G. Sepold: The Influence of Various Hybrid Welding Parameters on Bead Geometry, Supplement to the Welding Journal, May 2004.
- [51] Harald Scharner: Schutzgase für das Laserhybridschweißen, Air Liquide Austria, Presentation at the ÖGS Workshop Laser Hybrid Schweißen on 21.06.2013.
- [52] Klas Nilsson, Sebastian Heimbs, Hans Engström, Alexander F. H. Kaplan: Parameter Influence in CO2-laser/MIG Hybrid Welding, Luleå University of Technology, Sweden.
- [53] Hans Engström, Klas Nilsson, Jan Flinkfeldt et al: Laser Hybrid Welding of High Strength Steels, Luleå University of Technology, Sweden.
- [54] T. Graf H. Staufer: Laser-Hybrid Welding Drives VW Improvements, <http://www.aws.org/wj/jan03/feature1.html>, Accessed 14.01.2013.
- [55] H. Staufer: Laser Hybrid Welding in the automotive industry, Welding Journal October 2007.
- [56] Christoph Kammerhuber: Entwicklung und Anwendung des dioden-gepumpten Festkörperlaser-MSG Hybridschweißens zum Fügen von Wulstprofilen bei inseitigem Kehlnaht-Vollanschluss, Fronius International GmbH, Presentation at the ÖGS Workshop Laser Hybrid Schweißen 21.06.2013.
- [57] Jens Klæstrup Kristensen: State of art in shipbuilding applications of hybrid laser-arc welding, Force technology, Denmark NOLAMP 12 – Copenhagen, August 2009.
- [58] Dr S. Gook: Laserstrahl-MSG-Hybridschweißen an hochfestem Pipeline Stahl für die Großrohrproduktion, BAM Bundesanstalt für

R REFERENCES

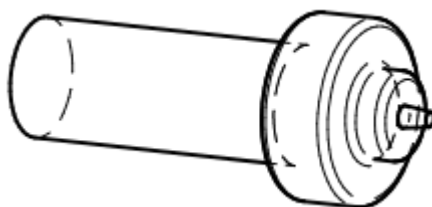
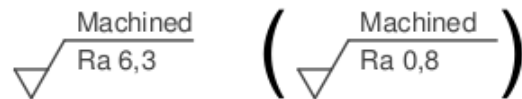
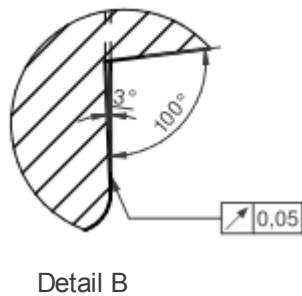
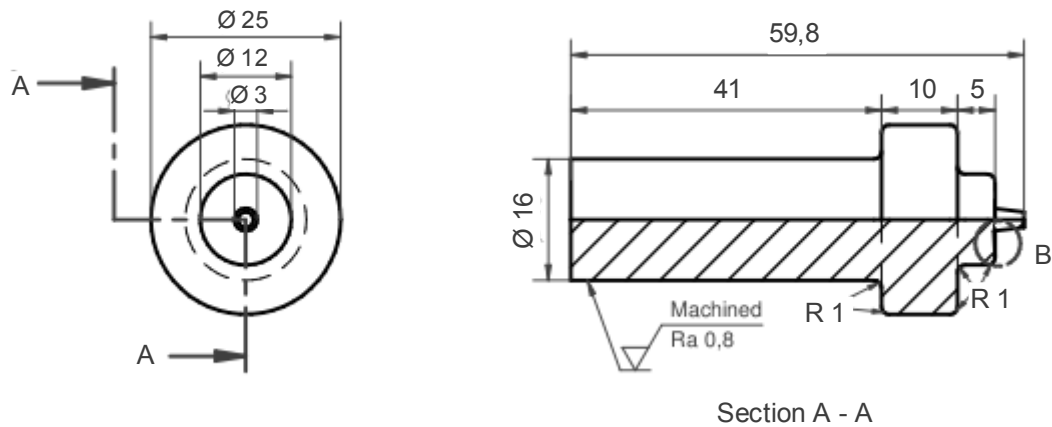
- Materialforschung; Presentation at the ÖGS-Workshop Laser Hybrid Schweißen on 21.06.2013.
- [59]** Steffen Keitel, Jan Neubert: Laser GMA Hybrid girth welding technologies for transmission pipelines, Schweißtechnische Lehr- und Versuchsanstalt Halle GmbH Presented at 5th Pipeline Technology Conference 2010.
- [60]** Lars Erik Stridth: Hybridlaser welding of pipes and the cost effectiveness compared to conventional welding,
<http://www.esab.com/global/en/education/Hybridlaser-welding-ofpipes.cfm> Accessed on 14.01.2013.
- [61]** Technisches Datenblatt AW-5754 <http://www.caro-prometa.wieland.de/>
Accessed on 15.01.2013.
- [62]** Technical data sheet of the GU-260 “Prvomajska” universal milling machine
<http://www.prvomajska.hr/products.php>,
Accessed on 15.01.2013.
- [63]** Technical data sheet of tool steel 1.2080
<http://www.metalravne.com/selector/steels/ocr12.html>
Accessed on 15.01.2013.
- [64]** Technical Data sheet filler AlMg4.5Mn <http://www.fidat.it>
Accessed on 21.1.2013.
- [65]** ISO 17637: Non-destructive testing of welds – Visual testing of fusion-welded joints; First edition 2003.7.15.
- [66]** EN ISO 25239-5 Friction stir welding — Aluminium; 2. Draft, 2009.
- [67]** Guide for Approval of friction stir welding in aluminum American Bureau of Shipping, October 2011.
- [68]** Schumann, H.: Metallographie. Deutscher Verlag für Grundstoffindustrie, Leipzig, 13., neubearbeitete Auflage, 1990.

- [69] P L Threadgill, A J Leonard, H R Shercliff and P J Withers: Friction stir welding of aluminium alloys, Paper presented at International Materials Reviews, vol.54. no.2. March 2009. pp. 49-93.
- [70] ISO 13919-2:Welding - Electron and laser beam welded joints - Guidance on quality levels for imperfections - Part 2: Aluminium and its weldable alloys, 2001.
- [71] ISO 10042 Welding - Arc-welded joints in aluminium and its alloys - Quality levels for imperfections, 2005.
- [72] EN ISO 25239-4 Friction stir welding — Aluminium; 2. Draft, 2009.
- [73] Technical Data sheet: ClaroCit Struer.
- [74] ISO 15614 Specification and qualification of welding procedures for metallic materials — Welding procedure test — Part 2: Arc welding of aluminium and its alloys, 2005.
- [75] M. Honoré, F. Boekhoff, J. K. Kristensen: Laser safety in non-confined welding areas, FORCE Technology, Innovation in Welding Technology, Brøndby, Denmark; Meyer Werft, Papenburg, Germany 2011
- [76] H. Hänninen, J. Mononen: Cost Comparison of FSW and MIG Welding, Laboratory of Engineering Materials, Helsinki University of Technology, 02/01/2004
- [77] <http://www.lowstir.com/Webpages/Product.html>
Accessed on 22.1.2013
- [78] Liming Liu, Xinfeng Hao and Gang Song: A New Laser-Arc Hybrid Welding Technique Based on Energy Conservation, State Key Laboratory of Material Modification & School of Materials Science and Engineering, Dalian University of Technology, Dalian 116024, P. R. China, Materials Transactions, Vol. 47, No. 6 (2006) pp. 1611 to 1614

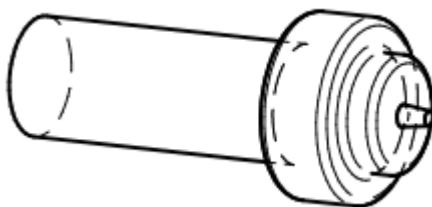
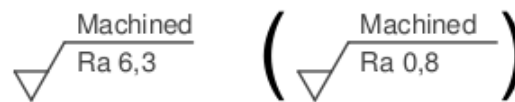
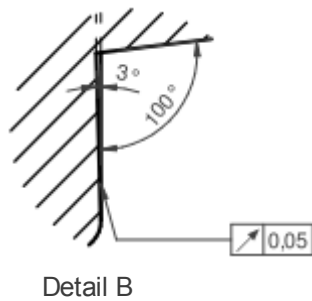
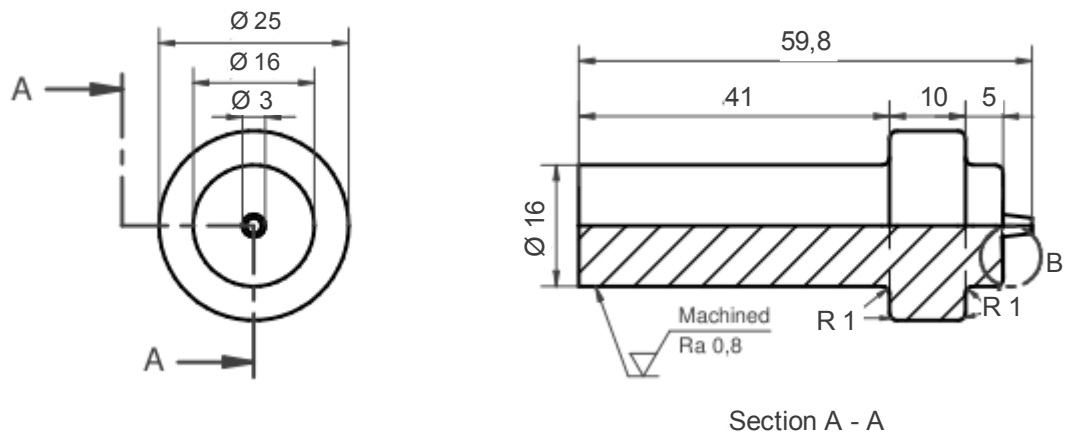
A APPENDIX



Appendix A-1: Blueprint and picture of tool with a shoulder diameter of 10 mm



Appendix A-2: Blueprint and picture of tool with a shoulder diameter of 12 mm



Appendix A-3: Blueprint and picture of tool with a shoulder diameter of 16 mm



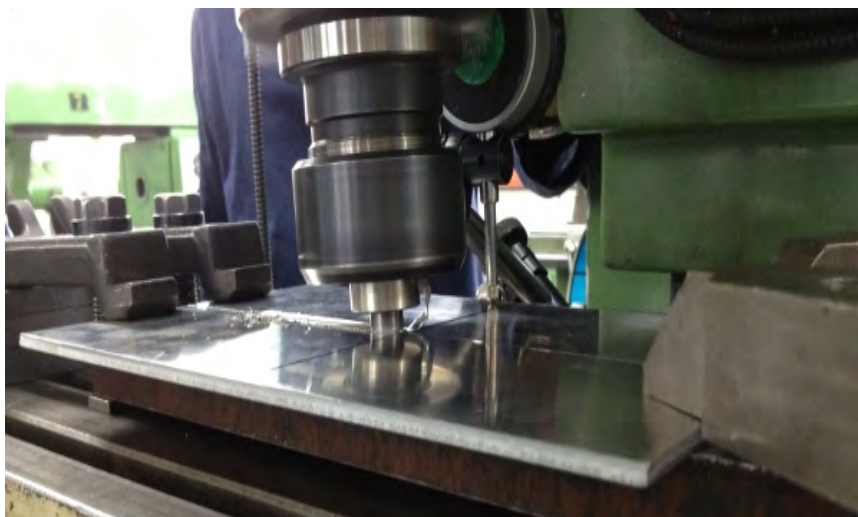
Appendix A-4: Tools manufactured and used during experimental procedure



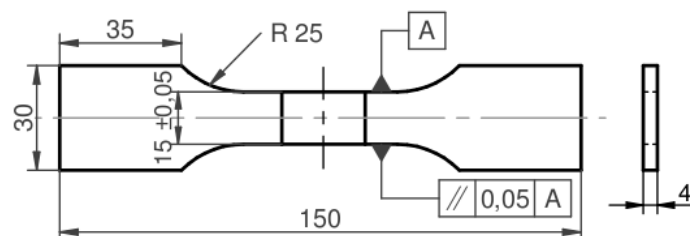
Appendix A-5: Machining of the FSW tools



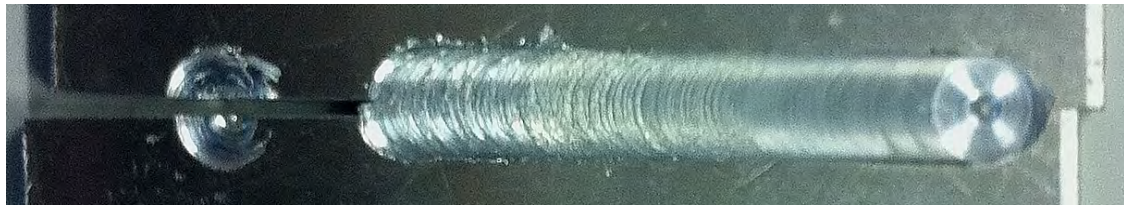
Appendix A-6: Securing of the workpieces with clamps before Welding



Appendix A-7: Friction stir welding in progress



Appendix A-8: Blueprint of tensile test specimen geometry



Appendix A-9: FSW specimen 1; lack of bonding due to failed fixture



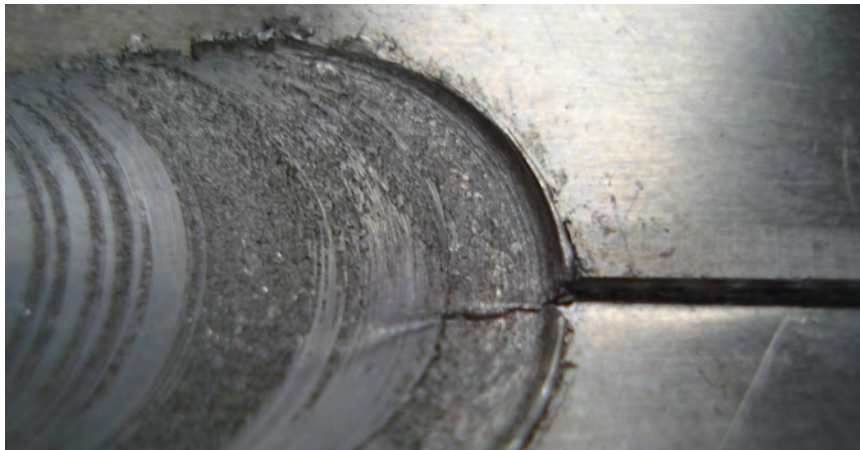
Appendix A-10: Face side of FSW specimen 2: irregular welding pattern and a small crack at the start of weld



Appendix A-11: Root side of FSW specimen 2: material discontinuity at the start of weld



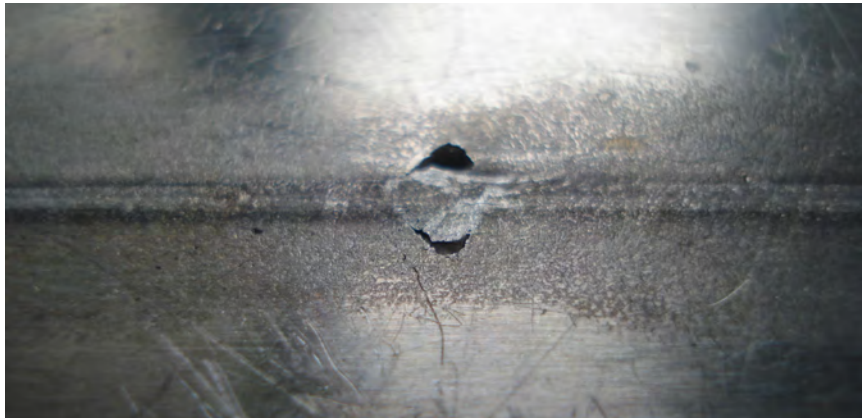
Appendix A-12: Flash alongside the weld of specimen 5



Appendix A-13: FSW specimen 4 showing irregular welding pattern and a small disruption at the start of weld



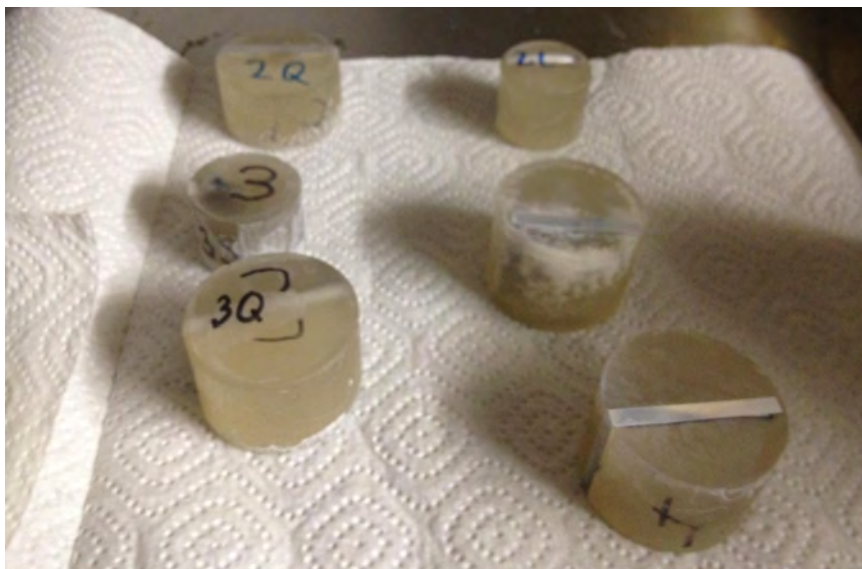
Appendix A-14: A cavity on the face side of FSW specimen 7



Appendix A-15: FSW specimen 7 – cavity observed from root side



Appendix A-16: Tensile specimen of the FSW weld 7 after fracture



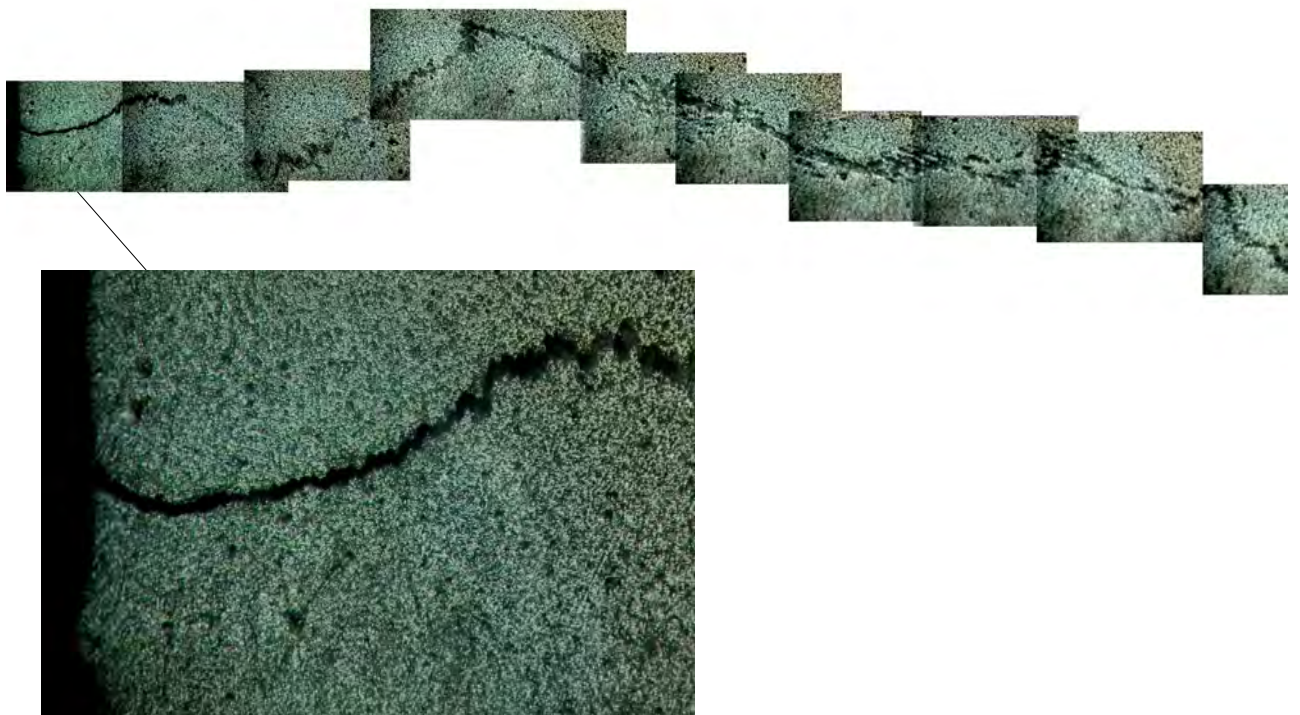
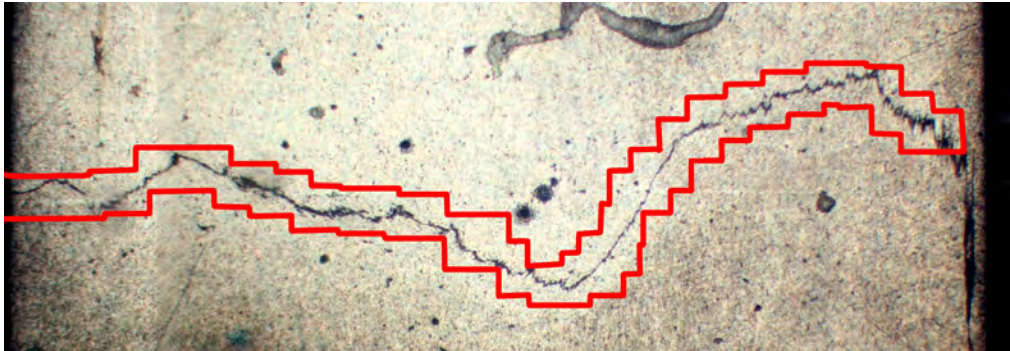
Appendix A-17: FSW specimens mounted and ready for polishing

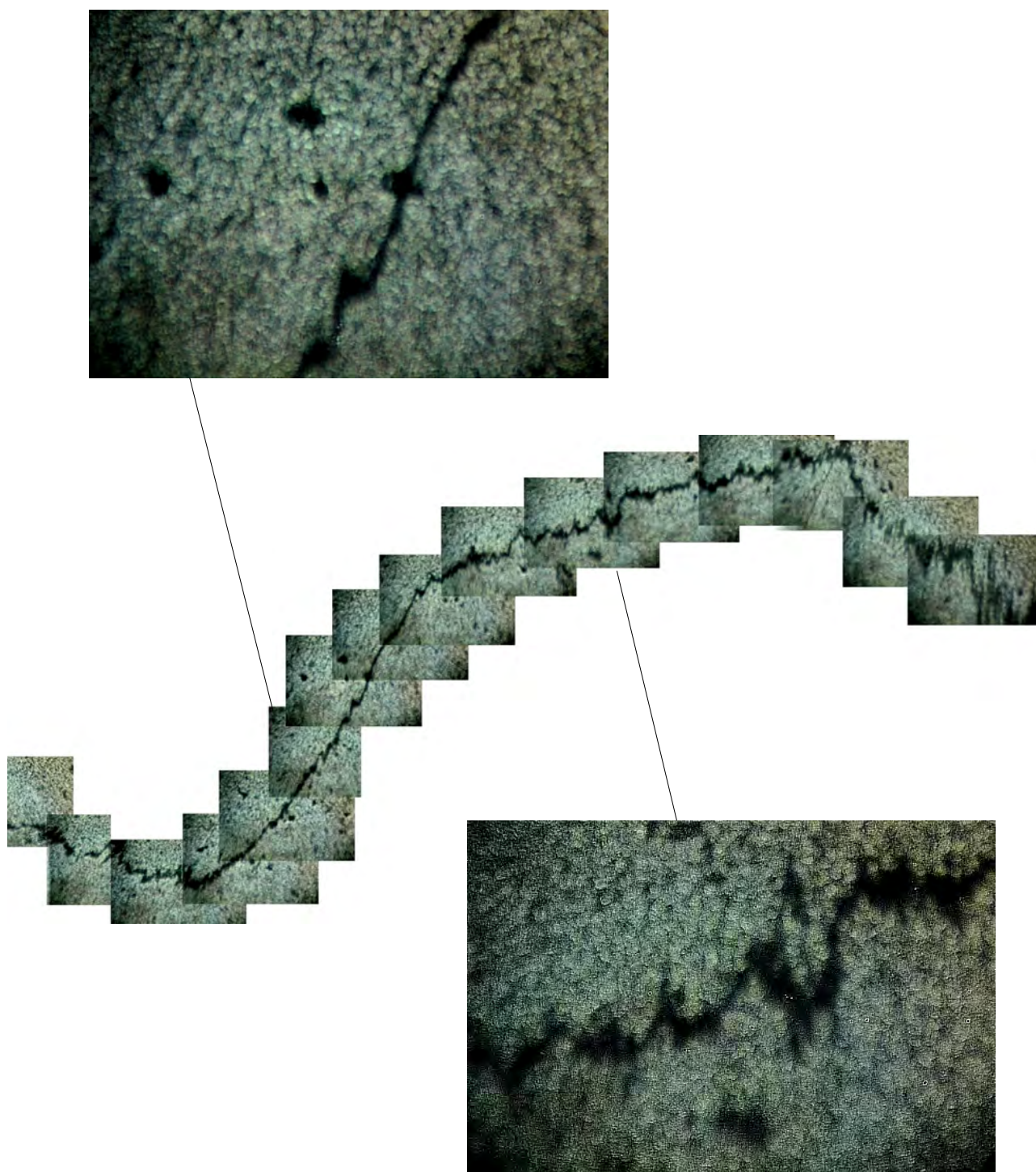


Appendix A-18: Setup for the macroscopic examination

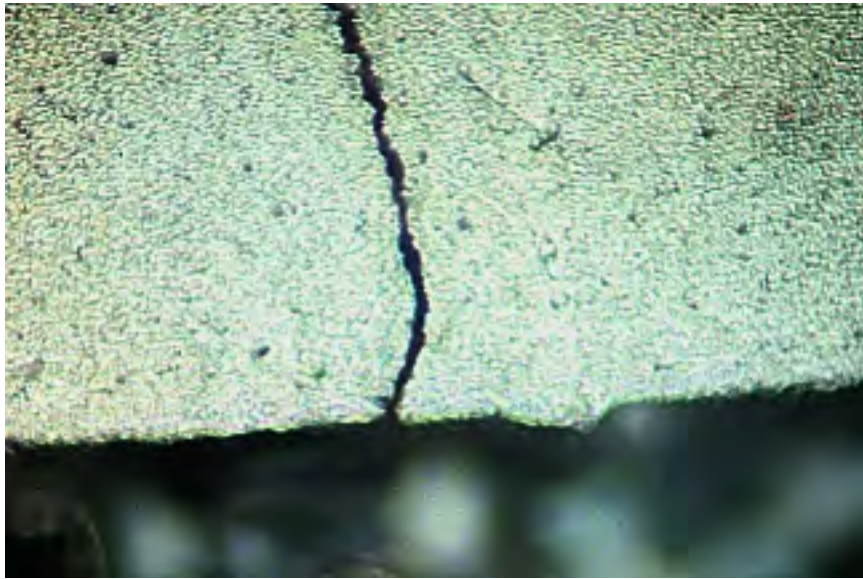


Appendix A-19: Longitudinal macroetch of specimen 2





macroetch of specimen 2



Appendix A-21: Diagonal macroetch of specimen 2 revealing a close-up of a root flaw



Appendix A-22: Transversal macro-etch of specimen 3 revealing a root flaw on the left



Appendix A-23: Transversal macro-etch of specimen 3 : the oxide layer at the edges of the joint result in the wavelike inter-phase



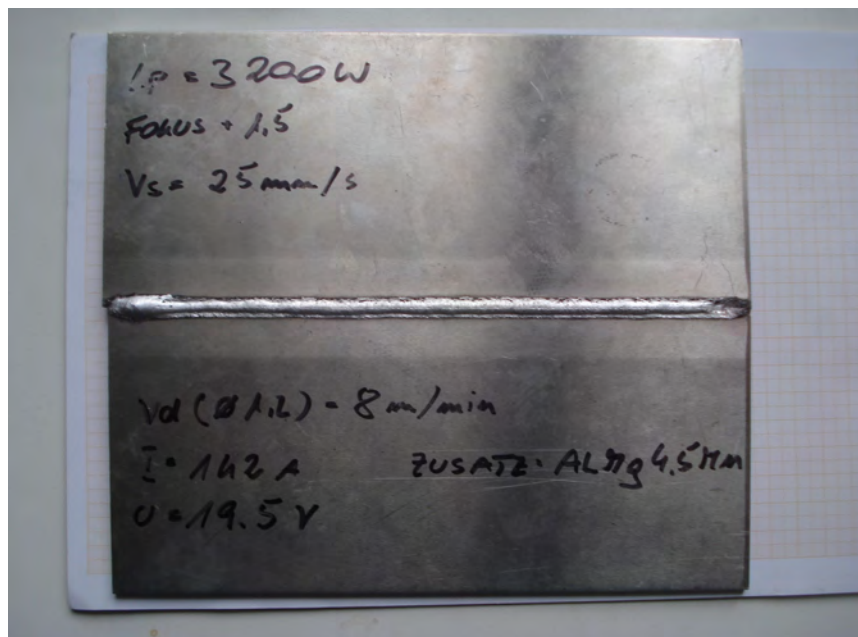
Appendix A-24: Diagonal macroetch of specimen 3 revealing a root flaw on the right the oxide layer at the edges of the joint result in the wavelike inter-phase



Appendix A-25: Transversal macro-etch of specimen 4: the brighter region represents the dynamically recrystallized zone DXZ; the oxide layer at the edges of the joint result in the wavelike inter-phase



Appendix A-26: Diagonal macroetch of specimen 4, revealing a root flaw on the left the oxide layer at the edges of the joint result in the wavelike inter-phase



Appendix A-27: LHW specimen; the HAZ can be distinguished as the bright region alongside the weld



Appendix A-28: Root side of LHW specimen



Appendix A-29: Close-up of root of LHW specimen; HAZ is represented by the bright region along the weld root



Appendix A-30: Distortion of the LHW specimen due to thermal stresses



Appendix A-31: Distortion of the LHW specimen due to thermal stresses

S SUPPLEMENTS

Technical data of GU-260 "Prvomajska" universal milling machine	
Characteristics	Dimensions
Table, length × width	1150 × 260 mm
Table travel, swivel	2 × 45°
Longitudinal- manual/automatic	785/770 mm
Cross travel-manual/automatic	270/260 mm
Vertical-manual/automatic	410/400 mm
Milling head, spindle taper	ISO-40
Pinola travel	80 mm
Speed number	18
Speed range	40-2200 r p m
El. engine	4.5 kW
Length	1750 mm
Width	1520 mm
Height	1650 mm
Machine weight	2150 kg



Picture of the GU-260 "Prvomajska" universal milling machine

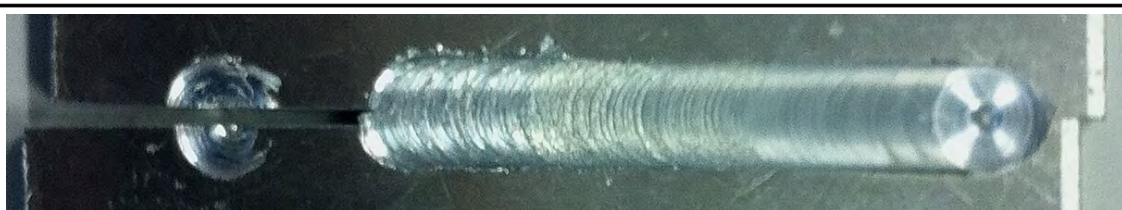
Supplement S-1: Technical data of the GU-260 "Prvomajska" milling machine [62]

Relevant technical data of tool steel 1.2080					
Tool material designation by standards					
Mat. No. EN 10027-2		DIN EN ISO 4957		AISI-SAE	
1.2080		X210Cr12		D3	
Physical properties of tool steel 1.2080					
Modulus of elasticity		N/mm ²		210000	
Density		g/cm ³		7.67	
Thermal conductivity		W/m*K		20	
Electric resistance		Ω*mm ² /m		0.65	
Specific heat capacity		J/g*K		0.46	
Chemical composition of tool steel 1.2080					
C	Si	Mn	P	S	Cr
1.9-2.2	0.1-0.4	0.15-0.45	max 0.03	max 0.03	11.0-12.0
Heat treatment of tool steel 1.2080					
Soft annealing		To secure uniform softness, heat to 800-840°C, cool slowly. This will produce a maximum HB of 250.			
Stress relieving		To remove machining stresses heat to 650°C, hold for one hour, followed by air cooling.			
Hardening		Harden from a temperature of 940-980°C by oil quenching or warm bath approx. 400°C. 64-66 HRC after quenching.			
Tempering		Tempering temperature: 150 – 400°C			
Applications of tool steel 1.2080					
Tools for: cutting, stamping, woodworking, drawing, deep drawing, pressing, cold work- ing rolls, measuring.					

Supplement S-2: Technical data of tool steel 1.2080 [63]
(HB: Brinell hardness; HRC: Rockwell hardness)

Technical Data of Lathe CTX210	
Swing	480 mm
Chuck diameter	140/165 mm
Turning length	305 mm
Bar capacity	45 mm
Drive power	7.5 kW
Speed range	20 – 6000 r p m


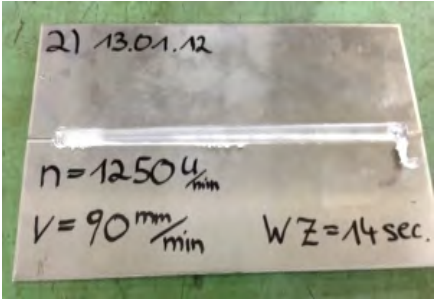
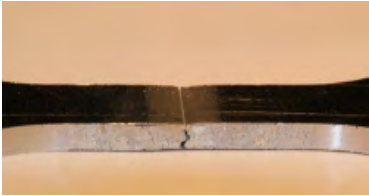
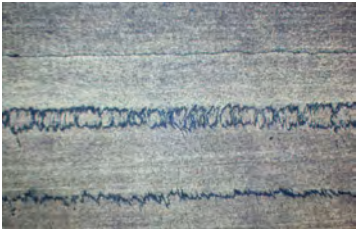

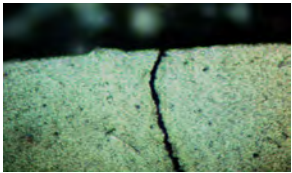
Supplement S-3: Technical data of lathe CTX210 by Gildemeister A.G.




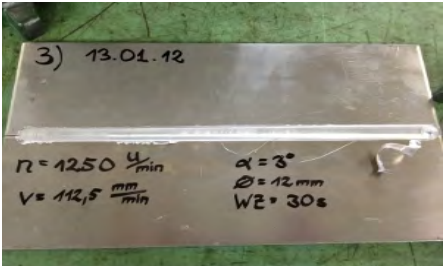


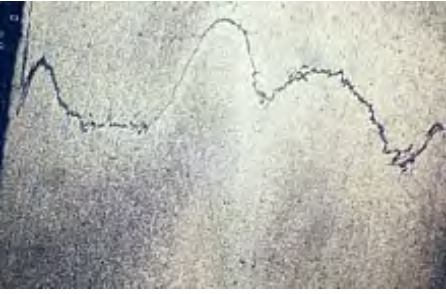
Rotation	1000 min ⁻¹	
Advance	12.5 mm/min	
Tool diameter	12 mm	
Tool angle	3°	
Time before advance	10	
Tensile Test	---	
Macroscopic examination	---	

Supplement S-4: FSW specimen 1 with parameters and test results

S SUPPLEMENTS

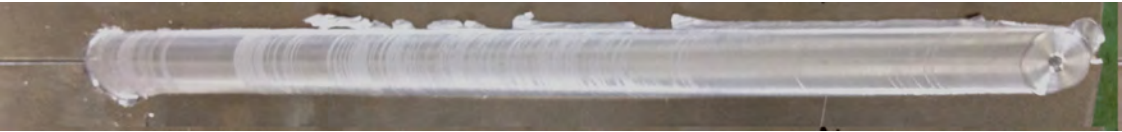
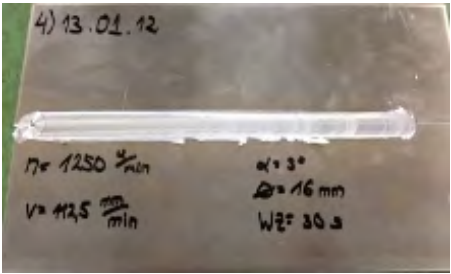
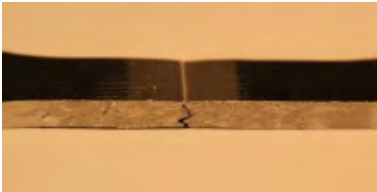


		
Rotation	1250 min ⁻¹	
Advance	90 mm/min	
Tool diameter	12 mm	
Tool angle	3°	
Time before advance	14 s	
NDT	VT	
Tensile test	Tensile test result: $R_m : 224.16 \text{ N/mm}^2$	
Macroetches	Longitudinal	
	Transverse	
	Diagonal	

*Supplement S-5: FSW specimen 2 with parameters and test results
(R_m : tensile strength)*


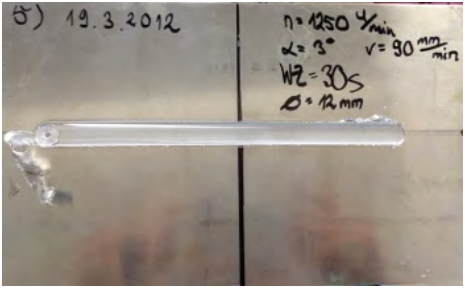

		
Rotation	1250 min ⁻¹	
Advance	112.5 mm/min	
Tool diameter	12 mm	
Tool angle	3°	
Time before advance	30 s	
NDT	VT	
Tensile test	Tensile test result: $R_m : 222.2 \text{ N/mm}^2$	
Macroetches	Transverse	
	Diagonal	

*Supplement S-6: FSW specimen 3 with parameters and test results
(R_m : tensile strength)*


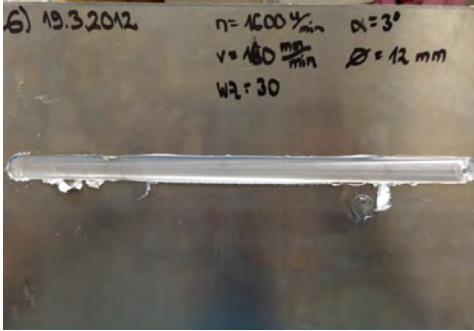
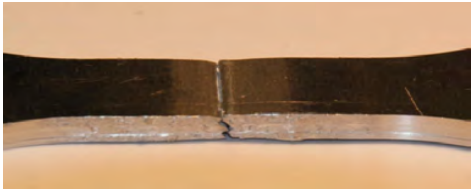
S SUPPLEMENTS

		
Rotation	1250 min ⁻¹	
Advance	90 mm/min	
Tool diameter	16 mm	
Tool angle	3°	
Time before advance	14 s	
NDT	VT	
Tensile test	Tensile test result: R _m : 165 N/mm ²	
Macroetches	Transverse	
	Diagonal	


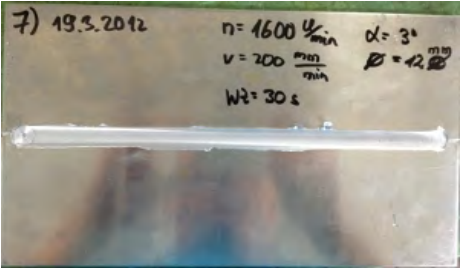

Supplement S-7: FSW specimen 4 with parameters and test results
(R_m : tensile strength)

		
Rotation	1250 min ⁻¹	
Advance	90 mm/min ?	
Tool diameter	12 mm	
Tool angle	3°	
Time before advance	30 s	
NDT	VT	
Tensile test	R _m : 241.3 N/mm ²	

*Supplement S-8: FSW specimen 5 with parameters and test results
(R_m : tensile strength)*

		
Rotation	1600 min ⁻¹	
Advance	160 mm/min	
Tool diameter	12 mm	
Tool angle	3°	
Time before advance	30 s	
NDT	VT	
Tensile test	Tensile test result: R _m : 208.3 N/mm ²	

*Supplement S-9: FSW specimen 6 with parameters and test results
(R_m : tensile strength)*

		
Rotation	1600 min ⁻¹	
Advance	160 mm/min	
Tool diameter	12 mm	
Tool angle	3°	
Time before advance	30 s	
NDT	VT	
Tensile test	Tensile test result: R _m : 242.3 N/mm ²	

Supplement S-10: FSW specimen 7 with parameters and test results
(R_m: tensile strength)

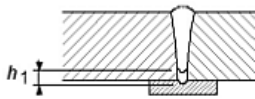
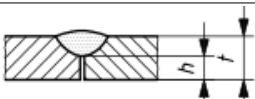
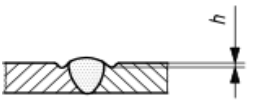
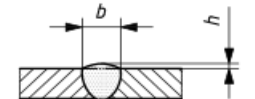

Technical data for AlMg 4.5 Mn filler material										
Designation		DIN: Al Mg 4,5 Mn; AA 5183; BS: 2901 Pt. 4 5183								
Chemical composition										
Si	Fe	Cu	Mn	Mg	Cr	Zn	Ti	Be	other	Al
0.2	0.4	0.1	0.5-1	4.3-5.2	0.05-0.25	0.25	0.15	0.0008	0.15	balance
Mechanical properties		R _m [N/mm ²]		R _{p0.2} [N/mm ²]		A [%]			T _f [°C]	
		300 - 330		125 - 145		25 - 35			565 - 638	
Description		Welding wires and rods for TIG and MIG welding magnesium and manganese alloyed aluminum with a magnesium content max 5%. This alloy shows very good mechanical properties that make it ideal for applications in shipyards, car and railway industry, construction of reservoirs and tanks.								

Supplement S-11: Technical data for AlMg 4.5 Mn filler material [64]
 (R_m: tensile strength; R_{p0.2}: 0.2% proof strength; A: tensile elongation;
 T_f: liquidus temperature interval)

Technical data of Wolpert U10 universal testing machine	
Capacity	100 kN
Strain range	250 mm
Load accuracy	EN ISO 7500-1 class 1
Dimensions	1000 x 500 x 2876 mm
Weight	750 kg

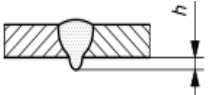
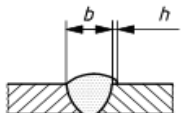
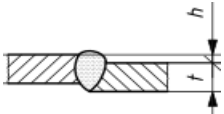
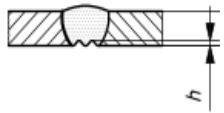
Supplement S-12: Technical data of Wolpert U10 universal testing machine

S SUPPLEMENTS

VT specifications of FSW and LHW welds part 1								
Quality criteria	Sketch and/or remarks	FSW ¹	ISO 10042			ISO 13919		
			Quality level ²			Quality level ³		
			D	C	B	D	C	B
Cracks	All types of detectable cracks	✗	✗	✗	✗	✗	✗	✗
Exit hole uniformity	Hollow left by the exit of FSW pin	... ⁴	---	---	---	---	---	---
Chevron marking	... ⁵	... ⁶	---	---	---	---	---	---
Flash	Material expelled by FSW process	... ⁷	---	---	---	---	---	---
Root reinforcement		... ⁸	---	---	---	... ⁹	... ⁹	... ⁹
Crater cracks	h = height or width of crater crack	---	$h \leq 0.4t$	✗	✗	✓	✓	✗
Porosity	l = maximum dimension of a pore	✗	✗	✗	✗	$l \leq 0.5t$	$l \leq 0.4t$	$l \leq 0.3t$
Surface pore	l = maximum dimension of a pore	✗	$l \leq 0.4t$	$l \leq 0.3t$	$l \leq 0.2t$	---	---	---
Crater pipe	h = height of crater pipe	---	$h \leq 0.4t$	$h \leq 0.2t$	✗	$h \leq 0.15t$	$h \leq 0.1t$	$h \leq 0.05t$
Lack of fusion	h – maximal height	---	$h \leq 0.1t$	✗	✗	$h \leq 0.25t$	✗	✗
Incomplete root penetration		✗	$h \leq 0.2t$	✗	✗	$h \leq 0.25t$	✗	✗
Thickness variation/ undercut		$h \leq 0.1t$	$h \leq 0.2t$	$h \leq 0.1t$	✗	$h \leq 0.2t$	$h \leq 0.1t$	✗
Excess weld metal		---	$h \leq 1.5 + 0.2b$ [mm]	$h \leq 1.5 + 0.15b$ [mm]	$h \leq 1.5 + 0.1b$ [mm]	$h \leq 2 + 0.3t$ [mm]	$h \leq 2 + 0.2t$ [mm]	$h \leq 2 + 0.15t$ [mm]
Sagging		---	$h_1 \leq 0.2t$	$h_1 \leq 0.1t$	$h_1 \leq 0.05t$	$h_1 \leq 0.3t + h_2$	$h_1 \leq 0.2t + h_2$	$h_1 \leq 0.1t + h_2$

Supplement S-13 part 1: VT of FSW and LHW welds according to relevant standards [70], and [71]

(✓ : permitted to pass VT; ✗ : not permitted to pass VT; --- : not relevant for specific weld; t: base material thickness; h, h₁, h₂ : height dimension as shown in the sketch, b: width dimension as shown in the sketch)

VT specifications of FSW and LHW welds part 2								
Quality criteria	Sketch and/or remarks	FSW ¹	ISO 10042			ISO 13919		
			Quality level ²			Quality level ³		
			D	C	B	D	C	B
Excessive penetration		---	$h \leq 5$ [mm]	$h \leq 4$ [mm]	$h \leq 3$ [mm]	$h \leq 0.2 + 0.3t$ [mm]	$h \leq 0.2 + 0.2t$ [mm]	$h \leq 0.2 + 0.15t$ [mm]
Overlap		---	$h \leq 0.2b$	✗	✗	---	---	---
Linear mis-alignment		$h \leq 0,2t$	$h \leq 0,4t$	$h \leq 0,3t$	$h \leq 0,2t$	$h \leq 0.25t$	$h \leq 0.15t$	$h \leq 0.1t$
Shrinkage groove		---	$h \leq 0.2t$	$h \leq 0.1t$	$h \leq 0.05t$	$h \leq 0.15t$	$h \leq 0.1t$	$h \leq 0.05t$
Test result								

Supplement S-13 part 2: VT of FSW and LHW welds according to relevant standards [70], and [71]

Notes:

FSW ¹ Quality criteria according to The Guide for Approval of friction stir welding in aluminum, by the American Bureau of Shipping.

² For base material thicknesses ≥ 5 mm.

³ For base material thicknesses ≥ 1 mm.

...⁴ The exit hole is to be examined and the uniformity has to be more than 75% complete.

...⁵ This type of marking is occasionally observed when welding aluminum alloys of the 5xxx series. These markings have not reported to affect the mechanical or corrosional behavior of FSW welds.

...⁶ The presence of such markings shall be noted and eventually removed prior to destructive testing.

...⁷ Prior to removal of flash, regions within friction stir welds containing excessive flash shall be marked on the plate, and these areas shall be inspected for dimensional conformance.

...⁸ Root reinforcement is to be less or equal to 10% of the base material thickness.

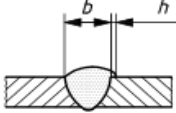
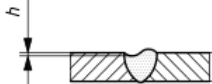
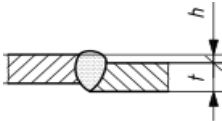
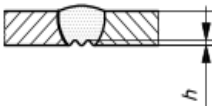
...⁹ Welding into the root backing is not permitted unless specified in certain applications.

S SUPPLEMENTS

VT protocol of FSW and LHW welds part 1									
Quality criteria	Sketch and/or remarks	FSW specimens							LHW weld
		1	2	3	4	5	6	7	
Cracks	all types of detectable cracks	✗ ¹	✗ ²	✗ ²	✗ ²	✓	✗ ²	✗ ²	✓
Exit hole uniformity	hollow left by the exit of FSW pin	✓	✓	✓	✓	✓	✓	✓	---
Chevron marking	... ³	✓	✓	✓	✓	✓	✓	✓	---
Flash	material expelled by FSW process	✓	✓	✓	✓ ⁴	✓ ⁴	✓ ⁴	✓	---
Root reinforcement		---	---	---	---	---	---	---	---
Crater cracks	h = height or width of crater crack	---	---	---	---	---	---	---	✓
Porosity	l = maximum dimension of a pore	✓ ⁵	✓ ⁵	✓ ⁵	✓ ⁵	✓ ⁵	✓ ⁵	✓ ⁵	✓ ⁵
Surface pore	l = maximum dimension of a pore	✓	✓	✓	✓	✓	✗ ⁶	✗ ⁶	l=1.8 [mm]
Crater pipe	h = height of crater pipe	---	---	---	---	---	---	---	h=1.7 [mm]
Lack of fusion	h – maximal height	---	---	---	---	---	---	---	✓
Incomplete root penetration		✗ ⁷	✗ ⁸	✗ ⁸	✓	✓	✓	✓	✓
Thickness variation / Undercut		✗ ¹	h=0 [mm]	h=0.1 [mm]	h=0 [mm]	h=0.1 [mm]	h=0 [mm]	h=0.1 [mm]	h=0.2 [mm]
Excess weld metal		---	---	---	---	---	---	---	h=0.29 [mm]
Excessive penetration		---	---	---	---	---	---	---	h=1.2 [mm]

Supplement S-14 part 1: VT protocol of FSW and LHW welds according to standards

(✓ : permitted to pass VT; ✗ : not permitted to pass VT; --- : not relevant for specific weld; t: base material thickness t = 4 mm for FSW and LHW specimens; h: height dimension as shown in the sketch, b: width dimension as shown in the sketch)

VT protocol of FSW and LHW welds part 2									
Quality criteria	Sketch and/or remarks	FSW specimens							LHW
		1	2	3	4	5	6	7	
Overlap		---	---	---	---	---	---	---	$h=0$ [mm]
Sagging		---	---	---	---	---	---	---	✓
Linear mis-alignment		✗ ¹	$h=0$ [mm]	$h=0$ [mm]	$h=0$ [mm]	$h=0$ [mm]	$h=0$ [mm]	$h=0$ [mm]	$h=0.3$ [mm]
Shrinkage groove		---	---	---	---	---	---	---	✓
Test result		✗	✗	✗	✗	✓	✗	✗	✗

Supplement S-14 part 2: VT protocol of FSW and LHW welds according to standards

Notes:

- ✗¹ the base material plates slipped apart due to fixture failing, resulting in a major gap and a crack at the start of the weld
- ✗² small crack can be observed at the start of the weld
- ...³ this type of marking is occasionally observed when welding aluminum alloys of the 5xxx series. These markings have not reported to affect the mechanical or corrosional behavior of FSW welds
- ✓⁴ excess flash upon the FSW weld, yet no dimensional deviations are accounted
- ✓⁵ as no destructive methods were used, subsurface porosity could not be detected
- ✗⁶ a cavity can be spotted. Cavity resulted from filing a hole prior to welding to ease tool plunge
- ✗⁷ the base material plates slipped apart due to fixture failing, resulting in a major gap on the root side of the weld
- ✗⁸ material discontinuity can be observed at the start of the weld resulting from a lack of penetration

